RISC-KIT

Resilience-Increasing Strategies for Coasts – Toolkit

Coastal Hazard Assessment Module

Deliverable No: D.2.1 – Coastal Hazard Assessment Module
Ref.: WP2 - Task 2.1
Date: May 2015

Deliverable Title	D.2.1 – Coastal Hazard Assessment Module
Filename	RISC-KIT_D.2.1
Authors	José A. Jiménez (UPC) Clara Armaroli (CRF) Marc Berenguer (UPC) Eva Bosom (UPC) Paolo Ciavola (CRF) Oscar Ferreira (UAlg) Haris Plomaritis (UAlg) Dano Roelvink (IHE) Marc Sanuy (UPC) Daniel Sempere (UPC)
Contributors	Tom Spencer (UCAM)
Date	01/06/2015

Prepared under contract from the European Commission
Grant Agreement No. 603458
Directorate-General for Research & Innovation (DG Research), Collaborative project,
FP7-ENV-2013-two-stage

Start of the project: 01/11/2013
Duration: 42 months
Project coordinator: Stichting Deltares, NL

Dissemination level

X	PU	Public
	PP	Restricted to other programme participants (including the Commission Services)
	RE	Restricted to a group specified by the consortium (including the Commission Services)
	CO	Confidential, only for members of the consortium (including the Commission Services)

Deliverable status version control

Version	Date	Author	Review
1.0	05/05/2015	José A Jiménez (UPC)	Christophe Viavattene (UM) Oscar Ferreira (UAlg)
2.0	27/05/2015	José A Jiménez (UPC)	Christophe Viavattene (UM), Ap van Dongeren (Deltares), Robert McCall (Deltares)
3.0	31/05/2015	José A Jiménez (UPC)	Robert McCall (Deltares)
4.0	01/06/2015	José A Jiménez (UPC)	

Table of Contents

List of Figures

List of Tables

Executive and Publishable Summary

The Resilience-Increasing Strategies for Coasts – Toolkit (RISC-KIT) EU FP7 project (2013- 2017) aims to produce a set of three innovative and EU-coherent open-source and open-access methods, tools and management approaches (the RISC-KIT) in support of coastal managers, decision-makers and policy-makers to reduce risk and increase resilience to low-frequency, high impact hydro-meteorological events. Within this general context, Task 2.1 has the aim of developing a Coastal Hazard Assessment module to describe the dynamic response of the coast to the impact of extreme hydro-meteorological events such as inundation and erosion. The final goal is to characterize in probabilistic terms the magnitude of storm-induced hazards along the coast at regional scale (O(100 km)) to be integrated within the CRAF to identify coastal hotspots.

The current deliverable 2.1 presents the Hazard Assessment module to be used in the RISC-KIT project. First, the general framework is presented which is followed by the description of the different tools to be used to quantify considered hazards. Coastal hazards included in this module have been selected taking into account the general characteristics of the European coastline. Thus, three main hazard types have been included: coastal-flooding related ones, coastal-erosion related ones and flash floods. For all of them, simple parametric models have been selected to quickly assess their magnitude for a large number of events (to obtain reliable probabilistic distributions) in large number of positions along the coast (to properly characterize hazards at regional scale). This permits, in a first phase, to quickly identify the existence of hotspots along the coast. In a second phase, these sensitive areas will be further analyzed by using detailed process-oriented models such as XBeach to properly define these hotspots based on a more precise assessment of the hazard magnitude.

In order to assess future storm-induced coastal hazards, we also propose a method to account for potential long-term climate change effects. The proposed methodology mainly focuses on the assessment of indirect effects, i.e. changes in the hazard due to induced changes in the coastal system state (e.g. SLR induced erosion and inundation).

1 Introduction

Recent and historic low-frequency, high-impact events such as Xynthia (impacting France in 2010), the 2011 Liguria (Italy) Flash Floods and the 1953 North Sea storm surge which inundated parts of the Netherlands, Belgium and the UK have demonstrated the flood risks faced by exposed coastal areas in Europe. Typhoons in Asia (such as Typhoon Haiyan in the Philippines in November 2013), hurricanes in the Caribbean and Gulf of Mexico, and Superstorm Sandy, impacting the northeastern U.S.A. in October 2012, have demonstrated how even larger flooding events pose a significant risk and can devastate and immobilize large cities and countries.

These coastal zone risks are likely to increase in the future (IPPC, AR5) which requires a re-evaluation of coastal disaster risk reduction (DRR) strategies and a new mix of prevention (e.g. dike protection), mitigation (e.g. limiting construction in flood-prone areas; eco-system based solutions) and preparedness (e.g. Early Warning Systems, EWS) (PMP) measures. Even without a change in risk due to climate or socio-economic changes, a re-evaluation is necessary in the light of a growing appreciation of ecological and natural values which drive ecosystem-based or Nature-based flood defense approaches. In addition, as free space is becoming sparse, coastal DRR plans need to be spatially efficient, allowing for multi-functionality.

1.1 Project objectives

In response to these challenges, the RISC-KIT project aims to deliver a set of open-source and open-access methods, tools and management approaches to reduce risk and increase resilience to low-frequency, high-impact hydro-meteorological events in the coastal zone. These products will enhance forecasting, prediction and early warning capabilities, improve the assessment of long-term coastal risk and optimise the mix of PMP-measures. Specific objectives are:

1. Review and analysis of current-practice coastal risk management plans and lessons-learned of historical large-scale events;
2. Collection of local socio-cultural-economic and physical data at case study sites through end-user and stakeholder consultation to be stored in an impact-oriented coastal risk database;
3. Development of a regional-scale coastal risk assessment framework (CRAF) to assess present and future risk due to multi-hazards (Figure 1-1, top panel);
4. Development of an impact-oriented Early Warning and Decision Support System (EWS/DSS) for hot spot areas consisting of: i) a free-ware system to predict hazard intensities using coupled hydro-meteo and morphological models and ii) a Bayesian-based Decision Support System which integrates hazards and socio-economic, cultural and environmental consequences (Figure 1-1, centre panel);
5. Development of potential DRR measures and the design of ecosystem-based and cost-effective, (non-)technological DRR plans in close cooperation with end-users for a diverse set of case study sites on all European regional seas and on one tropical coast (Figure 1-1; bottom panel);

6. Application of CRAF and EWS/DSS tools at the case study sites to test the DRR plans for a combination of scenarios of climate-related hazard and socio-economic vulnerability change and demonstration of the operational mode;
7. Development of a web-based management guide for developing integrated DRR plans along Europe's coasts and beyond and provide a synthesis of lessons learned in RISC-KIT in the form of policy guidance and recommendations at the national and EU level.

The tools are to be demonstrated on case study sites on a range of EU coasts in the North- and Baltic Sea Region, Atlantic Ocean, Black Sea and Mediterranean Sea, and one site in Bangladesh, see Figure 1-2. These sites constitute diverse geomorphic settings, land use, forcing, hazard types and socio-economic, cultural and environmental characteristics. All selected regions are most frequently affected by storm surges and coastal erosion. A management guide of PMP measures and management approaches will be developed. The toolkit will benefit forecasting and civil protection agencies, coastal managers, local government, community members, NGOs, the general public and scientists.

1.2 Project structure

The project is structured into seven Work Packages (WP) starting with WP1 on 'Data collection, review and historical analysis'.; WP2–4 will create the components of the RISC-toolKIT containing an 'Improved method for regional scale vulnerability and risk assessment' (WP2), 'Enhanced early warning and scenario evaluation capabilities for hot spots' (WP3) as well as 'New management and policy approaches to increase coastal resilience' (WP4). The toolkit will be tested through 'Application at case study sites' (WP5). WP6 will be responsible for 'Dissemination, knowledge transfer and exploitation' and 'Coordination and Management' are handled in WP7.

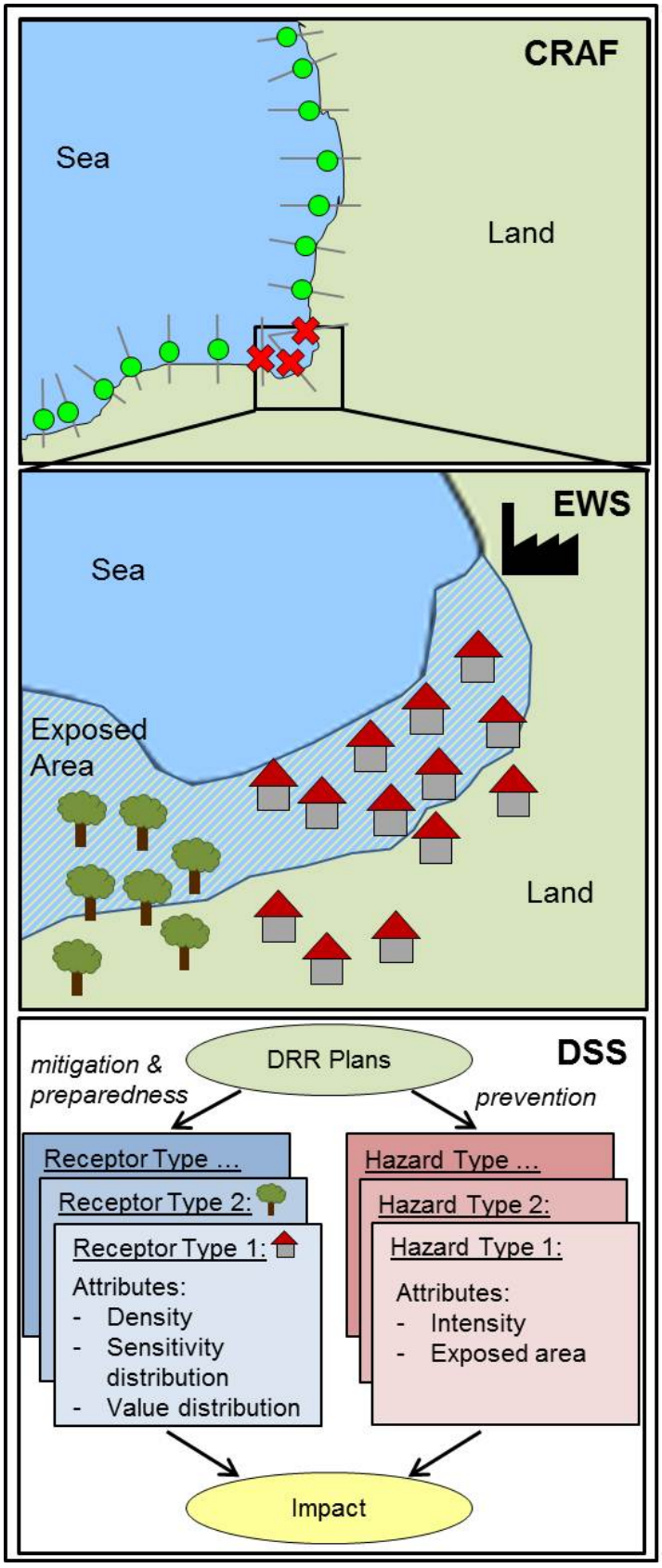

Figure 1-1: Conceptual drawing of the CRAF (top panel), the EWS (middle panel) and the DSS (bottom panel).

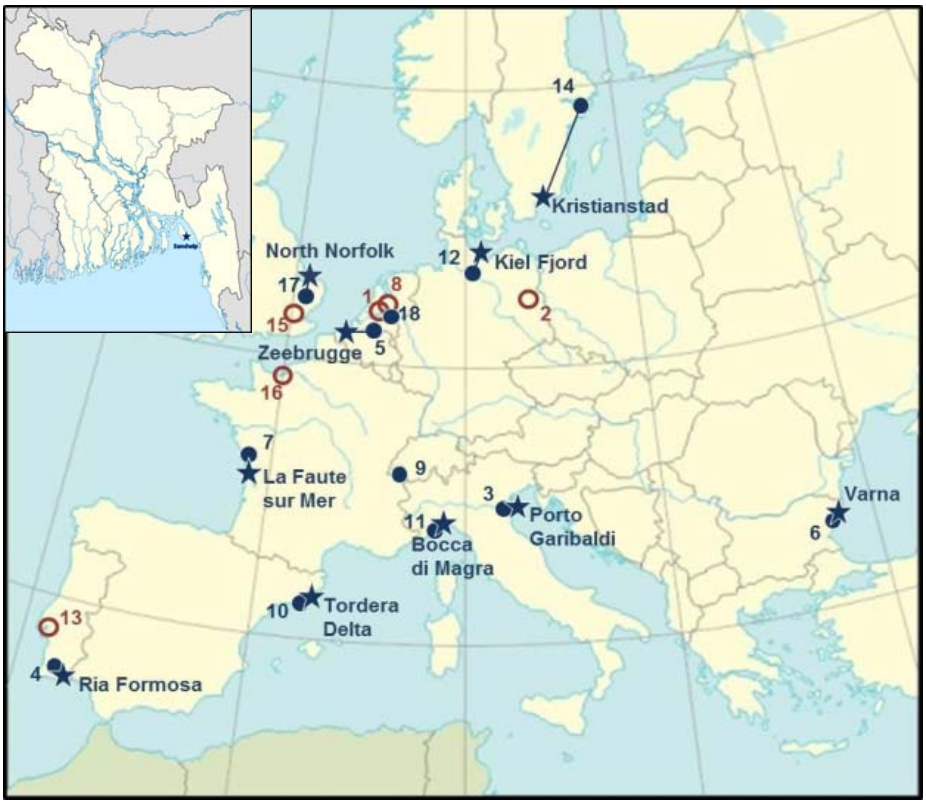

Figure 1-2: RISCKIT field sites.

1.3 Deliverable context and objective

The current deliverable 2.1 is part of WP 2. The objective of WP 2 are to develop a

- Coastal Hazard Assessment Module to assess the magnitude of hazards induced by the impact of extreme hydro-meteorological events in the coastal zone at a regional scale (O(100 km)).
- Set of Coastal Vulnerability Indicators for the receptors exposed to coastal hazards.
- Coastal Risk Assessment Framework (CRAF) for extreme hydro-meteorological events which, integrating hazards and vulnerability inputs, can be used to assess potential impacts and identify hot spot areas where detailed models can be applied.

This task (2.1) will develop a Coastal Hazard Assessment Module (D2.1) that describes the dynamic response of the coast to the impact of extreme hydro-meteorological events such as inundation and erosion. This module will be applicable at the regional scale (O(100 km)). The event scenarios (in terms of waves, storm surges and wind) will be derived from locally available observations, hindcasts (e.g. FP5 HIPOCAS) and regional or downscaled global climate change scenarios (e.g. IPCC AR5). Since they will be applied for regional scale assessment, they have to reproduce the spatial variability in process inputs in order to account for variations in forcing along the coast.

Once the forcing has been defined along the coast, the module will locally assess resultant hazard intensities (e.g. wind and wave setup, currents, wave impacts, overtopping, erosion and inundation). To this end, hazard intensities will be assessed using parametric models applicable to the characteristics of each type of coast present at the field sites (e.g. beaches, dunes, barriers, tidal flats, estuaries) and by applying open-source, process-based models (e.g. XBeach). The application of process-based models will be done in transect (1D) mode to optimize its usability at the regional scale for a significant number of events, representative of the local extreme climate.

These models forced by data on characteristic extreme events will allow the assembly of time series of hazards along the coast. Instead of the forcing, resultant hazard time series will be fitted to suitable extreme probability distributions. Using this approach, the Coastal Hazard Assessment module will map hazard intensities along the coast associated with given probabilities specified by stakeholders according to the target safety level.

This module will also account for potential long-term climate change effects on the intensity of future hazards. Such effects include changes in the background erosion rate, sea level rise and changes in extreme wind and wave patterns. The module will combine individual hazards to be later used in CRAF. The module will be validated and tested using existing laboratory and field datasets for coastal hazards."

This deliverable addresses the objective of WP 2 and Project Objective 3 "Development of a regional-scale coastal risk assessment framework (CRAF) to assess present and future risk due to multi-hazard" by providing methodologies to assess the magnitude of storm-induced coastal hazards at regional scale.

1.4 Approach

One of the elements/tools to be developed within RISCKIT is a quick-scan *Coastal Risk Assessment Framework (CRAF)* to identify hotspots coastal areas to the impact of extreme events at a regional scale of about 100 km of coastal length, a typical "administrative" or "jurisdictional" scale. These hotspots will be later analyzed in detail by using an impact-oriented *Early Warning System/Decision Support System (EWS/DSS)* to provide real-time (short-term) forecasts and early warnings, which is separate from the CRAF and is not discussed further in this report.

To this end, the Coastal Hazard Assessment Module will be used to assess the considered hazards in different sectors along the coast reproducing the existing spatial variability both in coastal morphology and in hydro-meteorological forcing. Taking into account that the main objective of this module is the identification of hotspots, the length of these sectors has been selected in the order of 1 km and they will be represented by a beach profile. The selection of the representative profile will be based on the use of an average profile and a "worst case" profile, which will be used to assess the magnitude of expected hazards in potentially weak points along the coast (e.g. coastal sectors with a low elevation).

Since the adopted approach is based on the probabilistic description of the considered hazards, this implies the use of use long-term data set to characterize the forcing and, in consequence, the induced hazards. In this sense, the module should be fed by long time series of wave and water level data. In the case that instrumental records do not exist and/or they are short enough to prevent a reliable extreme analysis, they will be

substituted by simulated (hindcast) data. As an example of this, long-term (44 years) series of waves and water level data obtained within the FP5 HIPOCAS project will be used to characterize the climatic forcing of considered hazards in the Mediterranean coast.

Coastal hazards included in this module have been selected taking into account the general characteristics of the European coastline. Thus, three main hazard types have been included which are present in the project study sites (where the proposed methodology will be tested): coastal-flooding related ones, coastal-erosion related ones and flash floods. For all of them, simple parametric models have been selected to quickly assess their magnitude for a large number of events (to obtain reliable probabilistic distributions) for a large number of positions along the coast (to properly characterize hazards at regional scale). This permits, in a first phase, to quickly identify the existence of hotspots along the coast. In a second phase, these sensitive areas will be further analyzed by using detailed process-oriented models such as XBeach to properly define these hotspots based on a more precise assessment of the hazard magnitude.

Regarding *coastal flooding*, different variables and processes have been included to characterize the overall hazard. The first considered source of hazard is the total water level where in addition to the *storm-surge* (which is usually given as data) we add the wave-induced component, i.e. the *runup*. This water level is then converted to associated hazards by accounting its consequences in terms of potential of inundation. This is done by assessing the magnitude of the floodwater volume entering the hinterland by means of two variables: *overwash* extension and *overtopping* discharge rates. The first one is characterized by the horizontal reach of the flooding event whereas the second one is characterized by means of a discharge rate which can be converted into a total floodwater volume which could be used as an input for more detailed inundation model. Finally, *inundation* is assessed by estimating the maximum potential land surface to be inundated. In this module we adopt the bathtub approach to delineate the maximum potential extension of this hazard along the coast by using the previously calculated total water level. Although this approach implicitly assumes that the storm duration is long enough to supply the required water volume to inundate such area, this approach allow the identification of sensitive areas to inundation in the first phase. They will be later analyzed in detail by using the process-oriented models in the second phase.

Regarding the assessment of the magnitude of the *coastal erosion hazard*, we have included two processes to characterize the overall hazard. The first one is, properly, *beach and dune erosion*. To this end, different simple parametric models are proposed to quantify the magnitude of the expected response of the impact of the storm on a sedimentary coast. The second one is *barrier breaching* and, in this case, a simple method assessing the susceptibility to suffer this hazard in a sandy barrier is proposed.

The assessment of the magnitude of these hazards will be revisited in the second phase of application, where in those areas identified as potential hotspots, we shall use detailed *process-oriented models* such as XBeach. This will permit to accurately quantify them in an optimized manner, since the model will be run for a large number of events (again to characterize the hazards in probabilistic terms) but just focusing on selected sensitive areas.

With respect to *flash-flood hazard*, we propose a simple method in which by combining basic and relevant variables characterizing the coast and the rainfall climate we identify which basins or sub-basins are susceptible to experience flash-floods, i.e. to be characterized as hotspots. These hotspots can be further analyzed by using quantitative methods such as the flash-flood model adapted in WP3 to be used in the FEWS (see deliverable D3.2, Roelvink et al. 2015).

In order to assess future storm-induced coastal hazards, we also propose a method to account for potential *long-term climate change effects*. This methodology mainly focuses on the assessment of indirect effects, i.e. changes on the hazard due to induced changes in the coastal system state (e.g. SLR induced erosion and inundation). This is because the inclusion of a potential CC-change in storminess will be straightforward since it will only imply to reassess the hazards by changing the forcing (e.g. wave and water level climates).

This Hazard Assessment Module is composed by a series of models that have previously been used and validated in different coasts worldwide. In spite of this , and as it occurs with all models, even the process-oriented ones, their application in a specific case requires to check its validity under local conditions.

A clear and simple example of this is the application of a simple predictive model to assess the magnitude of wave-induced runup in beaches. Here we have included 3 different models which predict different runup values for same wave conditions. If all models were good enough to predict runup at a given site, all of them had to predict the same result when fed by the same forcing conditions. Thus, before applying the module, it is the responsibility of each site to select the most proper one for the study site.

On the other end of complexity, within this Module, it is also envisaged to use the process-oriented model XBeach 1D. This model has been calibrated and validated in numerous sites and, recommended default values for most of coefficients have been provided. However, to produce reliable estimations of storm-induced hazards in a givens site, a specific calibration/validation should be required.

Due to this, to apply the Coastal Hazard Assessment Module in the RISC-KIT study sites in particular, and in any coastal site in general, a specific calibration/validation for local conditions has to be done. In some cases, this implies to select the best model to be used according to local characteristics (for those processes where more than one option is available). In other cases, this implies to look for the best set of coefficients to be used for local conditions (calibration/validation) of the model. Due to the range of different conditions to be analyzed within the Risc-kit project, this process will specifically be done for each study site in WP 5 (Application on case study sites).

1.5 Outline of the report

The following structure has been adopted in this report: (i) chapter 2 presents the general framework of the Hazard Assessment Module; (ii) chapter 3 covers the coastal flooding hazard and associated processes (runup, overwash, overtopping and inundation); (iii) chapter 4 covers the erosion hazard using structural functions based parametric models; (iv) chapter 5 covers the barrier breaching hazard; (v) chapter 6 presents a modulation of calculated hazards for the case of coasts protected by detached breakwaters; (vi) chapter 7 presents the XBeach 1D model to be used to

accurately quantify erosion and inundation hazards once hotspots had been identified; (vii) chapter 8 covers the flash flood hazard assessment; (viii) chapter 9 deals with the long-term variation of estimated hazards due to climate change; (ix) chapter 10 recommends how to select data and apply the Coastal Hazard Assessment Module at regional scale and (x) chapter 11 list all references used in this report.

2 General framework

2.1 Introduction

This chapter presents an overview of the general structure of the Coastal Hazard Assessment Module. As it was previously mentioned, storm-induced hazards will be described in probabilistic terms. This will permit to identify for a given probability of occurrence (selected by the stakeholder depending on the target safety level) which are the most sensitive areas along the coast, which are designated as hotspots. Section 2.2 introduces the concept of extreme events and discusses how to select the probability of occurrence of the hazards to be considered in the analysis. Section 2.3 presents the adopted approach to characterize the probabilistic description of the considered hazards. Section 2.4 briefly summarizes main characteristics of the study sites in terms of considered storm-induced processes and resulting hazards. Finally, section 2.5 presents the proposed general framework to assess the magnitude of storm-induced coastal hazards at the regional scale.

2.2 Extreme events

The main objective of the Coastal Hazard Assessment Module is to assess the magnitude of hazards induced by the impact of *extreme* hydro-meteorological events in the coastal zone. Thus, by using the Coastal Hazard Assessment module we shall be able to map hazard intensities along the coast associated with given *probabilities* specified by stakeholders according to the target safety level. Within this context, it is relevant to discuss what we understand by extreme event and how to select relevant probabilities of occurrence for the analysis.

There is not a unique way to define what an extreme event is and, usually, the concept of extremeness strongly depends on the context (Stephenson, 2008). In a simple way, an extreme event can be defined as an event having extreme values of hydro-meteorological variables. It is generally defined as that value exceeding some threshold. They are generally rare (low probability of occurrence), and for our main purposes they can be considered as having potential to cause damage.

In any case, extreme events can be defined and/or quantified based on (e.g. Beniston and Stephenson, 2004):

- How rare they are, which involve notions of frequency of occurrence.
- How intense they are, which involves notions of threshold of exceedance.
- The impacts they exert (e.g. in social, economic and/or environmental terms).

Within the context of this work, it is clear that an extreme event should be able to cause morphological and/or socio-economic consequences. While at a given study area that will occur for small return periods[1] (e.g. few years), at another study area (e.g., protected/armored) that will probably occur at longer return periods (100 years or more). The definition of the extreme event is, therefore, site dependent.

[1] The *return period* is the estimated time interval between events of of a similar intensity. The event associated with a return period *Tr* is the event that has a 1/*Tr* chance of being exceeded in any given year.

With respect to the selection of probabilities to be considered in the analysis one possibility is, in spite of this site dependency, to analyze common probabilities of exceedance. This is the approach adopted in the EU Floods Directive (EC, 2007), which specifies that flood hazard maps and flood risk maps will identify areas with a medium likelihood of flooding (at least 1 in 100 year event) and extremes or low likelihood events. The application of the Floods Directive in Catalonia (Spain) to fluvial inundation risk mapping has been done for 3 return periods (*Tr* = 10, 100 and 500 years), whereas for coastal inundation risk mapping included *Tr* of 100 and 500 years (ACA, 2014). For the Belgian coast a similar approach was used. EU Floods Directive reporting was done for return periods 10, 100 and 1000 year. Additionally, a return period of 4000 year was used because the existing protection level at some locations is already high.

An alternative approach is to assess the most used and relevant return periods for coastal management purposes at each site. For areas with coastal management plans that consistently consider a maximum return period of 50 years, there is probably no point on defining a coastal index hazard for 1000 years. The reverse is also true. Therefore, the coastal management life-span of each area should be taken into consideration when choosing the appropriate return periods for hotspot identification. Also, the perception of risk varies in each study area (Martinez et al. 2004) and, these differences need to be considered to select return periods relevant for local stakeholders.

A possible approach to select the *Tr* to be used in the analysis is based on the use of the concept of *lifetime* or *design life* of a coastal structure. In this case, we are considering the beach as a coastal protection measure protecting the hinterland against the impact of a storm. Here the *lifetime* is the period over which the beach is expected to continue providing protection against the "design" condition, which in this case corresponds to the target storm (see e.g. Reeve, 2010). With this, we can make use of the relationship predicting the probability of exceedance, *P*, as a function of the lifetime, *L*, and the return period,

$$P = 1 - \left(1 - \frac{1}{Tr}\right)^{L} \qquad (2.1)$$

To select appropriated or relevant *Tr* values, we can fix *L* as the desired minimum lifetime of the beach and *P* as the accepted probability of occurrence of the event within such lifetime as a function of the importance of the site (Figure 2.1).

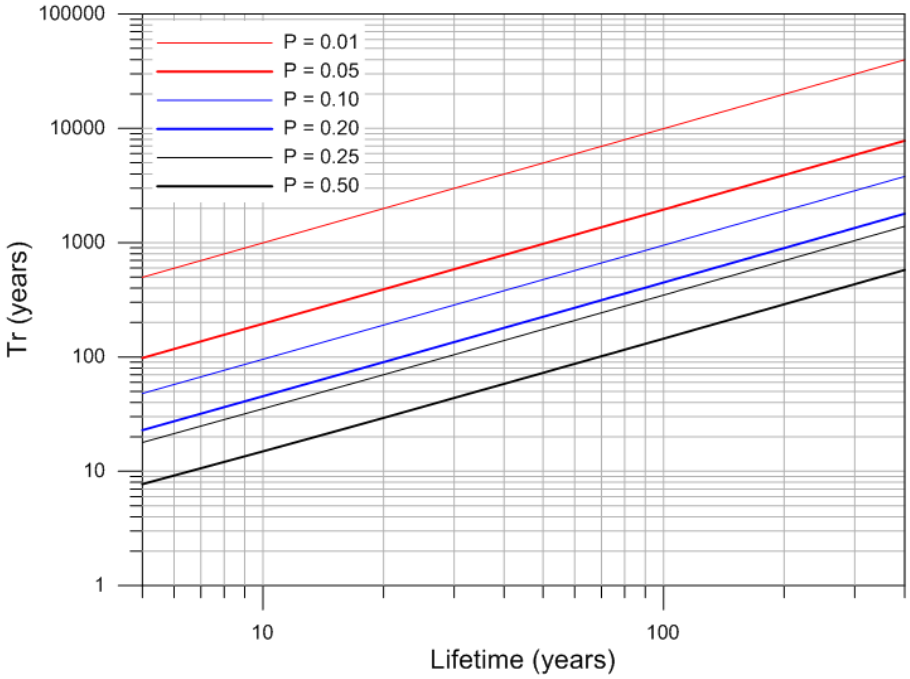

Figure 2-1: Event return period (Tr) for given probabilities of exceedance (P) within given lifetimes (L).

As rule-of-thumb as higher the importance (e.g. in economic, environmental and/or social-cultural terms) of the hinterland is, the lower the accepted probability of a hazard will be. This means, for instance, that for high (economic, social and/or environmental) interest areas where the exceedance of the protection capacity provided by the beach against the storm (inundation and/or erosion) should induce significant consequences, relative long lifetime and low probabilities of exceedance should be adopted.

From the practical standpoint, the selection of the lifetime and the accepted probability of exceedance determines the return periods for the events to be analyzed.

The first one, the *lifetime*, will make reference in the context of the objective of CRAF to the expected time horizon of the analysis. In other words, if we are analyzing the risk to coastal storms in a given coast, how long we assume that the coast is providing the current protection level? A conservative answer should be that we want to do the analysis for a very long time period. However, we have to consider that sedimentary coasts are usually subjected to coastal processes affecting their stability and, in consequence, the current beach configuration (and the corresponding level of provided protection) is not likely to be steady (in fact, the most probable situation is that the coastal configuration will change). On the other hand, if we assume that the beach is behaving like a coastal protection measure, we can make an analogy with usual lifetimes for such works. As an example, the Spanish Ministry of Public Works in their recommendations for procedures of design maritime structures (Puertos del Estado, 2001) proposes some values that could be used in this application, which have been selected as a function of the importance of expected consequences (Table 2-1).

Table 2-1: Recommended minimum lifetime for coastal protection works (Puertos del Estado, 2001).

Type of work	Importance	Minimum lifetime (years)
Defense against big floods*	High	50
Margins protection and defense	Medium	25
Beach nourishment and protection	Low	15

* It refers to defense works that in the case of failure may cause an important inundation of the hinterland.

The second one, the *probability of exceedance*, is also dependent on the importance of the implications of the hazard. Table 2-2 shows some recommended values of maximum allowable probabilities of failure for coastal protection works as a function of the (social, economic and/or environmental) consequences.

Table 2-2: Recommended maximum values of failure probability for coastal protection works as a function of their importance (Puertos del Estado, 2001).

Importance	Maximum probability
Very High	0.0001
High	0.01
Medium	0.10
Low	0.20

2.3 Response vs event approaches

When assessing the magnitude of the hazards associated with the impact of an event of a given probability of occurrence, one of the points introducing uncertainty to the analysis is the assignment of the probability of occurrence. In hazard analysis in general and, in coastal flooding in particular, two main approaches exist, commonly known as the event and response methods (Garrity et al. 2006).

The ***event approach*** is a kind of deterministic methodology, where the starting point is determined by the extreme probability distribution of wave heights and storm surges, plus some empirical relationships between other storm parameters of interest, such as wave period and storm duration *vs.* significant wave height. This method is mainly employed when the existing information for hazard analysis consists of pre-analyzed forcing (wave and water level) information that is provided without access to the original time series.

Once the probability of occurrence of the event is selected, wave height and storm surge are obtained from the corresponding extreme distributions, and the remaining parameters required to fully characterize the event are calculated by using the

available deterministic relations (Figure 2-2). However, with this approach, each wave height is associated with just one value of other storm parameters, such as wave period and storm duration, which implies the loss of significant information about the natural variability of the process (e.g. Sánchez-Arcilla et al. 2009). Once the event associated to a given probability has been defined, the different hazard parameters (to characterize flooding and/or erosion) are calculated and associated with the corresponding probability of occurrence.

In the ***response approach***, the entire original wave and water level time series are used to establish the hazard (flooding and/or erosion) parameters of interest, such as runup, total water level, overtopping, eroded volume. Due to the nature of the analyzed problem, different combinations of wave conditions (events) will result in similar hazard conditions, and in order to properly assign a probability to such a response, it is necessary to jointly consider all possible options. A probability distribution of extremes is then fitted to the obtained dataset (Figure 2-2), that represents the entire variability of a given hazard for all tested conditions. From here, the hazard parameter of interest (associated with a given probability) will be directly calculated from its probability distribution. This method is especially recommendable when wave variables during storms (e.g., H_s, T_p and duration) which are determining the magnitude of the hazard of interest are poorly or partially correlated. It is also recommended by the FEMA guidelines for flooding studies (Divoky and McDougal, 2006).

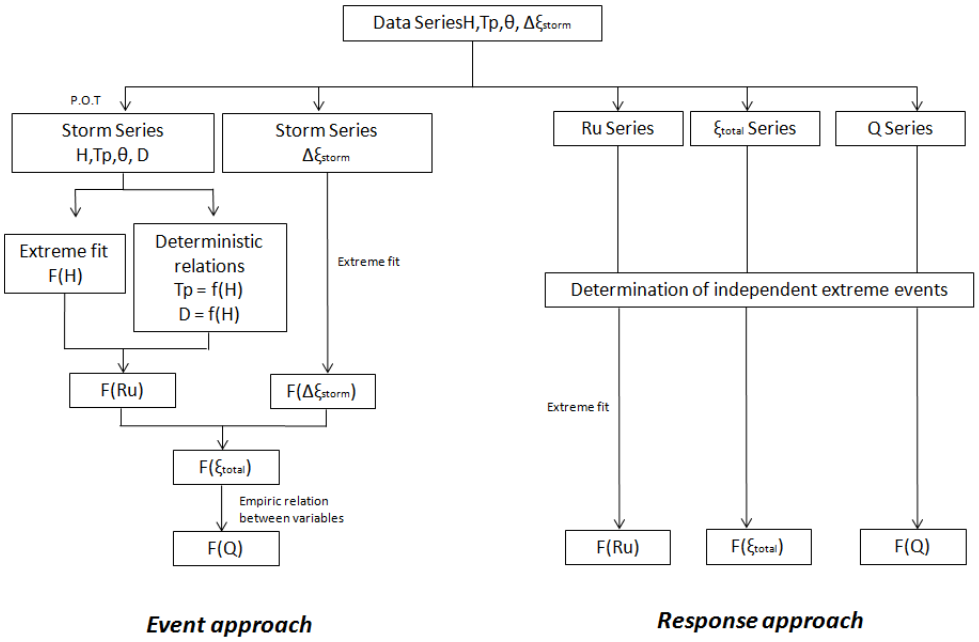

Figure 2-2: Event and response approaches to assess the probabilistic distribution of a given hazard. Example for inundation analysis (Sanuy et al. in review).

While analyzing storm-induced erosion, Callaghan et al. (2008, 2013) presented 4 different methods for determining extreme value beach erosion that could also be applicable to flood analysis or to assess the impact of a coastal storm in general. They are, in essence, different variations of the here denominated response approach. The

simplest one consists of fitting a probability distribution directly to the existing measurements of the process of interest (erosion and/or flooding). Although being the "most realistic approach", it should only be applicable when long term series of measurements do exist. One example of application should be when analyzing coastal inundation by storm surges when long-term water level records do exist. However, for some applications as e.g. the analysis of storm-induced erosion, this should not likely be the case, measurements are substituted by simulations, which are the basis for the other methods. The other proposed methods essentially consist of simulating a given hazard for a large set of forcing (hydro-meteo) conditions to be later fitted by a probability distribution, with the main difference among them given by the way of dealing with forcing (wave and water level) data.

In this project, we shall mainly follow the response approach to assess the magnitude of hazards at regional scale. This implies to obtain for selected locations along the coast the probability distribution of relevant storm-induced hazards (e.g. inundation, erosion) by building hazard time series to be later subjected to extreme analysis.

2.4 Processes and Hazards

When an extreme storm impacts on sandy coasts, it produces different morphodynamic responses which rapidly and significantly modify the coastal landscape. Induced processes and changes are controlled by a combination of different factors that essentially are storm characteristics and the coastal geomorphology (e.g., Morton, 2002; Morton and Sallenger, 2003). As these processes are potentially harmful for coastal stability and they should affect existing uses and resources in the coastal zone, they are usually considered as hazards.

The hazards to be studied in a given coastal zone will depend on the local coastal characteristics which will determine processes taking place during storm impacts. Table 2-3 summarizes the identified representative hazards for each of the RISCKIT study sites (Figure 1-2) and the corresponding storm-induced processes. As it can be seen, although apparently there is a relatively large variability in reported induced processes, they can be grouped in the following main hazard types: marine flooding (MF), erosion (E) and flash flood (FF). It has to be highlighted that, for the purposes of this report, we have grouped under flooding/inundation hazards all hazards related to variations in sea water level involving the temporary inundation of the coast at any degree. The lowest level correspond to overtopping and overwash hazards which essentially act on the most external fringe. On the other hand, the inundation hazard specifically refers to the inundation of a relative large portion of the coastal fringe due to an increased water level as a combination of storm-surge and wave-induced runup.

Thus, within this report we shall focus on how to characterize the following processes to assess storm-induced hazards in the RISCKIT sites:

- Marine flooding-inundation: runup, surge and total water level, overwash, overtopping and inundation.
- Erosion: beach erosion and barrier breaching.
- Flash flood .

Table 2-3: Processes and hazards acting on each of the study sites at regional scale (MF: marine flooding, E: erosion, FF: flash flood).

Site	Geomorphologic setting	Hazards	Processes (regional scale)
La Faute sur Mer, FR	Estuary behind sand barrier.	MF, E	[1] Beach erosion [2] Dune erosion/breaching [4] Runup/Overtopping [5] Storm surge
Ria Formosa, PT	Coastal lagoon with barrier islands.	MF, E	[1] Beach Erosion [2] Dune Erosion [3] Barrier breaching [4] Runup/overwash
Tordera delta, ES	Deltaic sandy shoreline. Sandy beaches. Rubble mound revetments.	MF, E, FF	[1] Beach erosion [4] Runup/Overtopping [6] Flash floods
Bocca di Magra, IT	Small catchments. Pocket bays.	MF, E, FF	[1] Beach erosion [4] Runup/ Overtopping [6] Flash flood
Porto Garibaldi, IT	Navigation inlet on urban coast.	MF, E	[1] Beach erosion [2] Dune erosion [4] Runup/overtopping
Varna, BG	Open Bay, Lake.	MF, E	[1] Beach erosion [4] Runup/ Overtopping
Kristianstad & Åhus, SE	Lowland river valley. Wetlands. Dunes.	MF, E	[1] Beach erosion [2] Dune erosion [4] Run-up [5] Storm surge [6] Flooding
Kiel Fjord, DE	Fjord. Bay.	MF, E	[1] Beach erosion [4] Runup/ Overtopping
North Norfolk, UK	Barrier islands. Saltmarshes.	MF, E	[1] Beach erosion [2] Dune erosion [3] Barrier breaching [4] Run-up/overtopping [5] Storm surge
Zeebrugge, BE	Large port urban. Beach.	MF, E	[2] Dune erosion [4] Runup/ Overtopping [7] Extreme wind speeds
Sandwip, BD	Island in the GBM. Delta.	MF	[5] Storm surge

2.5 Assessment framework

Figure 2-3 shows the proposed framework for the assessment of storm-induced hazards within the RISC-KIT project. The assessment is designed to be generally applied in two phases or steps:

- A first phase (identification of hotspots) in which the magnitude of the induced hazards (erosion and inundation related ones) is calculated by using simple models at regional scale. This will permit to make a first identification of sensitive areas along the coast to the impact of extreme events. This selection will be based on the frequency and intensity of the induced impacts in geomorphic terms.
- A second phase (hotspot selection), where the XBeach advanced model is applied in identified sensitive stretches to better (more accurately) quantify the magnitude of storm-induced hazards.

This two-phase approach has been selected to optimize the number of computations to be done as a compromise between accuracy and complexity. The application of the framework at a regional scale implies to cover a large extension of the coast (in the order of 100 km) which is schematized by sectors of about 1 km length which are represented by means of a beach profile. Moreover, the adoption of a probabilistic approach implies to use long-term forcing data time series (in the order of several decades) which may result in a number of modeled events in the order of several hundreds. The use of a detailed model for a combination of hundreds of beach profiles with hundreds of events will not be necessarily more efficient, especially taken into account that the objective of the framework is not to model in detail the beach response under specific storm conditions but to identify coastal hot spots.

As it can be seen in Figure 2-3 the Coastal Hazard Assessment Module is composed by different units:

- **Data input**, where data about coastal geomorphology and forcing (e.g. wave and water levels) are selected and used to characterize the extreme event forcing and the coast in the study site.
- **Hazard assessment**, where the magnitude of storm-induced hazards (e.g. erosion, inundation) is calculated in probabilistic terms.
- **Identification of geomorphic sensitive areas** to be later analyzed in the second phase.
- **Transfer of identified coastal hazards to the hinterland** by mapping their extension and intensity. This final stage is the link with the vulnerability module to integrate their induced socio-economic consequences to identify coastal hotspots. This part is included in the CRAF module.

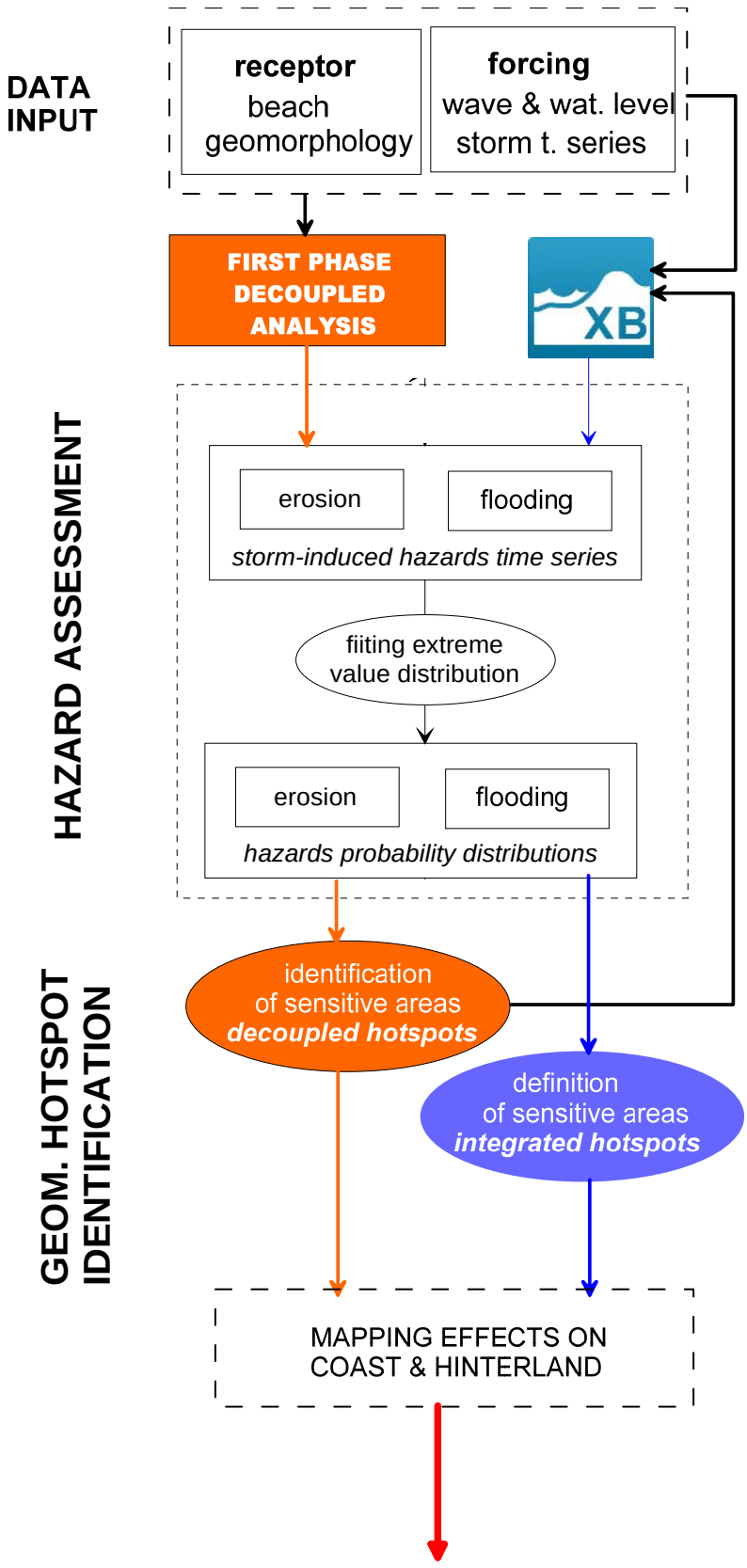

Figure 2-3: General Storm-induced Hazard Assessment Module. Flooding and erosion are the generic names used to designate a series of related hazards.

3 Flooding

3.1 Introduction

Coastal flooding is generally caused by a combination of high water levels (storm surges plus high tides) and wave action, and in consequence, a joint probability analysis of storm surges and wave run-up should be needed to properly characterize the total water level in probabilistic terms. The total water level at the shoreline, ξ_t, is composed by different contributions (Figure 3-1),

$$\xi_t = MSL + \xi_a + \xi_m + Ru \tag{3.1}$$

where MSL is the mean sea level; ξ_a, is the astronomical tide; ξ_m, is the meteorological tide or storm-surge and Ru is the wave runup (including both the wave setup and swash oscillations).

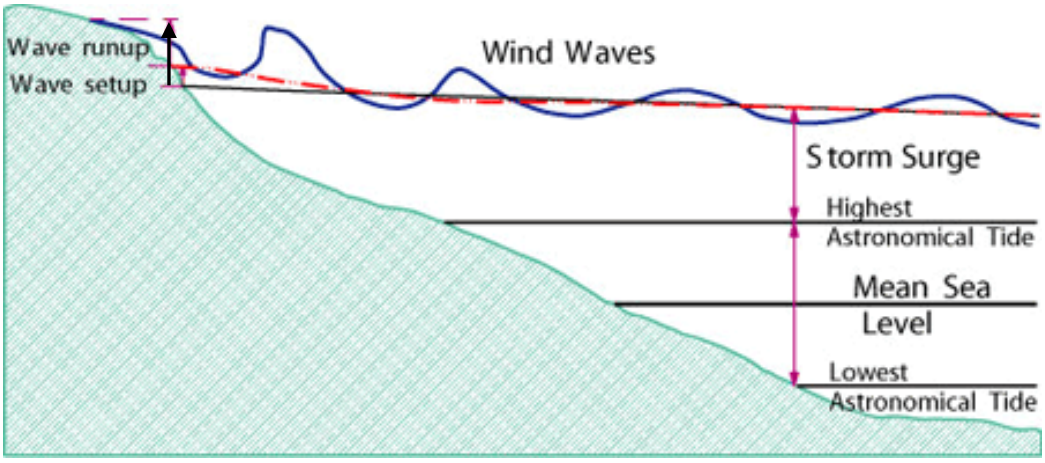

Figure 3-1: Components of total water level at the shoreline (www.ozcoasts.gov.au). (Note that storm surge can take place at any phase of the astronomical tide and, not necessarily from HAT as figure seems to suggest).

To properly assess the magnitude of flooding hazard different variables and processes will be characterized.

First, the main source of the hazard has to be characterized, i.e. the total water level. In open coasts/beaches, to determine the value of (3.1), we can assume that MSL and ξ_a, ξ_m is (or can be) extracted from measured/modelled time series and, the remaining part, the wave-induced runup, Ru, is the one to be calculated within the Coastal Assessment Hazard Module for a given wave climate scenario.

If the total water level exceeds the height of the beach or the structure, the hinterland will receive a given amount of floodwater and, in consequence, it will be flooded. This water level is then converted to associated hazards by assessing the magnitude of the floodwater volume entering the hinterland by means of two variables: *overwash* extension and *overtopping* discharge rates. The first one is characterized by the

horizontal reach of the flooding event whereas the second one, it is characterized by means of a discharge rate which can be converted into a total floodwater volume which could be used as an input for more detailed inundation model.

The worst condition will be given by an *inundation* extent of all the area connected to the sea with an elevation below the total water level. However, this would only occur in the case that such water level would remain in place for a time long enough to ensure that the required volume of water to fill such basin (coastal topography till the considered level) would flow towards the hinterland during the storm duration. In this module we adopt the bathtub approach to delineate the maximum potential extension of this hazard along the coast by using the previously calculated total water level.

In many situations, this bathtub approach is seldom realistic to properly determine the real extent of the area to be flooded under coastal storms. Thus, the affected area will depend on the real floodwater volume entering the hinterland during storm and, in consequence, in addition to runup values, associated overtopping volumes should also be computed. Thus, to delineate the final extension of the surface to be potentially flooded values obtained using the bathtub approach will be later compared with overwash extension values in those cases where wave-induced runup is dominant. In any case, identified sensitive areas will be later analyzed in detail by using the process-oriented models in the second phase.

3.2 Wave runup

3.2.1 Generalities

Wave-induced runup is defined as the height above the still water level (including wave set-up) reached by swash at the shoreline (Figure 3-1). It will serve to define which will be the **potential maximum elevation** of the water level at the shoreline during the event of interest.

In the simplest way, its assessment is usually done by applying empirical-derived models, which will predict its magnitude as a function of wave conditions (H and T; usually given as deepwater values). There are numerous formulas to predict it, most of them derived in laboratory experiments for fixed beds and/or, specifically, sloping structures (e.g. Burcharth and Hughes, 2011; Pullen et al. 2007).

For the use on open sedimentary coasts, there are a number of models that have been derived or specifically calibrated to be applied to beaches. They have been built by analysing laboratory and/or field measurements of beach runup under different conditions and, in this sense, they should be representative of expected conditions in most of RISC-KIT case studies.

One of the problems of having different models is that when they are applied to the same field conditions, they usually produce different estimations of maximum runup. The key question, therefore, is which is the best model to use to estimate extreme beach runup? This question has been analyzed by different authors by making specific validation exercises in which different models have been compared against runup data.

Roberts et al. (2010) analyzed data obtained in a large wave flume against different runup formulas. They concluded that for the analyzed data the best predictor for irregular runup was simply the significant wave height at breaking. The exception to

this general rule was found for profiles with a dune or a scarp, where the swash is limited by this topographic break.

Mather et al. (2011) also compared different runup formulas against field data gathered in South Africa. They found that the best tested models were Stockdon et al. (2006) and a new empiric model they presented (and derived from their data).

Shand et al. (2011) compared different runup models with data gathered in New Zealand and Australia beaches. They concluded that for predicting extreme runup on sandy beaches using the upper beach slope, the Mase (1989) and Hedge and Mase (2004) were the most accurate models.

Vousdoukas et al. (2012) also analyzed the performance of different runup models to predict runup in different beach profiles at Faro (South Portugal). They obtained a best-fit parametric model and, also found that runup predictions improved when wind speed and tidal elevations were included in the parameterizations.

Matias et al. (2012) analysed a large set of wave runup predictors and estimated their applicability for gravel barriers. The authors considered that the formula produced by Stockdon et al. (2006) was the best predictor of runup conditions.

3.2.2 Runup in beaches

For the use in open sedimentary coasts, we have made a preliminary selection of the runup models most used in beaches. The choice of the proper model to be used in each study site will be based on previous experience on the assessment of runup in the study area. In the case of no previous local experience, the use of selected models will permit to bound the expected runup magnitude within a reasonable "confidence band".

The first selected model is the one proposed by Stockdon et al. (2006) which has specifically been derived to be applied in beaches. This empirical model has been built by analysing a large data set of field measurements under different conditions. This model has been (and it is) extensively used to estimate runup on beaches under real field conditions, although other beach models are available and have also been used (e.g. Mather et al. 2011). The Stockdon model predicts the runup magnitude, $Ru_{2\%}$, as:

$$Ru_{2\%} = 1.1\left(0.35\tan\beta\,(Hs\,Lo)^{1/2} + \frac{\left[Hs\,Lo\,(0.563\tan\beta^2 + 0.004)\right]^{1/2}}{2}\right) \tag{3.2}$$

and, under extremely dissipative conditions ($\xi o < 0.3$) by:

$$Ru_{2\%} = 0.043\,(Hs\,Lo)^{1/2} \tag{3.3}$$

where H_s is the deepwater significant wave height, Lo is the deepwater wave length associated to the wave peak period, Tp, and $tan\ \beta$ is the beachface slope and ξ is the Iribarren number, which is given by:

$$\xi = \frac{\tan\beta}{\sqrt{Hs/Lo}} \tag{3.4}$$

Although the Stockdon model is, at present, one of the most used in beaches worldwide, some authors have reported underprediction of observed runup (e.g. Laudier et al., 2006; Almeida et al. 2012). Due to this, other runup models can potentially be considered for the RISC-KIT case study sites. Thus, two additional runup models are also included here as alternatives, the Holman (1986) and the Nielsen and Hanslow (1991) models.

The Holman (1986) model predicts the runup magnitude, $Ru_{2\%}$, as:

$$Ru_{2\%} = Hs\left(0.83\xi + 0.2\right) \tag{3.5}$$

The Nielsen and Hanslow (1991) model predicts the runup magnitude, $Ru_{2\%}$, as

$$Ru_{2\%} = 1.98 Lzwm \tag{3.6}$$

where,

$$Lzwm = 0.60\sqrt{H_{orms} Lo}\tan\beta \qquad \text{for } \tan\beta > 0.1 \tag{3.7}$$

$$Lzwm = 0.05\sqrt{H_{0rms} Lo} \qquad \text{for } \tan\beta \le 0.1 \tag{3.8}$$

3.2.3 Runup in artificial slopes

Although most of the coasts to be covered in the project are sedimentary ones, some stretches are composed by artificial slopes (dikes and/or revetments) and, therefore, we have also included here a runup model to be applied in this kind of environments.

For rock or rough slopes the 2% mean run-up prediction value can be described by (EurOtop; Pullen et al. 2007):

$$\frac{Ru_{2\%}}{Hs} = 1.65 \cdot \gamma_b \cdot \gamma_f \cdot \gamma_\beta \cdot \xi \tag{3.9}$$

with a maximum of,

$$\frac{Ru_{2\%}}{Hs} = 1.00 \cdot \gamma_b \cdot \gamma_{f\ surging} \cdot \gamma_\beta \cdot \left(4.0 - \frac{1.5}{\sqrt{\xi}}\right)$$

The *surface roughness parameter* γ_f describes the influence of the kind of revetment existing on the beach slope. The value of γ_f for typical elements is shown in Table 3-1 for coastal dikes and embankment seawalls and Table 3-2 for rubble mound structures.

From ξ = 1.8 the roughness factor $\gamma_{f\ surging}$ increases linearly up to 1 (when ξ = 10) as:

$$\gamma_{f\ surging} = \gamma_f + (\xi - 1.8) * (1 - \gamma_f)/8.2 \tag{3.10}$$

$$\gamma_{f\ surging} = 1.0 \ \ for \ \ \xi > 10$$

Table 3-1: Surface roughness factors for typical elements in coastal dikes and embankment seawalls (Pullen et al. 2007).

Reference type	γ_f
Concrete	1.0
Asphalt	1.0
Closed concrete blocks	1.0
Grass	1.0
Basalt	0.90
Small blocks over 1/25 of surface	0.85
Small blocks over 1/9 of surface	0.80
¼ of stone setting 10 cm higher	0.90
Ribs (optimum dimensions)	0.75

Table 3-2: Surface roughness factors for permeable rubble mound structures with slopes of 1:15. Values in italics are estimated / extrapolated (Pullen et al. 2007).

Type of armour layer	γ_f
Smooth impermeable surface	1.00
Rocks (1 layer, impermeable core)	0.60
Rocks (1 layer, permeable core)	0.45
Rocks (2 layers, impermeable core)	0.55
Rocks (2 layers, permeable core)	0.40
Cubes (1 layer, random positioning)	0.50
Cubes (2 layers, random positioning)	0.47
Antifers	0.47
HARO's	0.47
Accropode™	0.46
Xbloc®	0.45
CORE-LOC®	0.44
Tetrapods	0.38
Dolosse	*0.43*

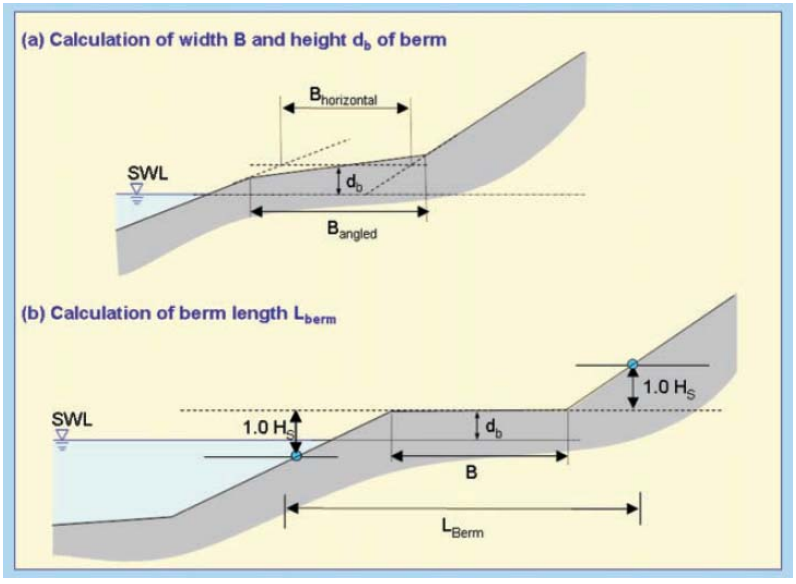

Figure 3-2: Determination of the characteristic berm length for γ_b (Pullen et al. 2007).

The *berm influence factor* γ_b describes the influence of the presence of a berm in the slope (Figure 3-2) and it can be calculated as:

$$\gamma_b = 1 - r_b\,(1 - r_{db}) \quad 0.6 < \gamma_b < 1.0 \tag{3.11}$$

where r_b stands for the width of the berm:

$$r_b = \frac{B}{L_{berm}} \tag{3.12}$$

Being B the berm width and L_{berm} the berm length (Figure 3-2), and r_{db} stands for the vertical difference between the still water level (SWL) and the middle of the berm (d_b):

$$r_{db} = 0.5 - 0.5\cos\left(\pi \frac{db}{Ru_{2\%}}\right) \quad \text{for a berm above still water level} \tag{3.13}$$

$$r_{db} = 0.5 - 0.5\cos\left(\pi \frac{db}{2 \cdot Hs}\right) \quad \text{for a berm below still water level} \tag{3.14}$$

For a permeable core a maximum is reached for $Ru_{2\%}/Hs = 1.97$.

The *influence factor of wave direction* γ_β, which describes the influence of the angle of wave attack β (see Figure 3-3), is given by:

$$\gamma_\beta = 1 - 0.0022|\beta| \;\; for \;\; 0 < |\beta| \leq 80$$

$$\gamma_\beta = 0.824 \;\; for \;\; |\beta| > 80 \tag{3.15}$$

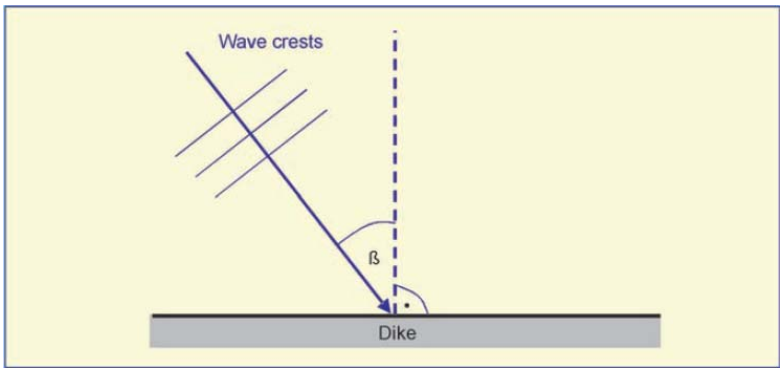

Figure 3-3: Definition of angle of wave attack β (Pullen et al. 2007).

In most of the cases, this correction factor will be very close to 1 and, in practice, this reduction factor can be neglected for wave directions less than 20°, which is a reasonable value for wave angles at the coast after refraction with the exception of areas where storm waves have a large obliquity with respect to the shoreline.

3.2.4 Example of application

In order to calculate the wave-induced runup in any of the RISC-KIT case study sites, the following data are required: *Hs* and *Tp* (deepwater values) and the beachface slope (tan β) or revetment configuration (slope, berm dimensions, roughness, etc).

The procedure to apply the tool is as follows:

1. Select the *conditions for application* by using two main criteria: (i) wave climate and (ii) beach representative profiles. The first one will be determined by the existing wave time series (measured or hindcast), representative of the local wave climate which will be used as input wave data. Ideally, wave time series should be long enough to produce a representative hazard time series that will be fitted to an extreme probability distribution (i.e. time series in the order of 20 years long). The second one will be determined by the values of the local beach slope, tan β, or revetment configuration representative of the site which will be used as input beach data. To take into account potential spatial variability in beach configurations, beach profiles at a given spacing along the beach should be taken to properly characterize the variability of required parameters (e.g. slope, berm height) (see chapter 10).
2. Select the *runup model* to be used and input the selected wave time series and beach configuration to obtain the corresponding $Ru_{2\%}$ time series. Ideally, the chosen model should be the one providing the "best fit" for local *Ru* measured episodes, and therefore should have been previously validated (whenever possible). In case these measurements are not available, the use of the different models will permit to bound the run up value within a reasonable confidence band. The conservative option should be to choose the model predicting the highest *Ru* values for a given return period.
3. Once the $Ru_{2\%}$ time series has been obtained, the *probability distribution of the water level* at the shoreline will be obtained. Here there are two possibilities depending on the kind of data available and the significance of surge in the study site:

   (i) to directly use the calculated $Ru_{2\%}$ time series to obtain the extreme probability distribution in the case that surge is not significant in the study area and/or there aren`t any data of simultaneous storm surge;
   (ii) to combine (add) the calculated $Ru_{2\%}$ time series with simultaneous surge data, $\xi_{m,}$ to obtain the total water level time series. This will be used to obtain the extreme probability distribution and it should be the "most accurate" way to proceed in case all needed data are available. Surge data can also be substituted by modelled ones when relevant (absence of data and/or hindcast time series).

To obtain the extreme probability distribution of the total water level at the shoreline, the following procedure is recommended:

1. First, maximum events of total water level are identified by using the Peak-Over-Threshold (POT) method with the threshold value being locally defined as a function of the calculated time series. To do this, we propose to use a significant enough quantile of the water level cumulative distribution (for NW

Mediterranean conditions the 99.5% quantile was used obtaining an average of about 3 storm events per year, but the value of the quantile to be used should be selected according to the local conditions for each study site). In order to ensure significance level and independence between extreme events a minimum duration and minimum time separation between events must be set (e.g. in the enclosed example in the NW Mediterranean coast, a 6 h minimum duration and 72 h minimum separation for extreme runup events have been selected, which are consistent with the local storm definition, Mendoza et al. 2011).

2. Second, the extreme probability distribution of the so-obtained maximum values is modelled using the Generalized Pareto Distribution (GPD) which is a family of extreme distributions comprising other extreme models such as the Weibull distribution and the Gumbel distribution.

Figure 3-4 shows the probabilistic distribution of runup in the Tordera delta (RISC-KIT case study in the Catalan coast) characterized through the runup magnitude calculated by using 3 proposed runup models for beaches. In this case, the hazard has been characterized by using as input data a 44-year hindcast wave time series (Hipocas data) whereas the local beach has been represented by means of a reflective beach profile (the used representative slope for computations was 0.14).

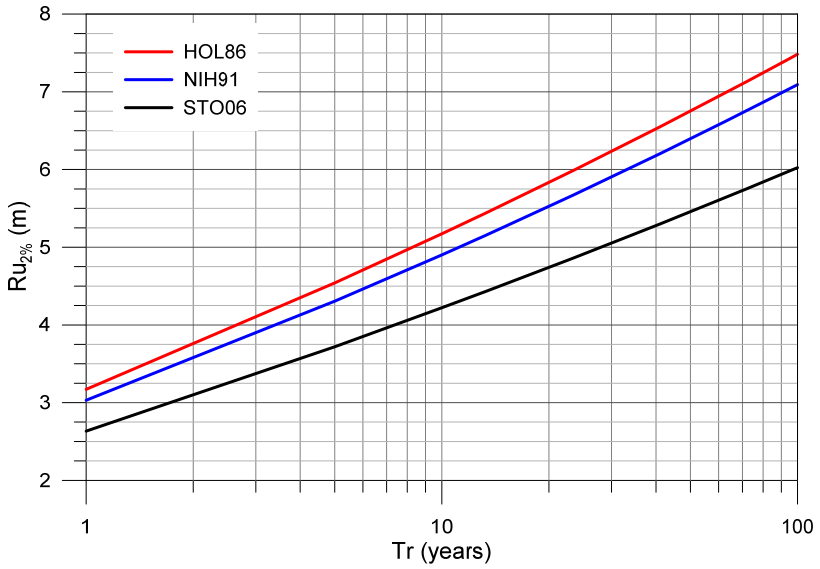

Figure 3-4: Extreme probability distribution of Ru2% at the Tordera delta using different runup models for beaches (HOL86, NIH91,STO06).

As it can be seen, the runup estimations for these reflective beach conditions are bounded within a maximum value given by the Holman (1986) model and a minimum one given by applying Stockdon et al. (2006). Table 3-3 shows the obtained values for selected return periods where the practical implications of selecting a given model can be easily identified.

Table 3-3: Runup values (m) associated to selected return periods calculated for the Tordera delta area using different runup models.

Tr (y)	HOL86	NIH91	STO06
1	3.2	3.0	2.6
5	4.5	4.3	3.7
10	5.2	4.9	4.2
25	6.1	5.7	4.9
50	6.8	6.4	5.5
100	7.5	7.1	6.0

3.3 Wave overwash and overtopping

3.3.1 Overwash extension

For those situations where the *Ru* exceeds the highest natural barrier (beach/dune height), the backbarrier will be temporarily flooded. In low-lying coasts such as barriers where it is quite usual to have elements of interest in that area, it is relevant to estimate not only the probability of occurrence of *Ru* >beach/dune height but also the extension of the overwash and, also, the flow depth. In the following, a simple approach to calculate the magnitude of this hazard is presented.

Figure 3-5 shows the sketch of the problem to be solved, which is determined by a situation where the water level reaches a maximum vertical elevation with respect to SWL given by the runup (R) at an horizontal distance from the shoreline X_R (overwash reach).

The h_c can be calculated assuming a similarity relationship (Figure 3-5) and applying the equations of Donnelly 2008:

$$h_c = \frac{h_o}{x_R}(x_R - x_c) \tag{3.16}$$

where x_c is the horizontal distance from SWL to the beach crest and x_R is he horizontal projection of maximum runup from SWL (Figure 3-5). The value of x_R can be estimated as the product of the runup magnitude R (estimated by applying any of the existing models, see section 3.2) and the beach slope. The value of x_C (distance from the waterline SWL to the maximum beach/dune height) can be directly measured from existing beach topography (e.g. from a DTM).

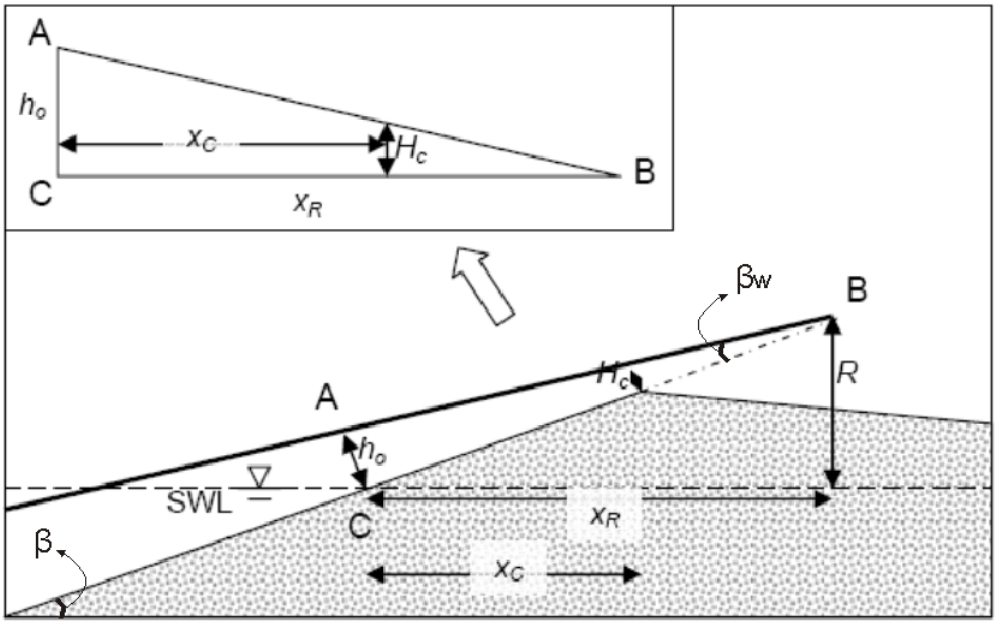

Figure 3-5: Sketch showing assumed water level at point of maximum run-up, with inset of triangle ABC showing linear relationship used to estimate water depths (after Schuettrumpf and Oumeraci, 2005).

To estimate the h_o-values two approaches can be applied:

(1) Substitute the h_o/x_R term by a constant value based on the laboratory measurements made by Schuettrumpf and Oumeraci (2005). Typical values are presented in Table 3-4 for different slopes. This constant value is also the tangent of the run-up lens ($tan\beta_w$) assuming a linear water surface.

(2) The equation (3.16) can be rearranged using the same similarity relation to:

$$h_c = \frac{tan\beta_w x_c}{x_R \cos\beta}(x_R - x_c) \tag{3.17}$$

where β is the beach slope. The values of $tan\beta_w$ can be again obtained from Table 3-4.

The flow velocity at the crest of the dune, u_c, can be calculated following Donnelly (2008):

$$u_c = C_u\sqrt{g h_c} \tag{3.18}$$

where C_u is the bore front coefficient that can take the following values: 1.53 (Donnelly 2008, measurements on sandy beaches), 2 (analytical dam break solution) or 2.6 (Matias et al. 2014, gravel barrier).

Table 3-4: Run-up lens slope measured for dikes (laboratory measurements in slopes 1:6) after Schuttrumpf and Oumeraci (2005).

	$tan\beta_w$	$tan\beta$	r
$h_{c2\%}$	0.035	0.17	0.60
$h_{c2\%}$	0.028	0.25	0.42

The variation of h_c and u_c can be estimated analytically for the backbarrier zone (Donnelly, 2008). However, to simplify the present approach we will associate the evolution of the h_c in the backbarrier zone only with the loss of volume due to infiltration assuming that there is no lateral widening of the flow (profile approach) using the following equation:

$$h(x) = h_c \exp\left(-a\frac{x}{u_c}\right) \tag{3.19}$$

where a is the proportionality constant for infiltration. Based on this equation, we can parameterize the exposure of backbarrier infrastructures assuming an infiltration constant while the rest of the values will depend on wave conditions and the barrier geometry.

The evolution of 'u' (overwash velocity) through the backbarrier is also variable but has a more complicated analytical solution since it depends on the slope, the bottom friction and the water depth. Hence, in order to calculate it, we would need to add another parameter (friction coefficient) that is difficult to estimate. Thus, due to these limitations and complexity, as a first approach, we can work only with the crest velocity as a worst case scenario. Finally, total overwash volumes can also be calculated by multiplying the u_c and $h(x)$ and assuming a time frame (the duration of the overwash event during the storm, time during which water level exceeds beach/dune height).

3.3.2 Example of application

The approach presented above to calculate the extent of the influence of the overwash/overtopping event will be illustrated with an application to the Praia the Faro beach (Portuguese RISCKIT site).

The first step was to calculate the storm water levels impacting on the beach with a given probability. In this case, and as an example, we have selected a storm event associated to a probability of occurrence given by a T_R = 50 y, which corresponds to wave conditions of Hs = 8.5m and Tp = 14 s.

The associated tide and storm surge for this event resulted in a water level 2.33 m above MSL (Vousdoukas et al., 2012). The corresponding wave runup was calculated using the HOL86 model which is considered the best formula for the study area according to Vousdoukas et al. (2012) and Almeida et al. (2012). Please note that in this illustration in particular, we are using the before denominated event approach to calculate water levels associated with a given probability of occurrence.

Figure 3-6 shows a typical barrier profile of the central part of Praia de Faro (Ria Formosa). This profile was extracted from the most recent DTM (May 2011) available for the study area. Dune crest elevation, and beach and backbarrier slopes were calculated from the DTM, using as representative slope for the runup formula the beach face slope. Table 3-5 summarizes values used in the computations.

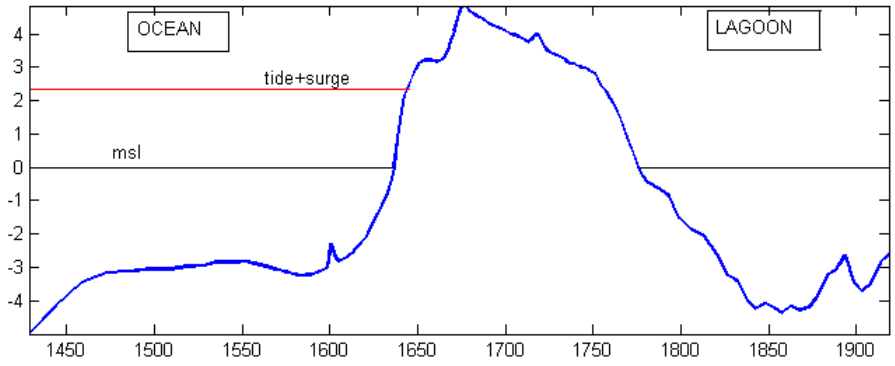

Figure 3-6: Praia de Faro typical barrier profile and key water levels for the event.

Table 3-5: Used values to estimate the overwash extension at Praia de Faro.

variable	value
Beach face slope	0.12
Dune crest	4.8 m above MSL
Tr	50 y
Runup	5.7 m
Surge + runup	8.5 m MSL

The point where the storm sea level (storm + tide) intersects with the beach was selected as a starting point for calculating the horizontal distances (x_C, x_R). These resulted in values of:

x_C = 32 m
x_R = 48 m

using equations (3.16) or (3.17) and (3.18) the runup water depth and velocity at the crest can be calculated:

h_C = 0.34 m
u_C = 2.9 m/s

Substituting the above values in equation (3.19) the overwash extension and depth at any given cross-shore distance can be calculated assuming a coefficient for the loss of water due to infiltration a. In Figure 3-7 the flow depth along the back barrier is calculated for two infiltration constant a=0.01 (almost impermeable bed) and a = 0.12 (typical values for barrier islands with similar sedimentary and morphological conditions as Ria Formosa (Donnelly et al., 2005)).

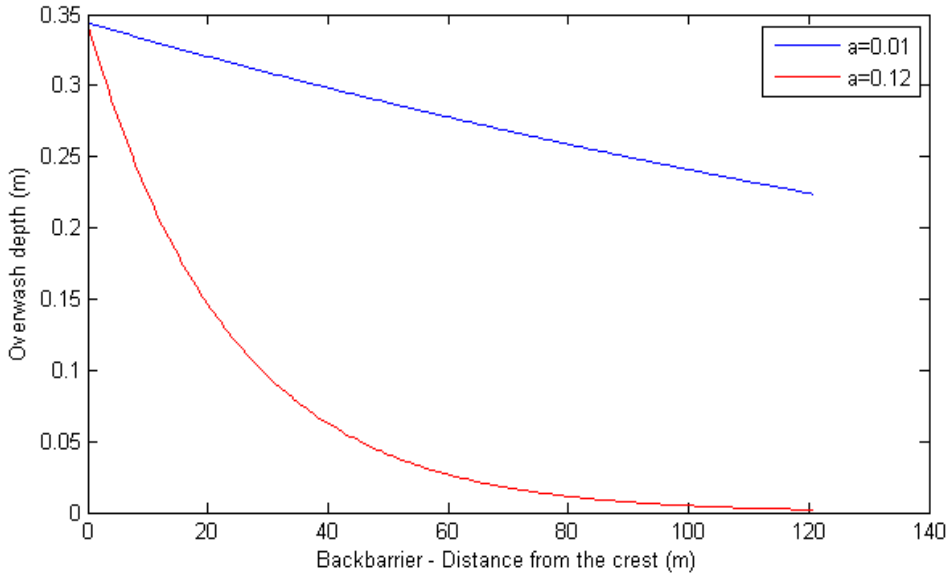

Figure 3-7: Overwash flow depth along the back barrier for three values of infiltration.

3.3.3 Overtopping

When wave-induced runup is significantly higher than the coastal structure elevation (dike/seawall), overtopping will occur and this will determine the total volume of floodwater entering into the hinterland and, in consequence, will largely control the extension of the hinterland area to be temporarily flooded.

Although, traditionally, overtopping has been calculated for coastal protection structures such as dikes and seawalls, there is an increasing number of studies where it is also applied for dunes and beaches in coastal flooding analysis, assuming beaches behave as a protection element against flooding (e.g. Kerper et al. 2006; Tuan et al. 2006; Figlus et al. 2010).

Overtopping is a function of the freeboard (*Rc*) during the event, i.e., elevation of a boardwalk, dike or seawall, or by the height of the dune/beach in the case of a natural environment, and the total water level at the coastline (Pullen et al., 2007) (Figure 3-8).

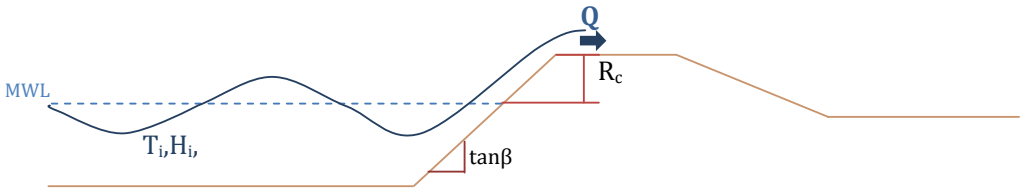

Figure 3-8: Scheme of overtopping conditions.

Different formulations exist to obtain the flow rate associated to overtopping from given wave conditions, with most of them being developed to characterize overtopping at seawalls and breakwaters (see Pullen et al., 2007). However, there is a number of studies where they are also applied and/or adapted to be also used in beach/dune (e.g. Kobayashi et al.. 1996; Tuan et al. 2006).

Among the different existing overtopping models, here we propose to use the overtopping model proposed by Hedges and Reis (1998) (hereinafter denoted as H&R), with the coefficients modified by Reis et al. (2008).

The overtopping discharge Q according to the H&R model is given by:

$$\frac{Q}{\sqrt{gR_{max}^3}} = \begin{cases} A\left(1-\frac{Rc}{\gamma_r R_{max}}\right)^B & 0 \le \frac{Rc}{\gamma_r R_{max}} < 1 \\ 0 & \frac{Rc}{\gamma_r R_{max}} \ge 1 \end{cases} \tag{3.20}$$

where R_{max} is the maximum wave runup value during the storm, γ_r is a roughness coefficient for the sloping bed (e.g. 1 for sand), Rc is the beach freeboard (elevation of the berm/embankment relative to the mean water level), A and B are coefficients, which are given by (Reis et al. 2008),

$$A = \begin{cases} 0.0033 & for\ 0.05 \le \tan\beta < 0.083 \\ 0.0033 + \frac{0.0025}{\tan\beta} & for\ 0.083 \le \tan\beta \le 1 \end{cases} \tag{3.21}$$

$$B = \begin{cases} 10.2 - \frac{0.275}{\tan\beta} & for\ 0.05 \le \tan\beta < 0.13 \\ 2.8 + \frac{0.65}{\tan\beta} & for\ 0.13 \le \tan\beta \le 1 \end{cases}$$

These coefficients were adjusted by Reis et al. (2007) to be used with a runup value given by $R_{max,37\%}$ which is about 8.5 % larger than $Ru_{2\%}$ assuming a Rayleigh distribution.

In the case of calculating overtopping discharges in a natural environment, we follow the Laudier et al. (2011) approach and used STO06 to estimate the wave runup for application of the H&R model. According to this, runup values calculated using STO06 are fed into (3.20) after proper transformation to $R_{max,37\%}$. This model predicts that beach overtopping will occur only when $\gamma_r R_{max} > Rc$.

The model can also be used with other runup formulas as those presented in section 3.2. However, it has to be considered that the change in the runup formula also implies a change in the discharge rates magnitude unless a specific calibration is performed. In any case, since the objective is to get a first assessment of the coastal vulnerability to temporary inundation to identify hotspots, the model can be used with other formulations although obtained values must be essentially interpreted in relative terms (i.e. to compare sites along the coast).

In this sense, when applied to natural environments, this should be equivalent to overwash computations, although in the previous section we have presented a method to assess the horizontal extension of the zone to be influenced by the temporary flooding whereas in this case, we are presenting a method to directly assess the rate of floodwater volume crossing the coastal barrier towards the hinterland.

Overtopping discharge rates will control the volume of floodwater entering the hinterland and, in consequence the extension of the inundated surface. However, overtopping is also a very important factor controlling direct damages along the coastal fringe. To stress its importance, Table 3-6 and Figure 3-9 show the expected damages under different overtopping rates (see also Geeraerts et al. 2007).

Table 3-6: Average overtopping flow and coastal vulnerability to flooding (adapted from FEMA (2007).

Order of magnitude Qov	Vulnerability to flooding
10^{-6} - 10^{-5} $m^3/s \cdot m$	Very low
10^{-5} - 0,001 $m^3/s \cdot m$	Low
0,001 - 0,01 $m^3/s \cdot m$	Medium
0,01 – 0,1 $m^3/s \cdot m$	High
> 0,1 $m^3/s \cdot m$	Very high

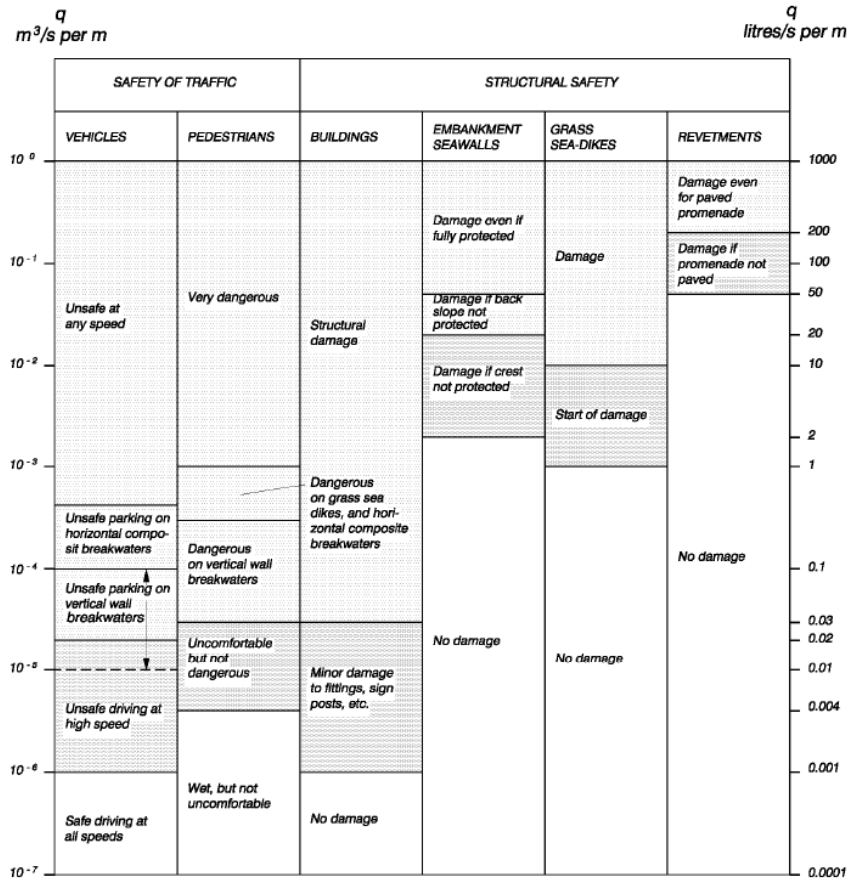

Figure 3-9: Critical values of average overtopping discharges (CEM, 2011).

3.3.4 Example of application

The implementation of this approach within the framework is straightforward. In this case, we are illustrating the calculation of overtopping in a natural environment with the final objective of assessing the floodwater discharge rates entering to the hinterland to produce its temporary flooding. It has to be considered that the application in a site protected by a dike/seawall will be the same, with the height of the structure the variable defining the elevation of the coast (Rc). The first step is obtained directly in the previous section, i.e. the estimation of the runup extreme climate for the study area (defined in terms of wave climate and beach morphology - slope) (Figure 3-10).

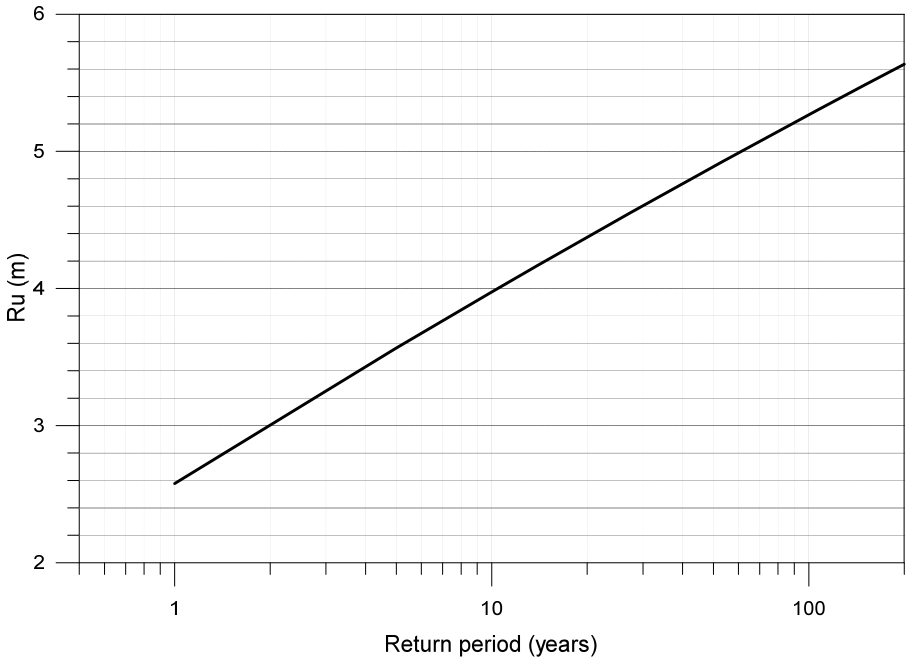

Figure 3-10: Runup extreme climate for the Tordera delta.

Now, the corresponding discharge rates are calculated for each return period for different elevations characteristics of the study area by applying equation 3.20 with the corresponding runup values. Figure 3-11 shows the obtained overtopping discharge climate for the Tordera delta for different beach elevations along the coast.

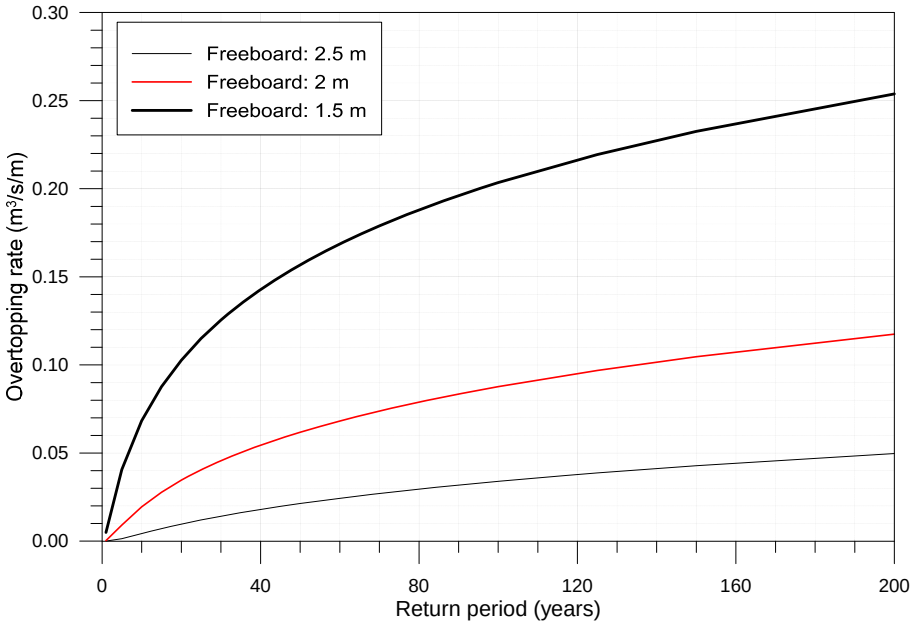

Figure 3-11: Overtopping discharge rates for different beach elevations for runup climate defined in Figure 3-10.

3.4 Inundation

Finally, the last used indicator to identify hotspots due to coastal flooding-related hazards will be the potential extension of the inundation. Although inundation models able to accurately model the extension of the inundation do exist (e.g. LISFLOOD, Bates and de Roo, 2000; Bates et al., 2005), since the objective is simply the identification of hotspots, in the first phase of the framework, the affected area will be delineated by using the *bathtub* approach.

The bathtub flooding approach essentially consists of assuming that all the coastal area connected to the sea with an elevation below the total water level will be inundated. As it was previously mentioned, this would only occur in the case that such water level would remain in place for a time long enough to ensure that the required volume of water to fill such basin (coastal topography till the considered level) would flow towards the hinterland during the storm duration. Thus, this approach is conservative (overprediction), in such a way that it characterizes the worst case scenario with the surface delineated being equivalent to the maximum potential inundation.

This approach is best suited in coastal areas characterized by a topography continuously increasing landward from the coast without presenting large low-lying areas.

To apply this method, the starting point is the total water level climate derived in section 3.2. Since the objective is identify hotspots by delineating the maximum extension/influence of flooding hazards, this water level climate will be characterized in a different way for protected and exposed coastal environments.

In *protected or sheltered environments*, such as estuaries, where waves are of secondary importance, the total water level climate will be characterized by the storm surge extreme climate. The procedure to obtain the extreme probability distribution is the same outlined for runup (section 3.2.4), although in this case, the variable used to define the storm events is the surge. The final result is a series of values of water levels (surge) associated with given return periods.

In *exposed environments*, such as open beaches where wave action during storms is important and, in many, cases induce water level changes of the same order of magnitude (in many cases larger) as surge, the total water level climate will be characterized by the storm surge plus runup extreme climate. The procedure to obtain the extreme probability distribution is the outlined in section 3.2.4. The final result is a series of values of water levels (surge+runup) associated with given return periods.

Once the water level associated to the selected return period is obtained, the next step is to delineate the land surface to be affected. In protected environments where the water level is given by the storm surge, this is easily done by using a GIS where all the area connected to the sea below that level is identified (see e.g. Figure 3-12).

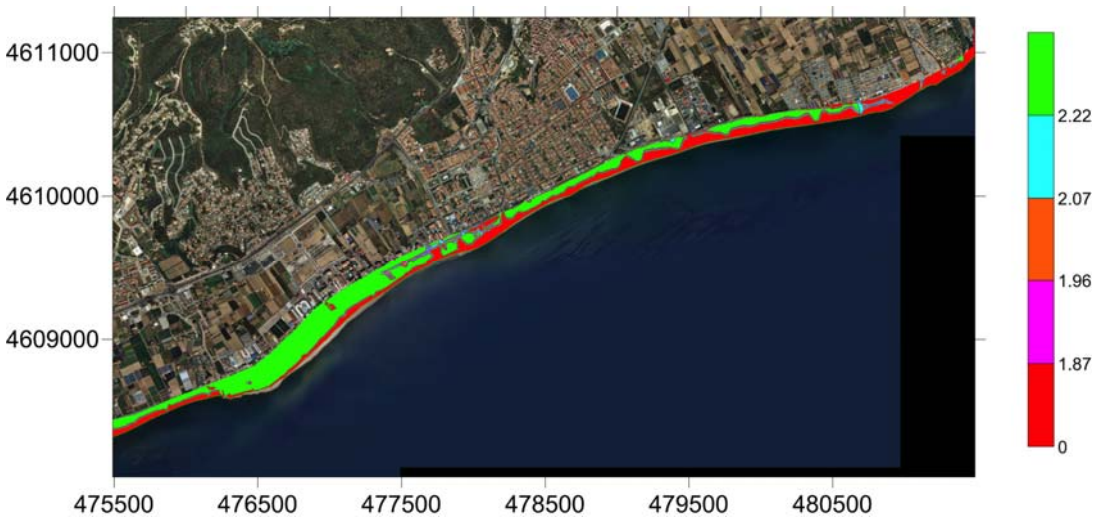

Figure 3-12: Simulation of coastal inundation for different water levels by using the bathtub approach in the Maresme coast.

In open environments where the water level is given by the storm surge and the wave-induced runup, the process is slightly different. First, for each beach profile representative of coastal sectors, we delineate the extension below the total water level associated with the target return period (Figure 3-13).

In the case of beach profiles with a morphology characterized by a monotonous increasing elevation in the landward direction, we can assume that the area thus delineated by using directly the bathtub approach is a good representation of the area to be (temporarily) affected by inundation (Figure 3-13, top).

.

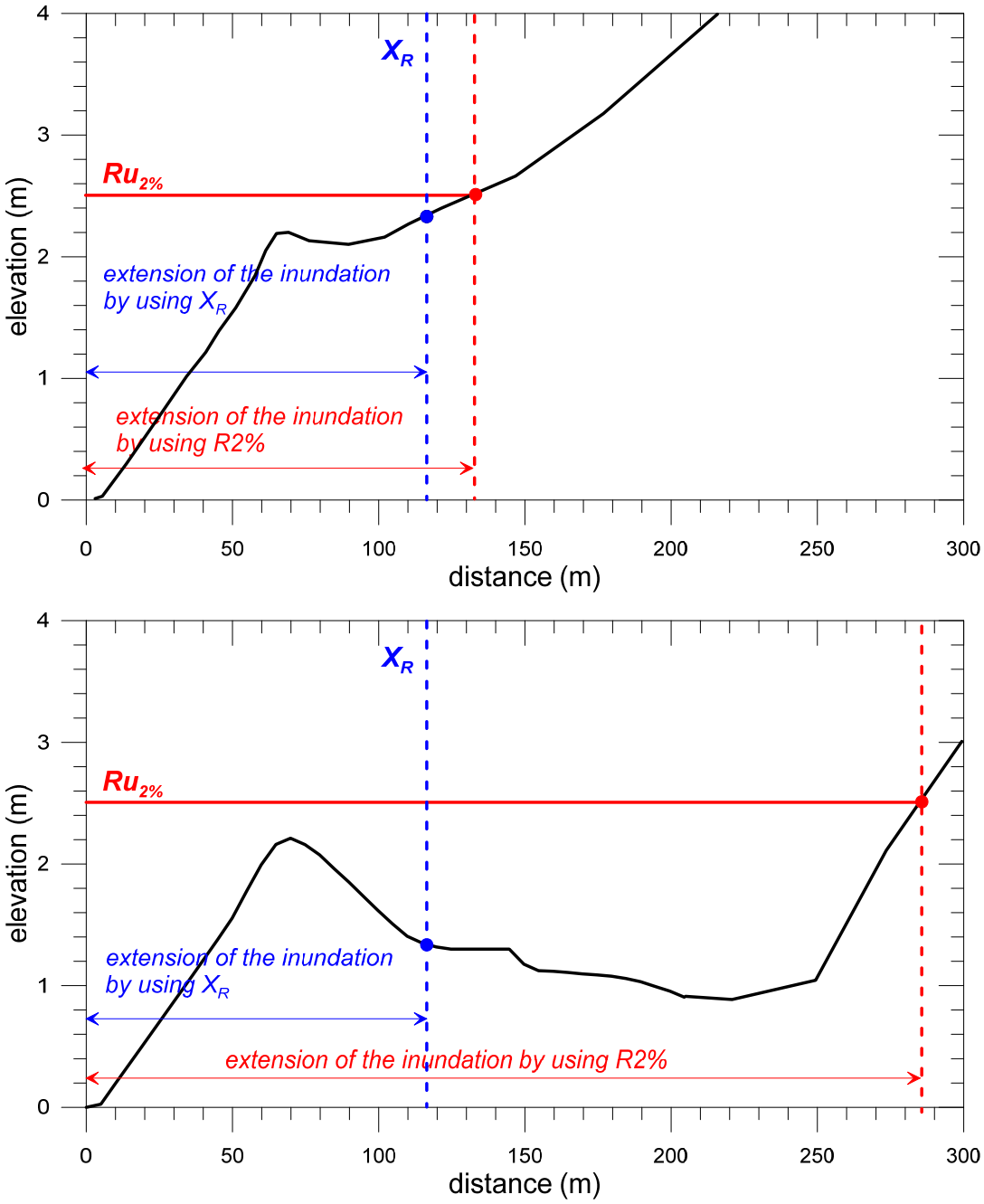

Figure 3-13: Delineation of the extension of the inundation of a beach profile using the bathtub approach (*Ru2%*) and the overwash extension (X_R). (*Top*: monotonous increasing elevation; *bottom*: varying elevation trend). (Note.- In this example mean water level was zero, otherwise it has to be added to calculated *Ru2%*).

In the case of coastal stretches characterized by the presence of low-lying areas landward of the beach, the direct use of this water level to delineate the area to be (temporarily) affected by inundation is clearly overpredicted (Figure 3-13, bottom). To reduce this effect, we shall use the above presented overwash extension (section 3.3). Thus, we shall assess which is the magnitude of the overwash extension for the corresponding profile and for the considered return period. As it can be seen, in the case presented in Figure 3-13, this results in a significantly reduced area. Once these two extensions are calculated, the shorter one will be retained (usually the one

defined by the overwash extension). In any case, it has to be also considered that if the intersection of the surge level exceeds the barrier elevation, then the bathtub approach should be used.

The final step to delineate the coastal surface susceptible to be inundated under a storm of a given return period, the points delineating the extension in each profile for all sectors along the coast are joined.

As a final point, coastal areas identified as hotspots will be analyzed in detail in the second phase where the use of detailed models such as XBeach will permit to accurately estimate the extension of the overwash.

4 Erosion

4.1 Introduction

As it has been described in chapter 2, one of the most important storm-induced hazards in sedimentary coasts is erosion. Thus, it is the first to appear during the initial stages of the storm and, once the beach is modified, the inundation of the hinterland will occur. In other cases, although hydraulic conditions during the storm are enough by themselves to inundate the hinterland, beach erosion during the storm will modify the coastal fringe (e.g. beach lowering) enhancing the inundation during the event. Due to this, it is necessary to include beach erosion in any storm-induced hazard assessment to properly identify sensitive stretches along the coast to the impact of extreme events.

The ideal manner to accurately calculate storm-induced erosion in an arbitrary beach should be to model acting processes with detailed process-oriented models developed to simulate these conditions such as XBeach (Roelvink et al. 2009). However, as it was already discussed in chapter 2, for hazard assessment at regional scale this approach is only suitable when a first reduction of selected cases to be analyzed is performed.

In this chapter we cover the assessment of storm-induced erosion using simple approaches able to efficiently work at large spatial scales and with a high number of events to obtain a probability distribution. Thus, to assess the magnitude of storm-induced erosion, here we have followed an approach in which the induced hazard is calculated with a structural function specifically derived for storm impacts on beaches, with the function to be selected depending on its performance for the site conditions (use of specific models calibrated for the site or for similar conditions).

4.2 Mendoza and Jiménez model

The first option considered in this framework is the structural erosion function proposed by Mendoza and Jiménez (2006) to characterize the impact of storms in Mediterranean beaches. It permits the calculation of the magnitude of the induced process (eroded volume and beach retreat,

Figure **4-1**) by means of a bulk model which depends on storm properties (*Hs, Tp* and duration) and beach morphology (sediment grain size and beach slope).

This structural erosion function consist of a bulk formula predicting the eroded volume in the inner part of the beach profile which have been derived by using the Sbeach model (Larson and Kraus 1989, Wise et al. 1996). This is a semi-empirical model to determine time dependent cross-shore sediment transport processes for an arbitrary beach profile. It has been verified against a variety of physical model and field data, and has been used extensively worldwide in planning studies and the design of beach nourishment projects. This model has already been used to simulate the dune lowering before the inundation of the hinterland during the impact of extreme storms (see e.g. Cañizares and Irish, 2008).

The structural function is derived by relating the storm-induced eroded volumes simulated with the Sbeach model with a coastal morphodynamic parameter. The

selected parameter was the one proposed by Jiménez et al. (1993) which uses the Dean parameter and the beach slope,

$$JA_0 = \left|D_{0,e} - D_0\right|^{0.5} \cdot m \tag{4.1}$$

where D es the Dean parameter ($H/T\ w_f$), D_{0e} corresponds to its value at equilibrium (2.5 when using waves given at deepwater) and m is the profile mean slope. This parameter was successfully used to predict the magnitude of eroded volumes in beach profile experiments obtained in large wave flumes and, in consequence, it can be considered a good predictor for storm cross-shore induced beach profile changes (Figure 4-2). It accounts for the effects of sediment grain size and initial beach profile slope.

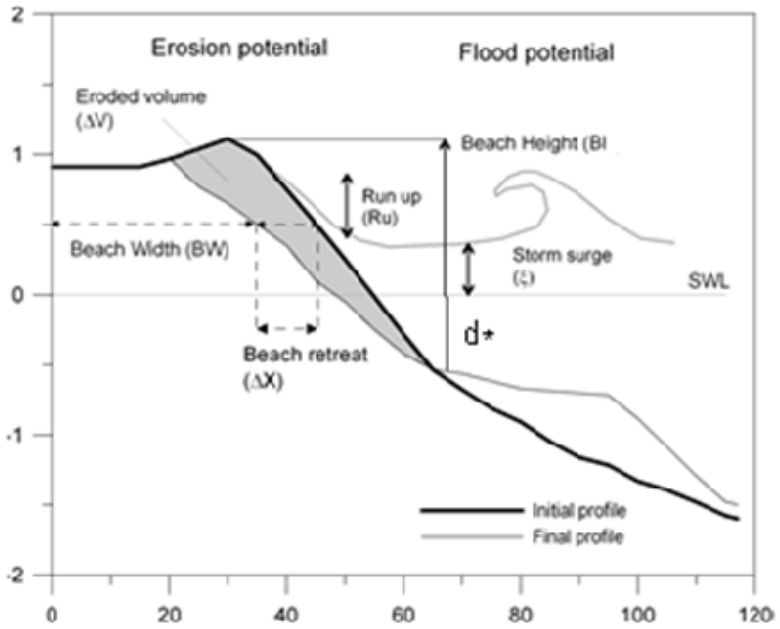

Figure 4-1: Scheme of storm-induced beach profile changes.

Figure 4-3 shows the relationship of computed eroded volumes by using Sbeach against values of the selected parameter JA (4.1) integrated during storm duration (dt) measured in hours. These values have been computed for storm conditions typical of the Mediterranean coast and for beach profiles representative of the Catalan coast (reflective and dissipative beaches). As it can be seen, the computed eroded volumes can be well represented by the used parameter and, taking into account the observed dependence a linear model is proposed, which in this case is given by,

$$\Delta V\ = 7.9\ JA\ dt + 3.6 \tag{4.2}$$

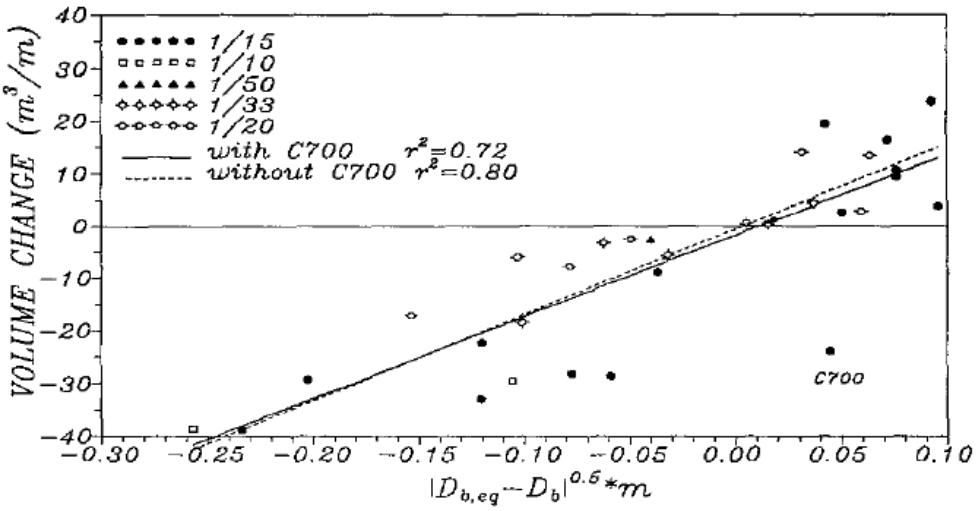

Figure 4-2: Eroded volume in the inner part of the beach profile vs JA parameter (Jiménez et al. 1993).

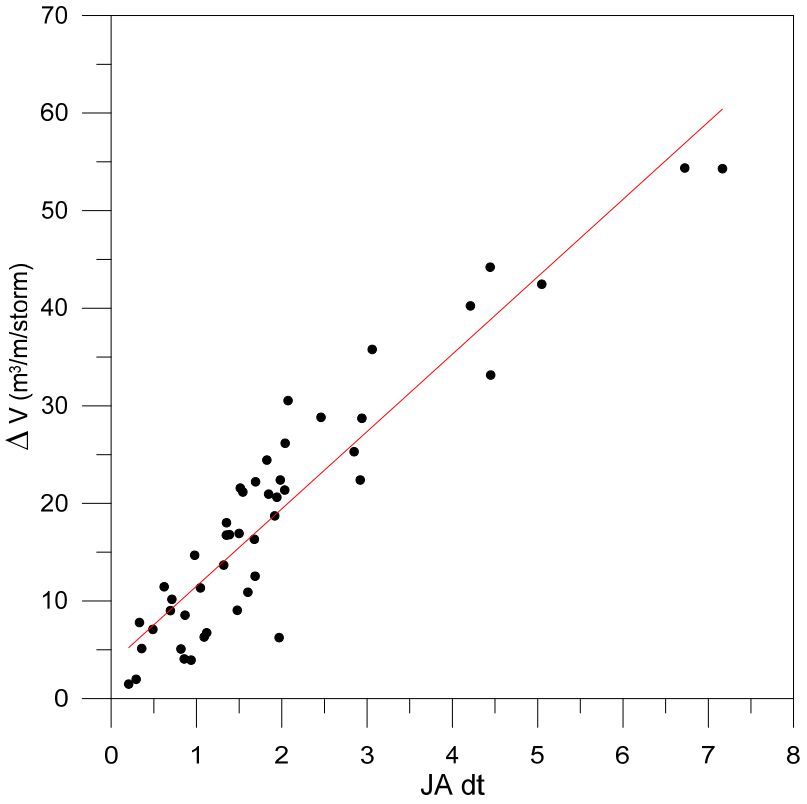

Figure 4-3: Computed eroded volumes vs values of JA-parameter (adapted from García Sorinas, 2014).

This approach can also be used to estimate the shoreline retreat induced during the storm, by relating the simulated shoreline retreat against corresponding values of the parameter. However, in some cases the induced retreat is not uniform in the emerged beach, with largest retreats in the highest beach levels and lower ones close to the

shoreline. To obtain a representative retreat for the emerged beach, we calculate a representative beach retreat, ΔXr , as,

$$\Delta Xr = \Delta V / (B + d*) \quad (4.3)$$

where B is the berm height and d^* is the depth down to which erosion of the inner part of the beach profile takes place. Figure 4-4 shows the calculated erosion depths d^* for different storm and profiles typical of Mediterranean conditions (Catalan coast), where it can be seen that it is possible to find a representative value for a range of representative conditions (here represented by a d^* value of 3 m). In any case, it is also possible to obtain a relationship as equation 4.2 but for the shoreline retreat.

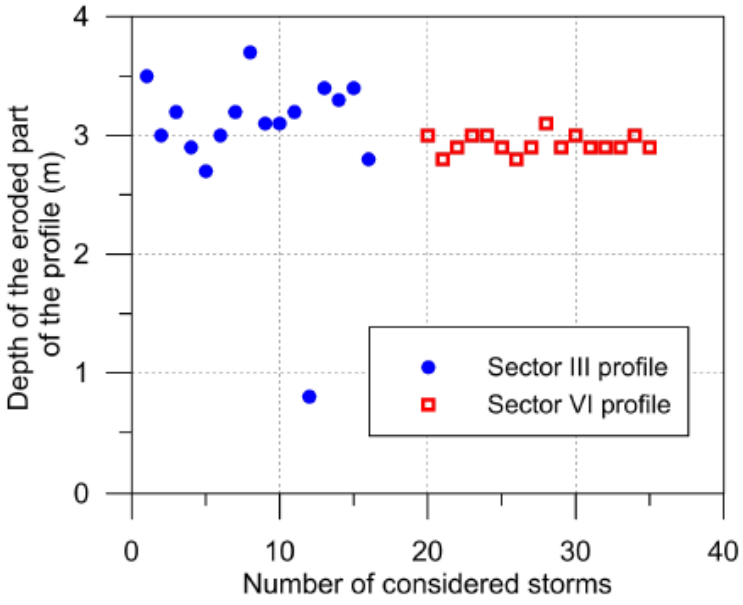

Figure 4-4: Depth of the eroded part of the profiles corresponding to Sbeach simulations (Bosom, 2014).

One of the main points to be considered when applying this approach is that the erosion structural function needs to be calibrated for the study site of interest to properly fit the coefficients of (4.2). Since it is obtained from simulations using a numerical model, its accuracy will depend on the accuracy of model runs. In the case of the non existence of pre- and post-storm data to obtain a calibrated set of coefficients for the specific site, values recommended in the literature should be used.

One of the points to be highlighted with respect to the use of this erosion structural function is that it also serves to parameterize eroded volumes computed using the XBeach model. As in the previous case, the coefficients to be used in the final formula (4.2) will be controlled by the proper calibration of the model. It has to be highlighted that in the case of using 2 models properly calibrated (Sbeach and XBeach), the set of coefficients should be the same. To illustrate the goodness of $JA \cdot dt$ to parameterize eroded volumes Figure 4-5 shows computed values using the XBeach model (1DV

transect version) in a highly reflective coarse sediment beach profile. As it can be seen, there is a linear relationship between both variables similar to equation 4.2.

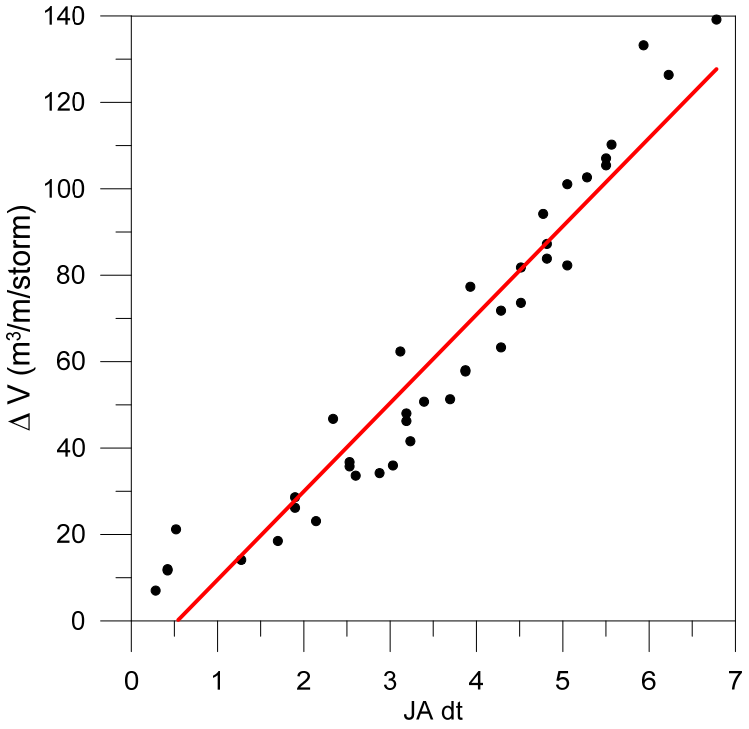

Figure 4-5: XBeach computed eroded volumes in a highly coarse sediment reflexive profile *vs* values of *JA*-parameter.

4.3 Convolution model

As an alternative to the previously presented erosion structural function, other simple models can be used to assess the magnitude of storm-induced erosion. Among them, one of the most used is the Kriebel and Dean (1993) convolution method (e.g. Callaghan et al. 2013). This approach is a simple analytical solution of the time dependent beach profile response to a storm event. In this approach the erosion is forced by wave breaking and water level variation due to storm surge. The basis for the convolution method is the observation that beach response to steady-state forcing conditions is approximately exponential in time. The duration of the storm and surge play an important role in the beach response and controls if the beach will reach to a steady-state or not. The final shoreline retreat, *R(t)* is then given by (Figure 4-6: *Definition Sketch for Beach-Profile Response (Kriebel and Dean, 1993)*:

$$R(t) = R_{\infty}(1 - e^{-t/T_s}) \quad (4.4)$$

where R_{∞} is the maximum retreat that occurs after the system reaches equilibrium; and *Ts* is the characteristic time scale of the exponential response.

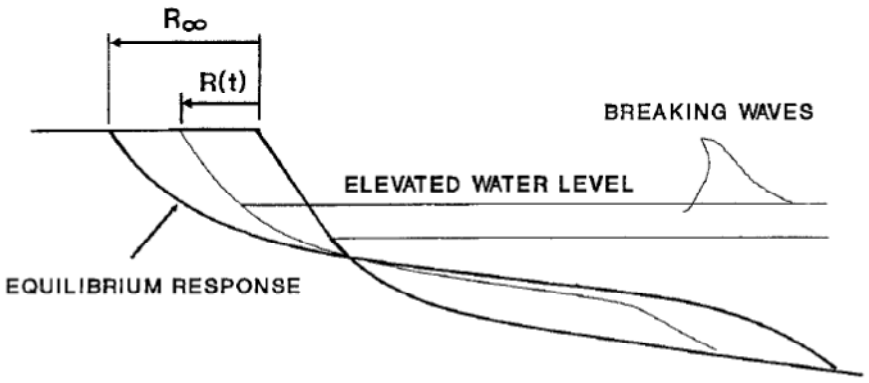

Figure 4-6: Definition Sketch for Beach-Profile Response (Kriebel and Dean, 1993).

The steady-state was calculated by the convolution of the surge with the beach profiles assuming that the profile will maintain its equilibrium shape and the total sediment volume remains unchanged. Different shapes of the subaerial beach were used (e.g. dune berm plus dune) in order to adjust total retreat to the sediment volume available for erosion. The dune (D) and berm (B) heights and the berm width (W), if present, as well as, the beachface slope (m) were used to calculate the subaerial sand volume. The submerged part of the beach profile is represented by the equilibrium profile (Dean, 1977). Based on the above assumptions the maximum potential retreat for a beach with a dune and berm is given by the following equation,

$$R_\infty = \frac{S(x_b - \frac{h_b}{m})}{B+D+h_b-\frac{S}{2}} - \frac{W(B+h_b-\frac{S}{2})}{B+D+h_b-\frac{S}{2}} \qquad (4.5)$$

Where S is the storm surge elevation, x_b is the surf zone width and h_b the depth of wave breaking.

At the same time and for the same profile case the maximum potential erosion volume above the MSL is given by the following equation,

$$V_{M\infty} = R_\infty D + (R_\infty + W)B + \frac{S^2}{2m} - \frac{S^{\frac{5}{2}}}{A^{\frac{3}{2}}} \qquad (4.6)$$

where A is the parameter that governs the overall steepness of the profile and is controlled by sediment grain size (Dean, 1977).

The time scale (Ts) required by the beach to reach the steady–state (at which the maximum potential erosion should occur) was parameterized based on numerical experiments and it was found to be strongly dependent on the breaking wave height and on the sediment size. The time scale varies by about one order of magnitude from the smallest wave heights to the largest, in such a way that the smaller wave heights have much shorter time scales (larger rate parameters) than larger wave heights. This is due to the fact that larger wave heights define a wider surf zone where sand must be

moved further offshore. As a result of this, a much longer time is required to reach the equilibrium state. In addition to this, it was found that values of *Ts* are smaller for coarser sediments, in such a way that the time scale is inversely proportional to the fall velocity (Kriebel and Dean, 1993). The resulting equation for *Ts* (after fitting an empirical equation to numerical data) is:

$$T_s = 320 \frac{H_b^{3/2}}{g^{1/2} A^3} \left(1 + \frac{h_b}{B} + \frac{m x_b}{h_b}\right)^{-1} \qquad (4.7)$$

Assuming that the time varying forcing of the storm surge has the form of $S^*\sin^2(\pi t/T_D)$ where T_D is the storm duration, the storm-induced shoreline retreat is:

$$R(t) = 0.5 R_\infty \left\{1 - \frac{\beta^2}{1+\beta^2} \exp\left(-\frac{t}{T_S}\right) - \frac{1}{1+\beta^2}\left[\cos\left({}^{2\pi t}/_{T_D}\right) + \beta \sin\left({}^{2\pi t}/_{T_D}\right)\right]\right\} \qquad (4.8)$$

where β is the ratio of the erosion time scale to the storm duration time scale $2\pi T_s/T_D$.

With these relationships (4.5, 4.6, 4.7, 4.8) we can estimate the magnitude of the storm-induced erosion (shoreline retreat) for any beach profile and storm characteristics.

4.4 Erosion under overwash conditions

During the impact of extreme storms with high waves and surged water levels, it is a common situation that the beach is overwashed and, as result of this, part of the sediment volume eroded from the beachface is transported landward. Since under these conditions, processes governing volume changes are different to those inducing standard offshore transport where undertow is the main forcing term, it should be desirable to check the validity of the above presented parametric relationships and/or to derive new ones to be used to predict storm-induced erosion for these conditions.

In this situation (Figure 4-7), three volume changes have been considered: the total eroded volume of the inner part of the profile (ΔV), the overwash deposit volume (ΔV_{ow}) and the difference between these two, which corresponds to the fraction of eroded volume transported seaward by undertow ($\Delta V_u = \Delta V - \Delta V_{ow}$).

Following the already implemented approach (section 4.2.1) a new structural function to assess the overwash volume (ΔV_{ow}) was derived. This is done by means of a bulk model which depends on storm parameters at deepwaters (*Ru* = f (*Hs,Tp*) and duration) and beach morphology controlling the expected overwash (berm height and beach slope). The function has been derived in a similar way that in section 4.2.1 but using the XBeach model. Thus, the model (in 1DV mode) has been used to simulate beach profile evolution under overwash conditions in 6 different beach profiles covering a wide range of beach slopes and berm heights (2 reflective profiles, 1 intermediate profile, 2 dissipative profiles and 1 additional reflective profile with a bar on its toe), using typical storm conditions for the NW Mediterranean coast (storm intensities covered a range of return periods from 1 year to about 200 years).

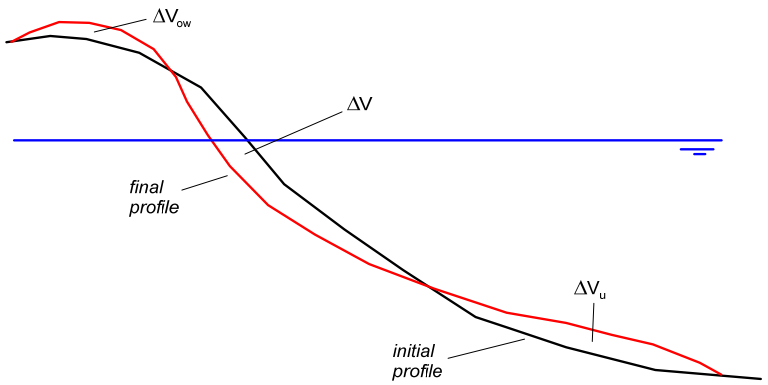

Figure 4-7: Storm-induced beach profile changes under overwash conditions.

This structural function predicts the magnitude of the overwash volume, ΔV_{ow}, as a linear function of an intermediate parameter, *SJ*, which accounts for the excess of wave-induced runup with respect to berm height (*Rc*). This *SJ* parameter is given by,

$$SJ = \left(\frac{Ru_{2\%}}{Rc}\right)^{1/2} \tag{4.9}$$

and where $Ru_{2\%}$ has been calculated using the Stockdon et. al (2006) model.

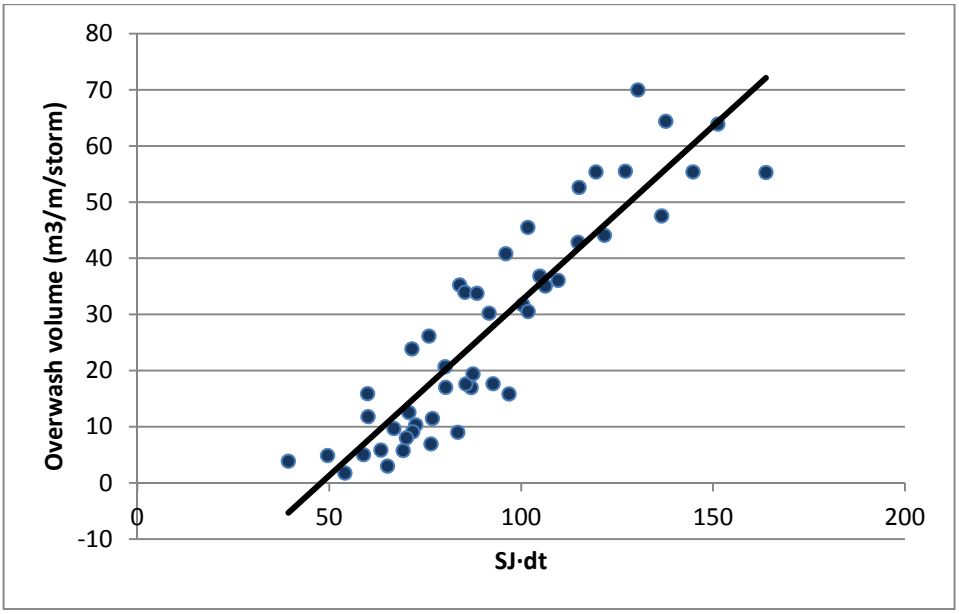

Figure 4-8: Computed overwash volumes *vs* SJ parameter.

Figure 4-8 shows the relationship of computed overwash volumes by using XBeach against the values of the *SJ* parameter integrated over storm durations. As it can be observed, computed volumes are well described by a linear function of the parameter, which is given by,

$$\Delta Vow = 0.62\ SJ\ dt \quad - \ 29.8 \tag{4.9}$$

To obtain this relationship, only overwash volumes larger than 1 $m^3/m/storm$ have been taken into account, which usually corresponds to a ratio *Ru/Rc* greater than 0.85.

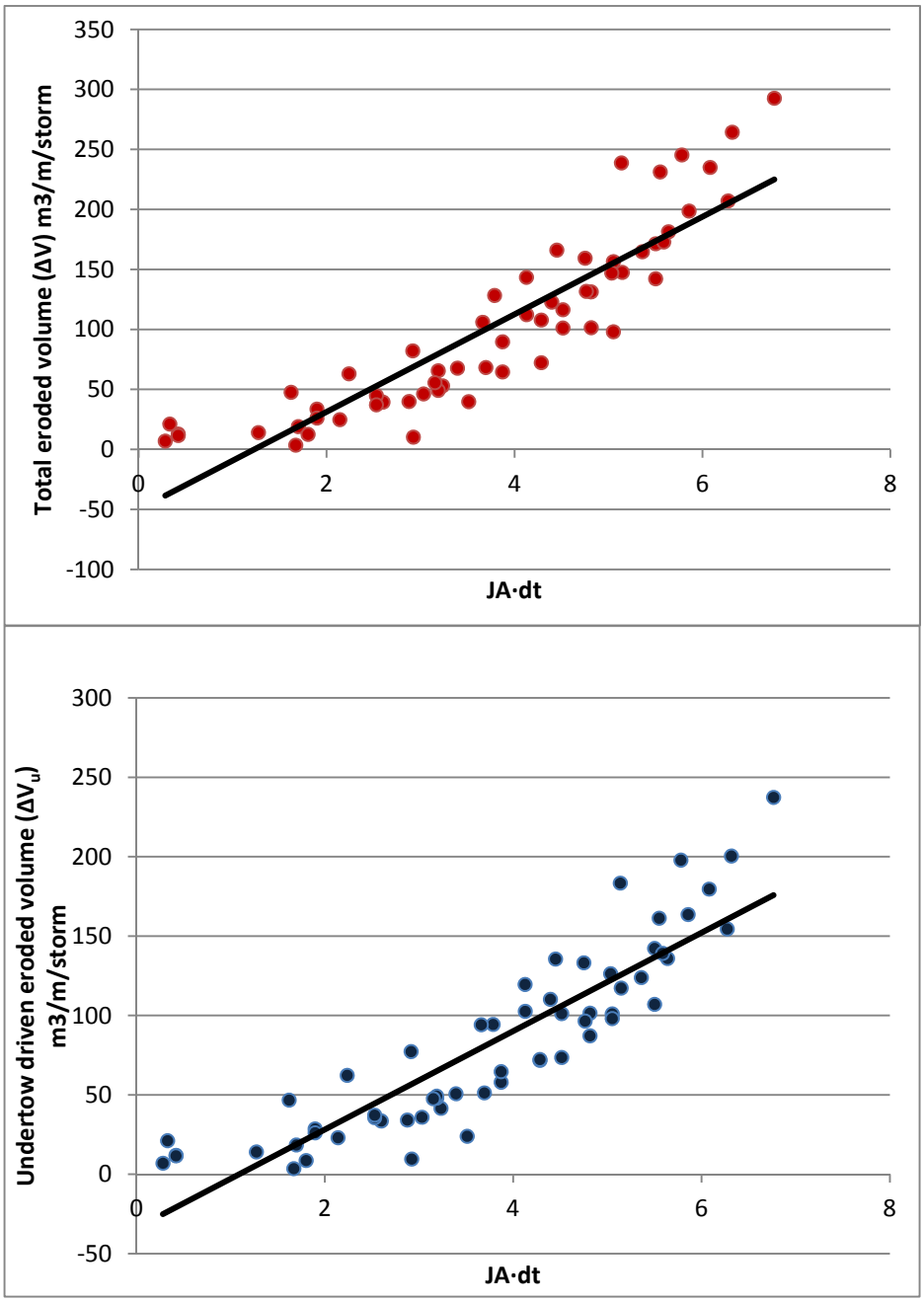

Figure 4-9: Computed total eroded volume (top) and undertow-driven eroded volume bottom) *vs* JA parameter.

Figure 4-9 shows the relationship between total and undertow-driven eroded volumes vs the *JA* parameter (Mendoza and Jiménez, 2006). As it can be seen, although the used data correspond to overwash conditions, this parameter is still able to reasonably model the observed behavior (obtained coefficients of determination for the linear model of r^2 = 0.809 and r^2 = 0.797 respectively).

In order to improve this predictive relationship under overwash conditions, the two parameters (*JA* and *SJ*) have been combined and integrated over storm duration (4.10)

to theoretically account for both undertow-driven and overwash-driven eroded volumes,

$$JA * SJ * dt = \left|D_{0,e} - D_0\right|^{0.5} \cdot m * \left(\frac{Ru_{2\%}}{Rc}\right)^{\frac{1}{2}} * dt \qquad (4.10)$$

Figure 4-10 shows the obtained linear model between computed total eroded volume and the aggregated parameter (4.10). As it can be seen the performance of the combined parameter is significantly better for the analyzed scenarios (r^2 = 0.9259), where the overwash process is rather relevant.

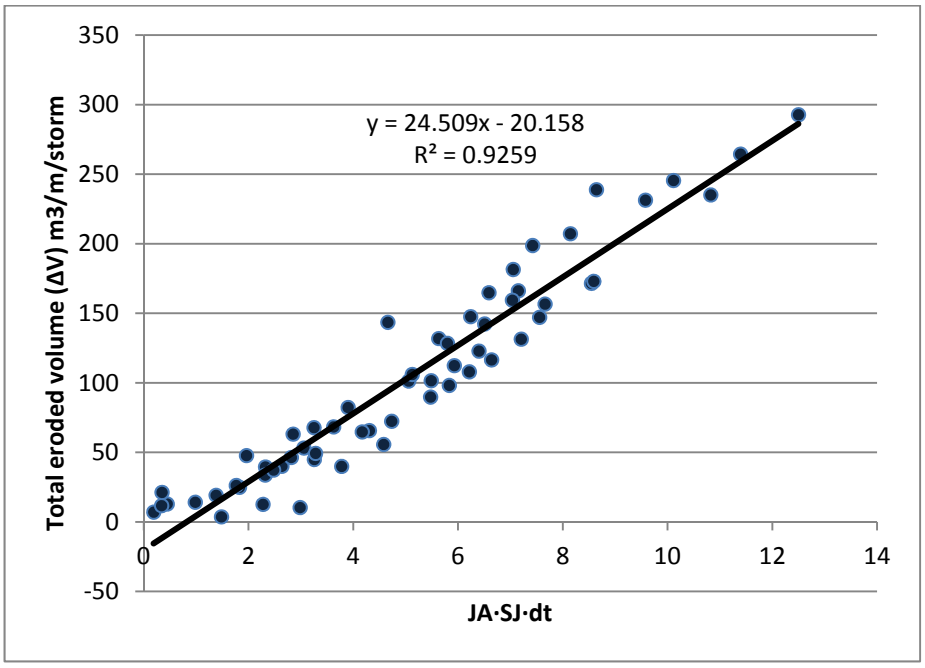

Figure 4-10: Computed total erosion volume vs JA•SJ parameter.

4.5 Example of application

To characterize the erosion hazard within the framework, we start from a set of storm characteristics (*Hs, Tp*, duration) obtained from a long time series of wave conditions in the study site. They are the same as the used ones to characterize overtopping (section 3.3.4).

For each storm, the magnitude of storm-induced erosion in terms of volume and shoreline retreat is calculated by using any of the above presented models. It is important to note that these parametric models have been derived/calibrated for specific conditions and, in consequence, it should be convenient to test/calibrate for representative conditions of the study site to be applied.

Figure 4-11 shows the computed extreme climate of beach erosion for two representative beach profiles of the Maresme coast (Catalonia, Spain). They are characterized by their corresponding beach slopes and sediment grain sizes whereas storm conditions are the same for both profiles. Once eroded volumes are computed using the structural erosion model for each storm, obtained results are fitted to a extreme probability distribution (GPD) to obtain the extreme erosion climate.

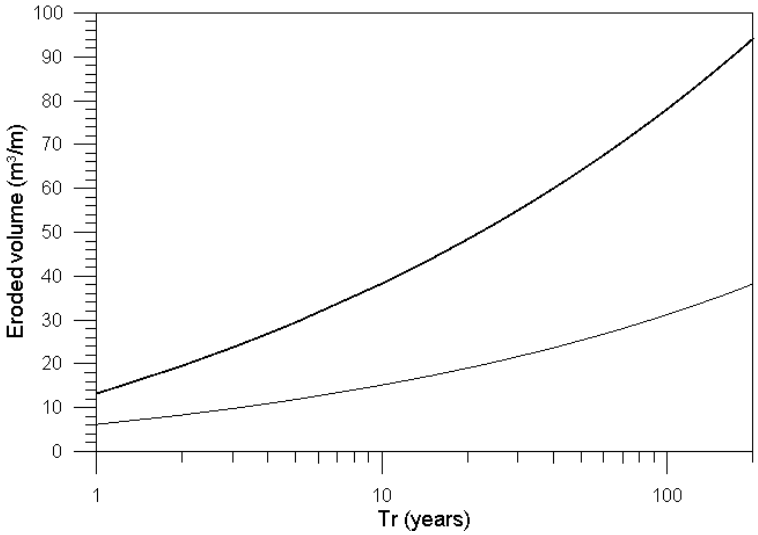

Figure 4-11: Erosion extreme climate for the Maresme coast (Catalonia) for different representative beach profiles.

Figure 4-12 shows the computed extreme climate of dune retreat for a representative beach profile in Ria Formosa (Portugal). Shoreline retreat for each storm has been calculated using the convolution model and obtained values are fitted to a extreme probability distribution (GPD) to obtain the dune retreat climate.

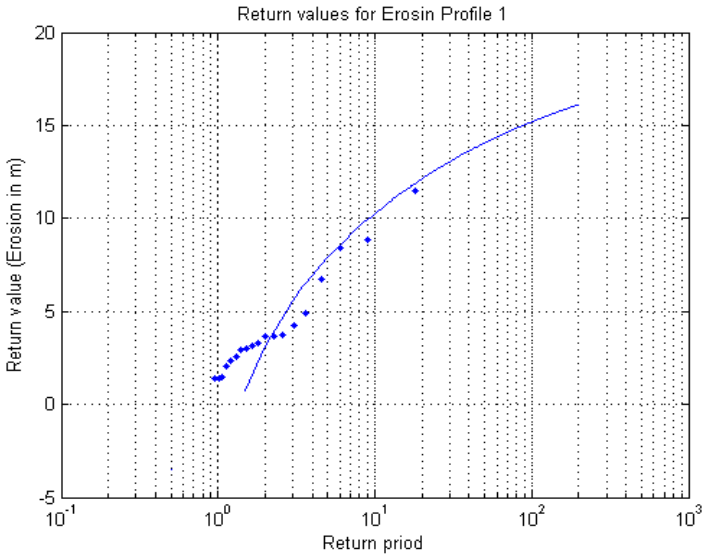

Figure 4-12: Erosion extreme climate for a dune in Ria Formosa (Portugal).

5 Barrier breaching

5.1 Introduction

Barrier island breaching is a complex process that can result in the transient or persistent (permanent) opening of a new inlet. The associated hazards are primarily related with coastal and dune erosion. Once the inlet is established secondary hazards can be associated with changes in erosion of the lagoon sediment; changes to the local hydro-ecological characteristics and also in the case of inlet migration the extension of the above hazards to the downdrift area.

The main process that produces the breaching is the local shoreline erosion, both structural and storm (or storm group) related accompanied by overwash, which can lower the dune height. In addition the overwash intrusion is a key element for the onset of a breaching. The barrier island geometry is also important; narrow and low barrier islands are more prone to breaching. Finally, the existence of a lagoon channel (i.e. large depths at the backbarrier area) can promote the hydraulic efficiency of the breach and help to the establishment of a new inlet.

5.2 Approach

Because of the complexity highlighted above there is not a simple formula to predict the occurrence of inlet breaching. As a result, the approach here defined will follow the work of Vila-Concejo et al. (2006) with some adaptation. This approach is based on determining a hazard area based on the potential occurrence or not of processes/morphologies that can contribute to barrier breaching and the formation of a new inlet. Table 5-1 shows a list of such processes and a brief description on the application. A simple index can then be created by the summation of the obtained proxies used to determine the breaching possibility. Alternatively a more complex index can also be formed taking into account actual values of the properties for different return periods.

The application of this index (Table 5-1) is restricted to sandy areas with coastal dunes. The approach cannot be applied to hard layers or beaches protected by seawalls and/or revetments preventing inlet breaching. Sectors incorporating an inlet should always be classified as 5 since breaching (or inlet migration) already existed and can continue to exist nearby (lowered areas).

This approach has the advantage of being user-friendly to get required input data from maps, aerial photographs or beach surveys along with other information already needed for CRAF application. The barrier island morphological characteristics can be easily obtained from the DTM or from a cross-shore profile data.

Table 5-1: List and description of the processes that lead to breaching.

Process /Morphology	Value	Description/occurrence
i. Overwash	1/0	0 – No overwash. 1 – Existence of recurrent overwash processes with barrier lowering at least at one spot inside the coastal sector.
ii. Structural erosion	1/0	0 – No structural erosion. 1 – Existence of structural erosion with continuous shoreline retreat (barrier width reduction) on the order of m/yr.
iii. Storm erosion	1/0	Storm induced retreat (Sir)/dune width (Dw). Storm induced retreat would be given by any model applied at CRAF for a given return period (e.g. 10yr, 50 yrs) depending on each coastal area. Dune width would be given by aerial photo analysis. 0 - Sir/Dw < 0.5. 1 - Sir/Dw >1.
iv.a Subaerial barrier volume	1/0	Geometric characteristics of the barrier island. Profile volume estimation (half of the width of barrier island multiplied by dune height, Sb = dune height*barrier width/2). A threshold (Sbcritical) should be established for values prone to breaching at each coastal area. 0 - Sb > 2*Sbcritical. 1 - Sb < Sbcritical. The value can be normalized over the CRAF area.
iv.b Washover width (Ww) to Barrier width (Bw) ratio	1/0	0 – Ww/Bw < 0.5. 1 – Ww/Bw > 1. Computed based on aerial photograph analysis of washovers and barrier width or from the overwash module at CRAF.
v. Backbarrier depth and morphology	1/0	0 – If the backbarrier is higher (eg dune ridges) than the dune front. 1 – If the backbarrier is lower than the dune front or if it has tidal channels that can promote the hydraulic efficiency of the inlet and make it permanent.
Breaching Index	0-5	A summation of all above expressed values. Intermediated values can be attributed to each parameter (e.g. 0.5).

Note: iv.b is only applied as an alternative to iv.a if enough data is missing to compute iv.a.

The **final classification** can be expressed as:

0 – No breaching
]0,1] – Very low breaching possibility
]1,2] – Low breaching possibility
]2,3] – Mean breaching possibility
]3,4] – High breaching possibility
]4,5] – Very high breaching possibility

6 The case of protected coasts with detached breakwaters

6.1 Background

Many of our coasts are already protected by coastal structures such as detached parallel breakwaters which significantly affect incident wave conditions during storms (Figure 6-1). Their existence along a coastal stretch will determine that, in general, any of the potential storm-induced flooding and erosion hazards presented in the previous chapters will be lower than under non-protected conditions. Due to this, in order to properly identify hotspots along the coast, it should be necessary to account their effect on such hazards to avoid an overprediction of their intensity which may lead to identify "false" hotspots.

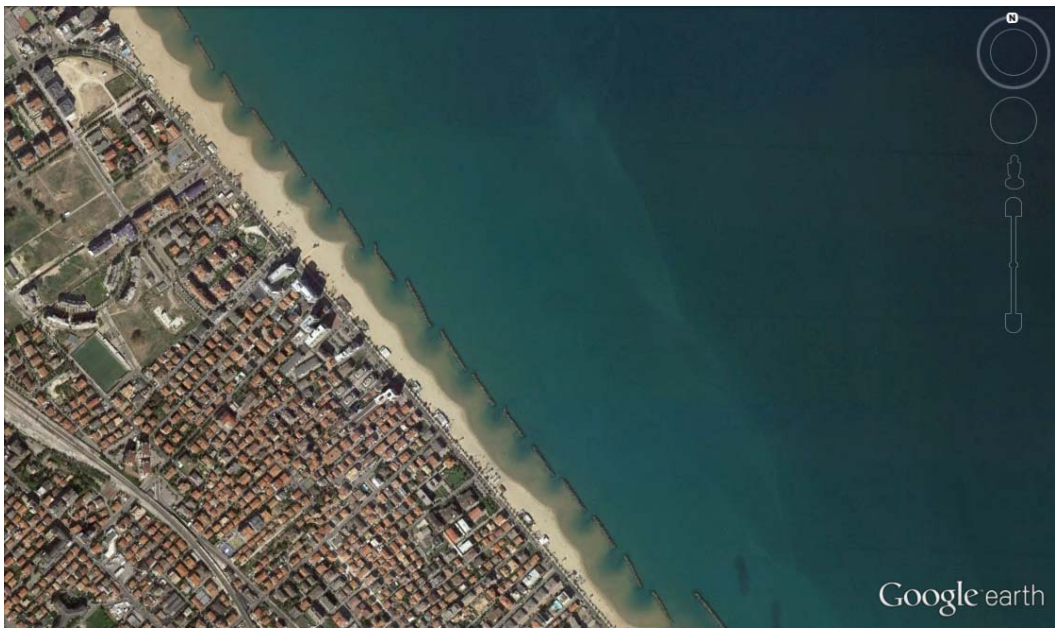

Figure 6-1: Coast protected by detached breakwaters in Pescara (Italy).

The real degree of protection results from the combination of structure's parameters and storm conditions which will determine wave conditions in the leeside of the structure and, thus, impacting on the shoreline. Due to this, to properly assess the impact of the storm in terms of flooding and/or erosion in this type of protected coasts, it is necessary to account for the effect of the presence of the structure on the incident wave field.

In the following, this problem is analyzed just focussing on its effect on coastal flooding as the main hazard, since most of the existing models (presented in chapter 3) use offshore wave information which clearly does not reflect the effect of protection. However, this procedure should also be applicable to assess erosion when the magnitude of the hazard is calculated using a structural function as outlined in chapter 4, which usually also depend on deepwater wave characteristics.

The procedure is here presented at the most detailed level, which implies to calculate the effect of a given structure on wave conditions by using detailed information.

However, since the spatial scale of application of the Hazard Assessment Module is regional (O(100 km)) and, the main objective is to identify hotspots which will be further defined by using detailed models, its application can be adapted. Thus, instead of applying the methodology individually to each structure, it could be possible to define a "characteristic structure" for a given coastal sector (O(1km)), in such a way that the estimated effect should be applicable to the entire sector. The scale of application of the methodology in each site will depend on local conditions (e.g. number of structures or extension of the protected coast, existing information) but, in any case, its application should imply that the magnitude of considered storm-induced hazards in the area will be lower than in non-protected coasts.

6.2 Wave Transmission

The computation of wave-induced runup in a beach protected by a detached breakwater during a storm requires to account for the dissipation effect generated by the breakwater on incident wave conditions. The first question that arises is how to compute the transmission coefficient (K_t) given a breakwater with specific characteristics, in order to calculate the transmitted wave height (H_t). The second question is how to use the transmitted wave height into common runup formulas for natural beaches considering that all formulas use the deepwater wave conditions.

In this chapter, we present the approach applied along the Emilia-Romagna coastline (Armaroli et al., 2009b; Harley and Ciavola, 2013), together with a short review of different formulas available in the literature to compute the transmission coefficient, namely Van der Meer and Daemen (1994), d'Angremond et al. (1996) and Van der Meer et al. (2005).

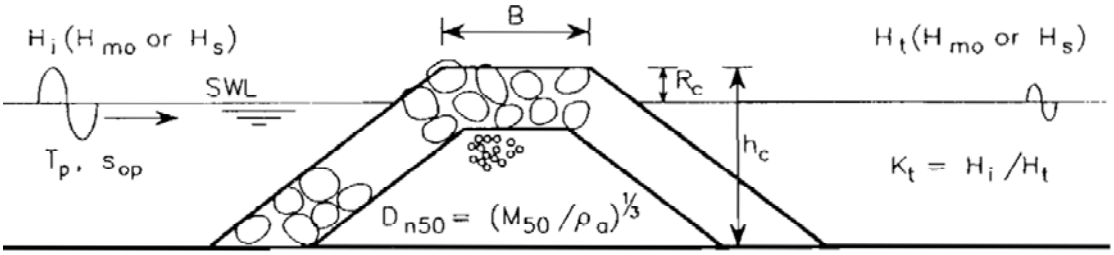

Figure 6-2: LCS and main parameters that have to be considered when dealing with wave transmission (Van der Meer and Daemen, 1994).

Figure 6-2 shows a typical section of a parallel breakwater used for coastal protection, a statically stable LCS, which is defined as "*low-crested breakwaters close to non- or marginally overtopped structures*" (Van der Meer and Daemen, 1994). These LCS are more stable than other structures because a large part of the wave energy can pass over the breakwater (Van der Meer and Daemen, 1994). When a wave approaches a LCS, part of its energy is dissipated through wave breaking, on and over the structure, and part of the energy is reflected. Thus, only part of it is transmitted through wave transmission and overtopping. Most of the wave energy is transmitted in the lee of the breakwater through overtopping, while a limited amount of energy is transmitted by wave infiltration through the permeable layer of the upper part of the rubble mound.

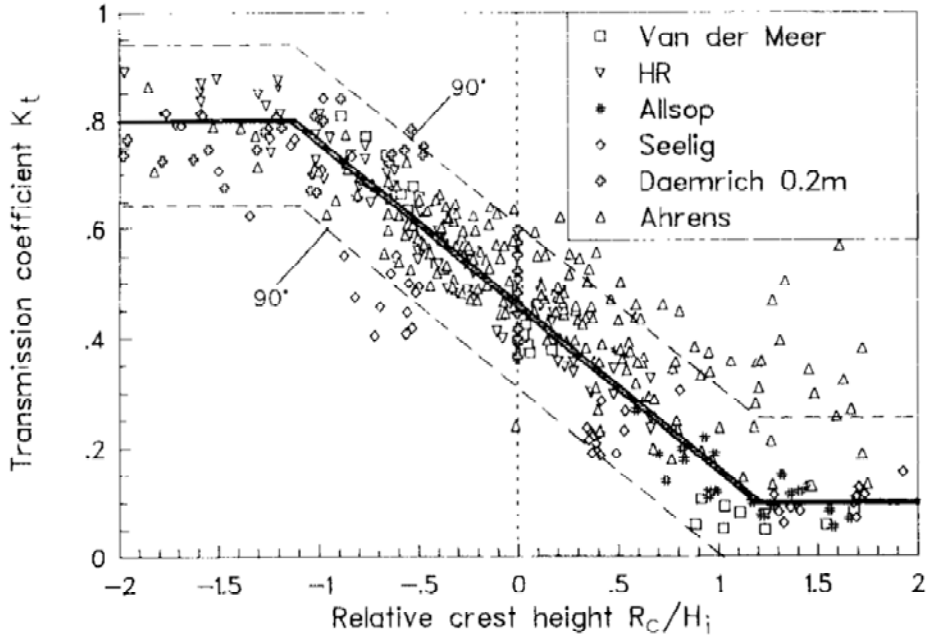

Figure 6-3: Transmission coefficient versus relative crest height. The dashed bands indicate the 90% confidence interval (Van der Meer and Daemen, 1994).

Figure 6-3 shows the results obtained by Van der Meer and Daemen (1994) in a reanalyse of a series of laboratory tests on wave transmission in form of transmission coefficient *vs* relative crest height (R_c/H_i). As it can be seen, although a clear trend is observed, a large scatter is also visible. According to the authors, the scatter is associated to the effects of wave period, the presence of extremely small waves and, also to the influence of crest width (B) and permeability (Dn_{50}).

The formula proposed by the Van der Meer and Daemen (1994) to compute K_t is:

$$\text{for } -2.0 < \frac{R_c}{H_i} < -1.13 \qquad K_t = 0.80$$

$$\text{for } -1.13 < \frac{R_c}{H_i} < 1.2 \qquad K_t = 0.46 - 0.3\,\frac{R_c}{H_i} \qquad (6.1)$$

$$\text{for } 1.2 < \frac{R_c}{H_i} < 2 \qquad K_t = 0.10$$

The 90% confidence levels are given by $K_t \pm 0.15$. Results showed in Figure 6-3 indicate that for large negative values of R_c/H_i (breakwaters with R_c largely below SWL), K_t should approach 1 (full transmission, $H_t \approx H_i$), while for large positive values (breakwaters with R_c largely above SWL), K_t should approach 0 (no transmission).

To take into account the effect of wave steepness (s_{op}), crest width (B) and nominal diameter of armour rocks (Dn_{50}) on the transmission coefficient, the authors reanalysed the data and found a new relation between K_t and the relative crest height (R_c/D_{n50}), relative crest width (B/D_{n50}) and wave steepness. The formula is:

$$K_t = a \frac{R_c}{Dn_{50}} + b \quad (6.2)$$

where,

$$a = 0.031 \frac{H_i}{Dn_{50}} - 0.024 \quad (6.3)$$

$$b = -5.42\, s_{op} + 0.0323 \frac{H_i}{Dn_{50}} - 0.017 \left(\frac{B}{Dn_{50}} \right)^{1.84} + 0.51 \quad (6.4)$$

where s_{op} is calculated using the peak wave period T_p. The formula is valid for $0.075 < K_t < 0.75$. The authors state that the formula is valid also outside the given range, but its reliability decreases.

Van der Meer et al. (2005) reanalysed a series of datasets collected in laboratory experiments in order to define the reliability of the Van der Meer and Daemen (1994) (6.2) and the d'Angremond et al. (1996) formula, which is given by:

$$K_t = -0.4 \frac{R_c}{H_i} + 0.64 \left(\frac{B}{H_i} \right)^{-0.31} (1 - e^{-0.5\xi op}) \quad (6.5)$$

Where ξ_{op} is the breaker parameter ($tan\alpha/(s_{op})^{0.5}$) that is related to the seaward slope of the structure ($tan\alpha$). This formula does not include the nominal diameter of armour rocks, while it considers the relative freeboard height (R_c/H_i) and the relative crest width (B/H_i). The formula is valid for K_t values between 0.075 and 0.8. The comparison between measured and calculated K_t using both (6.2) and (6.5) formulas revealed that the (6.2) formula of Van der Meer and Daemen (1994) gives a larger scatter than the d'Angremond et al. (1996) formula. Thus, only a reanalysis of the (6.5) formula is presented in Van der Meer et al. (2005), producing a different equation:

$$K_t = -0.35 \frac{R_c}{H_i} + 0.51 \left(\frac{B}{H_i} \right)^{-0.65} (1 - e^{-0.41\xi op}) \quad (6.6)$$

This formula is valid for rubble mound LCS with large and very large crest widths (i.e. $B/H_i > 10$). For LCS with small crest widths (i.e. $B/H_i < 10$) the d'Angremond et al. (1996) formula (6.5) is still valid. Because of a discontinuity of the given functions for $B/H_i = 10$, for practical application it is recommended to apply (6.5) for $B/H_i < 8$, (6.6) for $B/H_i > 12$ and to linearly interpolate K_t for $8 < B/H_i < 12$.

There are some important restrictions that were taken into account by Van der Meer et al. (2005) that have to be outlined. First, waves with high steepness values ($s_{op} > 0.07$) are not stable and are likely to break well before being transmitted and were not taken into account in the reanalysis. Furthermore, waves with very low steepness (long waves, $s_{op} < 0.002$) are difficult to be generated in a flume, where the studies presented here were undertaken, thus waves with $s_{op} < 0.002$ were discarded.

6.3 Procedure

In what follows, a description of the methodology to account for the effects of LCS on the computation of wave-induced runup adopted in the Emilia-Romagna region is presented together with an example of its application. A special emphasis is put on the description of the practical procedure to select/calculate each variable at the different steps.

As previously mentioned, this procedure is designed to be applied at the most detailed scale (to one specific structure). At regional scale, and depending on local characteristics (e.g. length of protected coastline) and/or level of detail required by local stakeholders, it can be simplified by applying it to a "characteristic structure" with average representative structure dimensions (e.g. crest width, depth, freeboard). Although this will result in a less precise quantification of wave height modification, it can be enough for the purpose of this framework, i.e. hotspot identification.

The first step when dealing with the calculation of H_t is to compute H_i values for deep water wave conditions during the storm. The required information is:

H_s, T_p, Dir = deepwater wave characteristics.

$tan\gamma$ = Seafloor slope seaward of the structure (at least down to the closure depth).

h_L and h = water depth at the toe of the landward and seaward sides of the structure.

Variables related to bottom configuration ($tan\gamma$, h_L, h) are derived from existing bathymetric data. To notice that some structures might show scour holes at the seaward foot generated by wave reflection. It is recommended not to measure the water depth at the scour hole but at a closer location, where the seafloor is more regular. If the water depth at the landward side of the structure is not available or difficult to measure, it can be assumed that the seafloor is symmetrical on both sides of the breakwater (same depth).

To find H_i at the toe of the structure, waves have to be propagated towards the coast. Unless a very complicated bathymetry does exist, as an approximation, the Snell law can be applied. Once H_i is known, it has to be transmitted in the lee of the structure using one of the formulas mentioned above. The most important information to know on LCS characteristics is the freeboard R_c. It can be derived from Lidar data or from direct surveys. Alternatively, if the original project document designed to build the structure is available, the nominal R_c value can be used. It should be considered that, if the LCS was built some time ago, the actual R_c value can be different from the original one. The difference can be due to subsidence, if applicable, compaction of seafloor sediments, both natural and induced by the weight of the structure itself, adjustment of armour rocks of the top of the structure and compaction of its finer core. Furthermore, the LCS could have been damaged by storm waves (e.g. the rocks could have fallen down), reducing the R_c height above SWL. The recommendation is to use the most recent information gathered through direct surveys, if possible. If only the R_c value is known, the van der Meer and Daemen (1994) equation 6.1 can be applied (Armaroli et al., 2009b), keeping in mind that the formulations are simple and the scatter of the data is significant (Figure 6-2).

Another information that can be derived from direct surveys is the crest width (B). Again, it can be extracted from Lidar data, if available, or through direct surveys of the

LCS crest (Harley and Ciavola, 2013). To notice that whenever a topographic Lidar is used, the effect of the tide in controlling the emerged width of the structure can be significant. In cases of sufficient water clarity, colour aerial photography may be used. Dn_{50} can be derived from information included in the document with the original project or, again, from direct measurements (Harley and Ciavola, 2013). It should be outlined that the nominal Dn_{50} value can be different from the actual value, because of maintenance interventions carried out to fix the structures or to renovate/modify the LCS through time, using different stones than the original ones. If B values, as well as Dn_{50} values, are available, the van der Meer and Daemen (1994) equation 6.2 can be applied. However, van der Meer et al. (2005) found that the equation of van der Meer and Daemen (1994) generates a significant scatter if compared to measured K_t, thus the authors recommend to use the d'Angremond et al. (1996) for $B/H_i < 8$ (eq. 6.5) and the formula of van der Meer et al. (2005) for values of $B/H_i > 12$ (eq. 6.6), and to linearly interpolate K_t values between these two boundaries. Both (6.5) and (6.6) formulas include ξ_{op} that is the breaker parameter, which includes the seaward slope of the LCS. This parameter is difficult to measure in prototype conditions (while in laboratory flumes it is easily measurable). The nominal value designed when the LCS was built can differ from the real value due to the modifications induced on the structure by waves, currents, sediment compaction, etc. Nevertheless, if it is not possible to directly measure $tan\alpha$, the seaward LCS slope can be assumed to be unchanged from the designed one and the nominal value can be used (Harley and Ciavola, 2013).

Once modified wave conditions due to the presence of the structure are computed (H_t) this has to be converted to deepwater wave conditions to be used in the selected runup model. To do this, transmitted waves have to be refracted back to deepwater by using, as it was previously done, the Snell law. If no wave direction is considered the only involved process to be modified should be shoaling. This will result in a deepwater wave height lower than the initial one since it is accounting for the effects of the coastal protection structure.

Harley and Ciavola (2013) applied this methodology to evaluate the efficiency of temporary flood protection measures created to prevent damage and inundation of the rear part of the beach along the Emilia-Romagna coast. The analysis was performed through the XBeach 2D model. Values of K_t calculated with the model were compared to those computed with the van der Meer et al. (2005) and d'Angremond et al. (1996) formulas, for different model configurations. Authors measured the LCS characteristics (R_c, B, Dn_{50}) with an RTK-DGPS at Lido di Classe, while for Lido di Dante the nominal values were used. The only information taken from the literature for both sites was the seaward slope of the structures (i.e. 1/2). The comparison between XBeach-derived K_t and empirical K_t, as stated by the authors, shows a good agreement at Lido di Dante (where the LCS freeboard is at 0.0 m MSL) under different storm and surge conditions, while the empirical values underpredict K_t for Lido di Classe, especially for low surge levels (LCS freeboard is 0.6 m above MSL). Nevertheless the authors conclude that equation 6.6 gives the best agreement.

Finally, it should be outlined that it is important to use the most reliable data, measured or extracted from charts/reports, because the computation chain includes a number of formulas with a relatively large uncertainty (van der Meer et al., 2005;

Harley and Ciavola, 2013), and, if an error is introduced together with the input information, it is then amplified down to the final output.

6.4 Example of application

In what follows the outlined methodology is applied to the protected coast of the Emilia-Romagna region. The analysis was carried out through cooperation activities between the University of Ferrara and the Regional Geological Service to define the vulnerability of the coastline along profile lines (extracted from a 2004 Lidar DTM), equally spaced along the coast (almost 500 m). Three worst case scenarios were designed for three return period events (1-in-1, 10 and 100 year), considering the concomitant happening of storms and surge levels with the same return period, plus Spring High Tidal levels (0.45 above MSL). Wave parameters were used to compute run-up along 187 profile lines. Beach slopes were computed along every profile. The resulting total water level was then compared to the elevation of the rear beach and to the location and elevation of infrastructures located on or close to the beach, in order to develop ten vulnerability typologies. Further details are given in Ciavola et al. (2008); Armaroli et al. (2009a,b; 2012a, b; 2013) and Armaroli and Perini (2012).

First, the freeboard elevation of LCS was extracted from Lidar data (2004). Using the Lidar Data Handler Tool (developed by USGS) of Arcgis®, a longitudinal section of each breakwater was extracted to obtain the R_c value. Because the breakwaters are quite old the values extracted from the Lidar grid were, most of the times, significantly different (even less than a half) than the nominal value (1.5 m above MSL; Idroser, 1982). Moreover, the longitudinal section of the Lidar grid, extracted with the Lidar Data Handler Tool, returned scattered elevation data. The scatter is generated not only by the non-uniform surface of the rubble mound, that is composed of large rocks, but also by maintenance activities carried out to fix or renovate the structures. The impact induced by waves on the upper part of the LCS is also an important component. The difference between the extracted elevations and the nominal values is also due to subsidence rates that, along the Emilia-Romagna coastline, can reach 0.02 m/year (Ravenna area; Teatini et al., 2005). Several structures were also modified through time (elevated, elongated, reshaped) to implement their efficiency. It was decided to compute a mean R_c value, excluding values below +0.5 m MSL, to take into account the resolution of the Lidar. The water depth at the seaward toe of the structure was instead evaluated through the analysis of cross-shore topo-bathymetric profiles carried out by ARPA (the Regional Environment Agency) in 2000. Scour holes, when present, were avoided and the water depth was measured at a closer location, where the seafloor was “regular”. The same bathymetric profiles were used to measure the seafloor slope (between 0.003 and 0.005 along the Emilia-Romagna coast) down to the closure depth, that is between 6 and 7 m below MSL. The wave height of each return period was then propagated to the toe of the structure. Because Dn_{50} values were not available for the whole coastline, the van der Meer and Daemen (1994) formula was used (6.1). Wave direction was set to 90° N (from the East for the Emilia-Romagna coastline) to exclude refraction, as waves approach is parallel to the breakwater.

Table 6-1: Wave conditions and surge associated to a T_R = 1 year used for the computation of the transmission coefficient and transmitted wave height.

Direction (° N)	Hs (m)	Tp (s)	Surge (m)
30°	3.3	7.2	0.85
60°	3.6	7.4	
90°	3.5	8.4	
120°	2.8	7.8	
mean	3.3	7.7	0.85

The values of R_c were corrected as follows (Armaroli et al., 2009b), to take into account the designed worst case scenarios where the tide and surge elevation are included:

$R_c^* = R_c - 0.45 - surge_{T1,10,100}$

where 0.45 is the tidal level (spring tides), R_c is the freeboard elevation extracted from Lidar data and $surge_{T1,10,100}$ are the surge elevations extracted from the literature, one level for each scenario. The same correction was applied to the water depth measured at the toe of the structure, landward and seaward sides:

$h^* = h - 0.45 - surge_{T1,10,100}$

$h_L^* = h_L - 0.45 - surge_{T1,10,100}$

Two examples are presented in what follows. The first one corresponds to a profile that is protected by a LCS that has a real freeboard higher than its nominal value (due to maintenance activities, a layer of rocks was added on the top of the structure to strengthen it). The second example is, on the contrary, a LCS with an elevation smaller than the half of its nominal value. In the example the T_R = 1 year scenario is used (Table 6-1). To notice that only wave shoaling was calculated, as it was decided to use a mean value of wave height and period for each return period event, to which it was associated a wave direction of 90° N.

1) Example 1: R_c above nominal value

h = –3.58 m $\quad$ h^* = –4.88 m

h_L = –2.10 m $\quad$ h_L^* = –3.40 m

R_c = 1.28 m $\quad$ R_c^* =–0.02 m

then:

H_i = 3.35 m

$\frac{R_c^*}{H_i} = -0.006$

Thus applying (6.1):

$K_t = 0.462$

And finally,

$H_t = K_t H_i = 1.55$ m

The value of H_t is then back-propagated to deep-water conditions to obtain $H_o = 1.43$ m, which is the value to be used to calculate run-up values along protected beaches.

2) Example 2: R_c less than a half of the nominal value.

$h = -3.76$ m $\quad h^* = -5.06$ m

$h_L = -1.85$ m $\quad h_L^* = -3.15$ m

$R_c = 0.68$ m $\quad R_c^* = -0.62$ m

Following the same procedure and applying (6.1) ($H_i = 3.33$ m, $R_c^*/H_i = -0.19$ and $K_t = 0.52$) results $H_t = 1.72$ m. The deep-water (transmitted) wave height H_o is then 1.57 m, thus higher than the previous example, as expected.

If the same examples are used to find K_t without the influence of surge and tide levels the results should be: Example 1, $H_{t\infty} = 1.04$ m; Example 2, $H_{t\infty} = 1.15$ m, both values are lower than the previous ones, as the dissipating effect of the breakwater is higher.

To assess the influence of this on the magnitude of the hazard, the previous example is now used to compute the wave-induced runup in a protected beach with and without the attenuation effect. A beach profile with slope, $tan\beta$, of 0.06, from the MSL to the dune foot, is taken here as example. The Iribarren number for the $T_R = 1$ year event (Table 6-1) is $\xi = 0.32$. By applying the Stockdon et al. (2006) model, $R_{u2\%}$ is 1.15 m. If the attenuation effect calculated in example 1 is taken into account ($H_{t\infty} = 1.43$ m, $T_p = 7.7$ s and $Dir = 90°$N), $R_{u2\%}$ is 0.76 m. If same computations are carried out considering the attenuation effect but excluding the influence of surge and tide levels ($H_{t\infty} = 1.04$ m, $T_p = 7.7$ s and $Dir = 90°$N), $R_{u2\%}$ should be 0.65 m. As it can be seen, the inclusion of the attenuation effect of the presence of the submerged breakwater results in a smaller hazard (wave-induced runup during the storm), which is also affected by the inclusion or not of a simultaneous storm surge.

The approach presented in these guidelines, although developed for LCS, can be adopted for other types of shore-parallel detached defences, even if different formulas may have to be applied. A similar methodological procedure can also be applied for the computation of run-up values on beaches protected by coral-reefs, which act in a similar way in dissipating incoming wave heights. In this case the literature of simple transmission formulas is scarcer and a recent work by van Dongeren et al. (2013) used a more sophisticated numerical approach like XBeach.

7 XBeach 1D

7.1 Introduction

In the previous chapters, a range of empirical formulations is provided for a number of identified hazards that can occur separately or simultaneously. These can be tuned to local conditions and since they require practically no computational effort are very suitable for a probabilistic approach.

However, in cases with unusual profile shapes, types of beaches or conditions for which such empirical approaches have not yet been derived, an alternative may be to use process-based modelling, for instance with the XBeach model (Roelvink et al., 2009, 2015).

In the report RISCKIT D.3.2 Improvement of Physical Processes previously published to the present report, validation of XBeach is reported for a number of hazards relevant to the CRAF, on top of proven skill for parameters such as dune erosion volume. Since 1D profile-mode simulations with XBeach are not too time-consuming, especially when one focuses on the period around peaks of storms, we present in this Chapter an alternative to the proposed parametric/empirical estimates for some of the considered hazards.

7.2 Short description of 1D XBeach

XBeach was originally developed as a short-wave averaged but wave-group resolving model, allowing resolving the short wave variations on the wave group scale and the long waves associated with them. Since the original paper by Roelvink et al. (2009) a number of additional model options have been implemented, thereby allowing users to choose which time-scales to resolve:

- Stationary wave model, efficiently solving wave-averaged equations but neglecting infragravity waves; This option is not appropriate for extreme-event modeling and will be skipped further.
- Surfbeat mode (instationary), where the short wave variations on the wave group scale (short wave envelope) and the long waves associated with them are resolved.
- Non-hydrostatic mode (wave-resolving), where a combination of the non-linear shallow water equations with a pressure correction term is applied, allowing to model the propagation and decay of individual waves.

In the following these options are discussed in more detail. It is important to note that all times in XBeach are prescribed on input in morphological time. If you apply a morphological acceleration factor (keyword: *morfac*) all input time series and other time parameters are divided internally by *morfac*. This way, you can specify the time series as real times, and vary the *morfac* without changing the rest of the input files (keyword: *morfacopt = 1*).

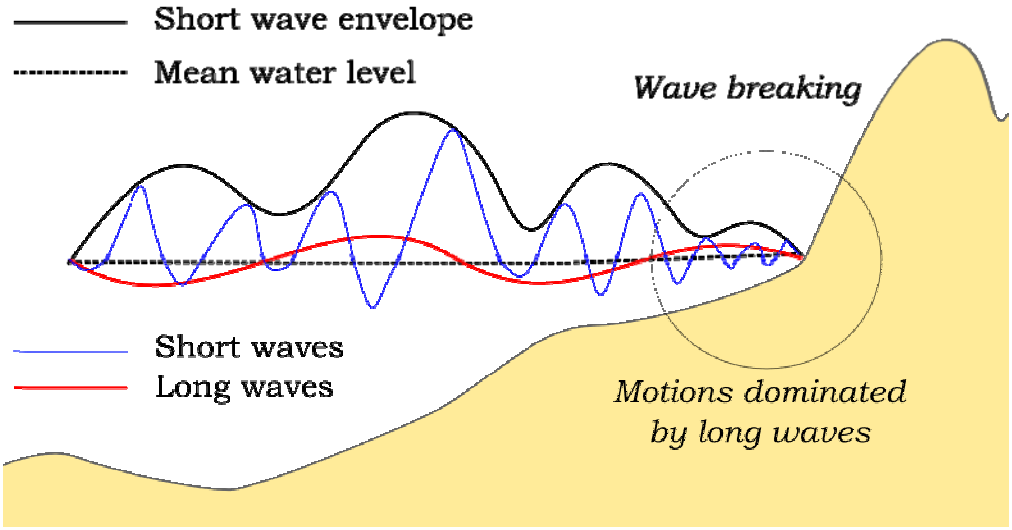

Figure 7-1: Principle sketch of the relevant wave processes.

7.2.1 Surf beat mode (instationary)

The short-wave motion is solved using the wave action equation which is a time-dependent forcing of the HISWA equations (Holthuijsen et al., 1989). This equation solves the variation of short-waves envelope (wave height) on the scale of wave groups. It employs a dissipation model for use with wave groups (Roelvink, 1993a; Daly et al., 2012) and a roller model (Svendsen, 1984; Nairn et al., 1990; Stive and de Vriend, 1994) to represent momentum stored at the surface after breaking. These variations, through radiation stress gradients (Longuet-Higgins and Stewart, 1962, 1964) exert a force on the water column and drive longer period waves (infragravity waves) and unsteady currents, which are solved by the nonlinear shallow water equations (e.g. Phillips, 1977; Svendsen, 2003). Thus, wave-driven currents (longshore current, rip currents and undertow), and wind-driven currents (stationary and uniform) for local wind set-up, long (infragravity) waves, and runup and rundown of long waves (swash) are included.

Using the surfbeat mode is necessary when the focus is on swash zone processes rather than time-averaged currents and setup. It is fully valid on dissipative beaches, where the short waves are mostly dissipated by the time they are near the shoreline. On intermediate beaches and during extreme events the swash motions are still predominantly in the infragravity band and so is the runup.

Under this surfbeat mode, several options are available, depending on the circumstances:

- **1D cross-shore;** in this case the longshore gradients are ignored and the domain reduces to a single gridline (keyword: *ny = 0).* Within this mode the following options are available:
    - Retaining directional spreading (keyword: *dtheta* < *thetamax* – *thetamin*); this has a limited effect on the wave heights because of

refraction, but can also allow obliquely incident waves and the resulting longshore currents.
  - Using a single directional bin (keyword: *dtheta* = *thetamax* – *thetamin*); this leads to perpendicular waves always and ignores refraction. If the keyword *snells = 1* is applied, the mean wave direction is determined based on Snell's law. In this case also longshore currents are generated.

- **2DH area;** the model is solved on a curvilinear staggered grid (rectilinear is a special case). The incoming short wave energy will vary along the seaward boundary and in time, depending on the wave boundary conditions. This variation is propagated into the model domain. Within this mode the following options are available:
  - Resolving the wave refraction 'on the fly' using the propagation in wave directional space. For large directional spreading or long distances this can lead to some smoothing of groupiness since the waves from different directions do not interfere but their energy is summed up. This option is possible for arbitrary bathymetry and any wave direction. The user must specify the width of the directional bins for the surfbeat mode (keyword: *dtheta*).
  - Solving the wave direction at regular intervals using the stationary solver, and then propagating the wave energy along the mean wave direction. This preserves the groupiness of the waves therefore leads to more forcing of the infragravity waves (keyword: *single_dir = 1*). The user must now specify a single directional bin for the instationary mode (*dtheta = thetamax - thetaminn)* and a smaller bin size for the stationary solver (keyword: *dtheta_s)*.
  - For schematic, longshore uniform cases the mean wave direction can also be computed using Snell's law (keyword: *snells = 1*). This will then give comparable results to the *single_dir* option.

In the figures below some typical applications of 1D and 2D models are shown; a reproduction of a large-scale flume test, showing the ability of XBeach to model both short-wave (HF) and long-wave (LF) wave heights and velocities (Figure 7-2); and a recent 2DH simulation (Nederhoff et al., 2015) of the impact of hurricane Sandy on Camp Osborne, Brick, NJ (Figure 7-3). Obviously, for use in the CRAF we envisage predominant use of the 1D mode.

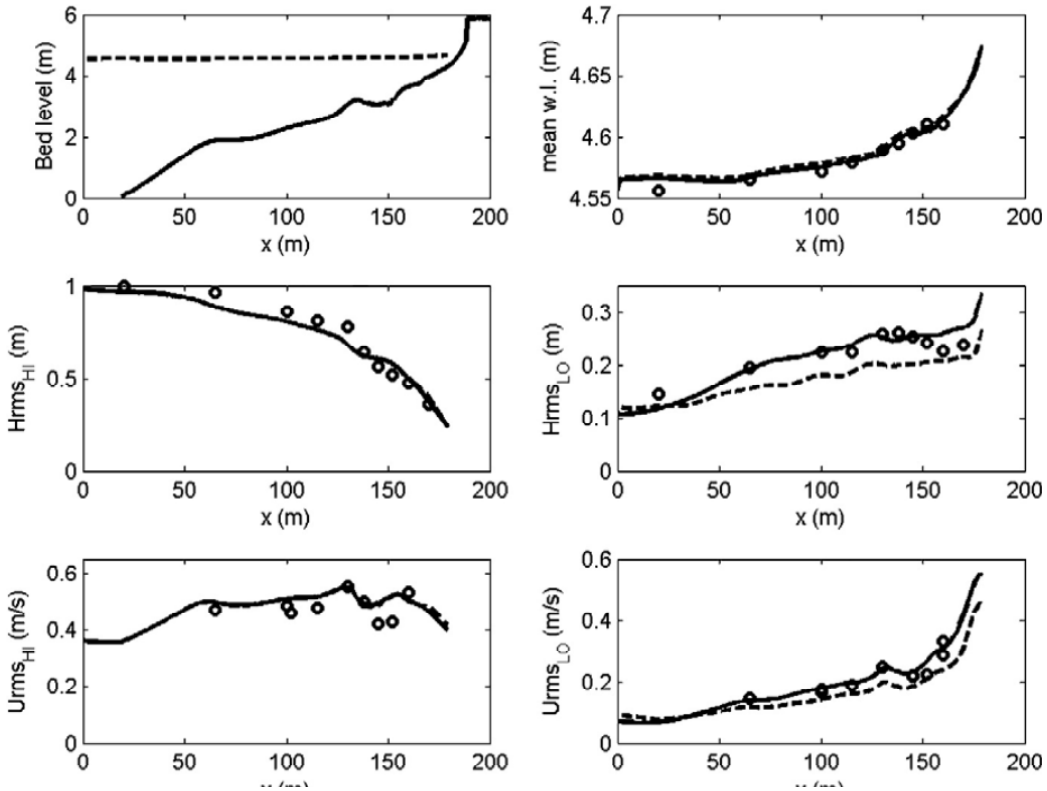

Figure 7-2. Computed and observed hydrodynamic parameters for test 2E of the LIP11D experiment. Top left: bed level and mean water level. Top right: measured (dots) and computed.

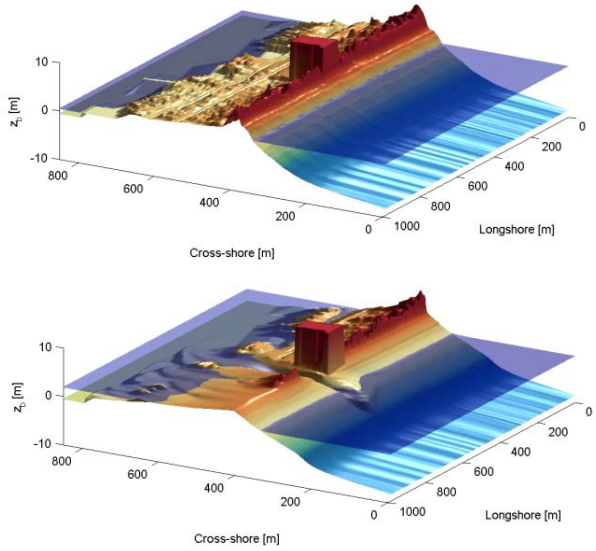

Figure 7-3. Pre (top) and post-Sandy (bottom) in a three dimensional plot with both bed and water levels as simulated by XBeach (Nederhoff et al. 2015).

7.2.2 Non-hydrostatic mode (wave resolving)

For non-hydrostatic XBeach calculations (keyword: *wavemodel = nonh*) depth-averaged flow due to waves and currents are computed using the non-linear shallow water equations, including a non-hydrostatic pressure. The depth-averaged normalized dynamic pressure (q) is derived in a method similar to a one-layer version of the SWASH model (Zijlema et al. 2011). The depth averaged dynamic pressure is computed from the mean of the dynamic pressure at the surface and at the bed by assuming the dynamic pressure at the surface to be zero and a linear change over depth.

Under these formulations dispersive behavior is added to the long wave equations and the model can be used as a short-wave resolving model. Wave breaking is implemented by disabling the non-hydrostatic pressure term when waves exceed a certain steepness, after which the bore-like breaking implicit in the momentum-conserving shallow water equations takes over.

In case the non-hydrostatic mode is used, the short wave action balance is no longer required. This saves computation time. However, in the wave-resolving mode we need much higher spatial resolution and associated smaller time steps, making this mode much more computationally expensive than the surfbeat mode.

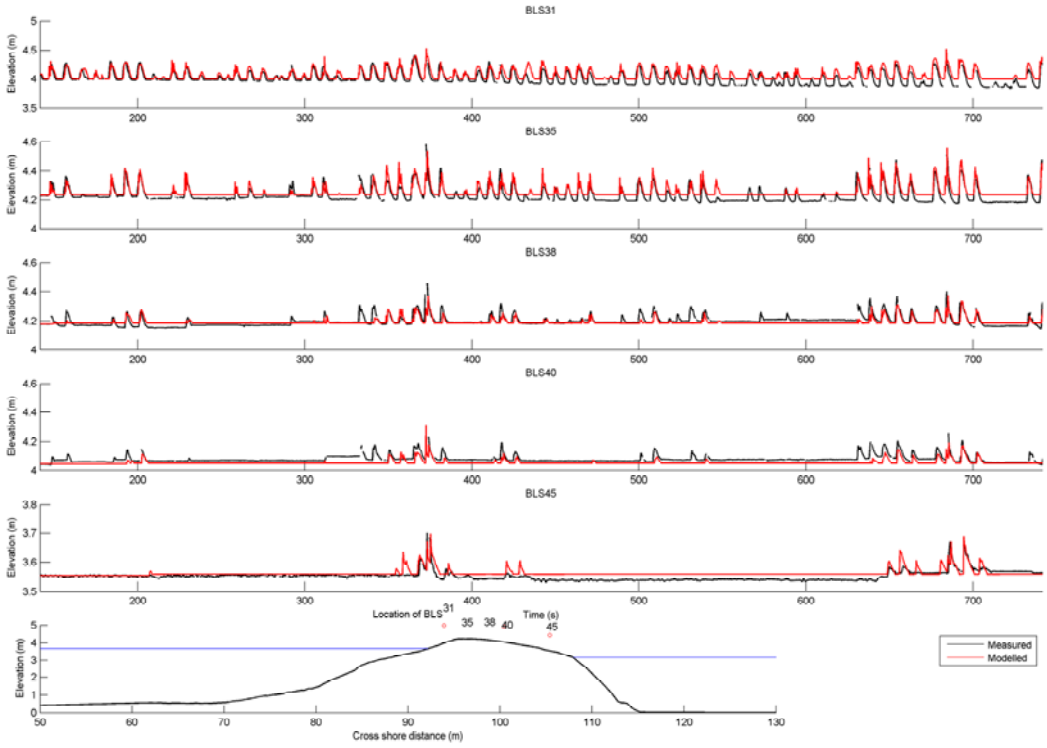

Figure 7-4. Measured (black) and modeled (red) time series of overtopping during BARDEX experiment (McCall et al. 2014).

The main advantages of the non-hydrostatic mode are that the incident-band (short wave) runup and overwashing are included, which is especially important on steep slopes such as gravel beaches. Another advantage is that the wave asymmetry and skewness are resolved by the model and no approximate local model or empirical formulation is required for these terms. Finally, in cases where diffraction is a

dominant process, wave-resolving modeling is needed as it is neglected in the short wave averaged mode. The XBeach-G formulations for gravel beaches (McCall et al. 2014) are based on the non-hydrostatic mode.

7.3 1D model setup and required inputs

7.3.1 Selection of simulation mode

Per section of coast, or sometimes per profile, a selection must be made which simulation mode to apply:

- Sandy beaches with dunes.
    - Standard XBeach approach applies; caution and local calibration is needed for open ocean beaches with coarser sediment, where asymmetry transport factor needs to be enhanced.
- Coasts with dikes or hard boulevards where overtopping is a major issue but morphology change is less important.
    - We recommend the nonhydrostatic version as it does not cost much more in 1D and gives much better representation of overtopping.
- Gravel beaches.
    - Nonhydrostatic version as implemented in XBeach-G.
- Sandy beaches mixed with steep slopes where overtopping may be a major issue.
    - Nonhydrostatic version including morphology change; we have carried out promising first tests but local validation is strongly recommended.

For simulating a large number of storms and profiles, an important choice is whether to run simulations over whole storm periods or just over the peaks of the storms, say approximately 3-6 hours where the real impacts take place.

7.3.2 Model setup

The model setup can be automated to a high extent using simple Matlab functions. The basic input structure is as follows; for a much more extensive overview we refer to the XBeach manual at XBeach.org.

- A *params.txt* textfile with keyword-oriented input, which describes,
    - Process choices.
    - General parameter settings.
    - Settings for flow, wave, sediment transport and morphology submodels.
    - Numerical and output settings.
    - References to grid and bathymetry files.
    - References to tide time series files.
    - References to wave spectra files or parametric wave spectral inputs.
    - References to sediment thickness file in case of unerodible layers (e.g. hard structures).
- All attribute files referred to in the *params.txt* file; typically files with simple structure that are easy to generate.

As an example of how to set up a series of automated runs we refer to the section on runup validation for Praia de Faro (Portugal) described in the report RISCKIT D.3.2 Improvement of Physical Processes.

An automated Matlab procedure was set up for this validation with the following structure:

- Read all records from the provided matlab datafile.
- For all records:
    - Create a schematized profile with the right swash zone slope; Create a grid with grid sizes decreasing from 10 m at offshore end to 1 m in the swash zone.
    - Interpolate schematized values to the grid.
    - Write XBeach grid and profile files; in case of 2D runs extend the profile uniformly in longshore direction.
    - Generate params.txt and jonswap.txt input files.
    - Run XBeach for 30 minutes.
    - Analyze $R_{2\%}$ runup height.
- Store results and produce time series and scatter plots with regression lines.

All input data, observations and Matlab scripts to generate the results are stored on the XBeach repository, under folder *testcases/Vousdoukas2012_Praia_de_Faro.*

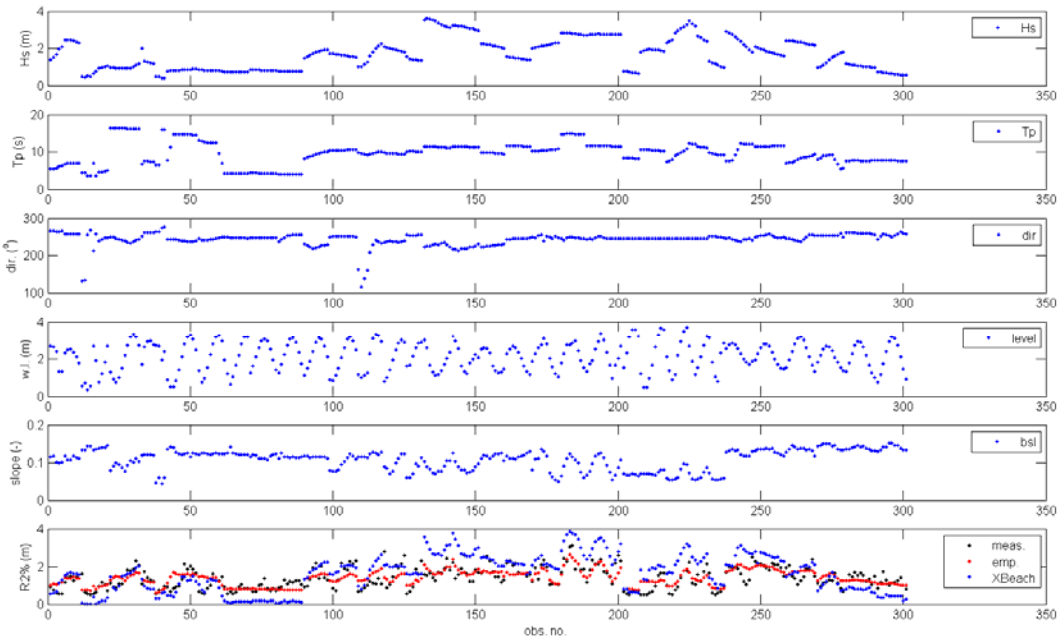

Figure 7-5 Simulations for Vousdoukas et al. 1D surf-beat mode. Panels from top to bottom: *Hs*, *Tp*, mean wave direction (not used in 1D), water level, beach slope in swash zone, $R_{2\%}$.

In this case, the R2% runup height was the only output parameter (hazard) of interest. To give an impression of the kind of results, Figure 7-5 and Figure 7-6 show some of the obtained ones which are fully detailed in the report RISCKIT D.3.2 Improvement of Physical Processes (Roelvink et al. 2015). The results shown are for 1D surfbeat mode simulations; even better reproduction of the measurements is possible with 2DH simulations, even on a longshore uniform grid with coarse resolution; the simulations shown here run very fast (in the order of tens of seconds per run) and are therefore suitable for use in CRAF.

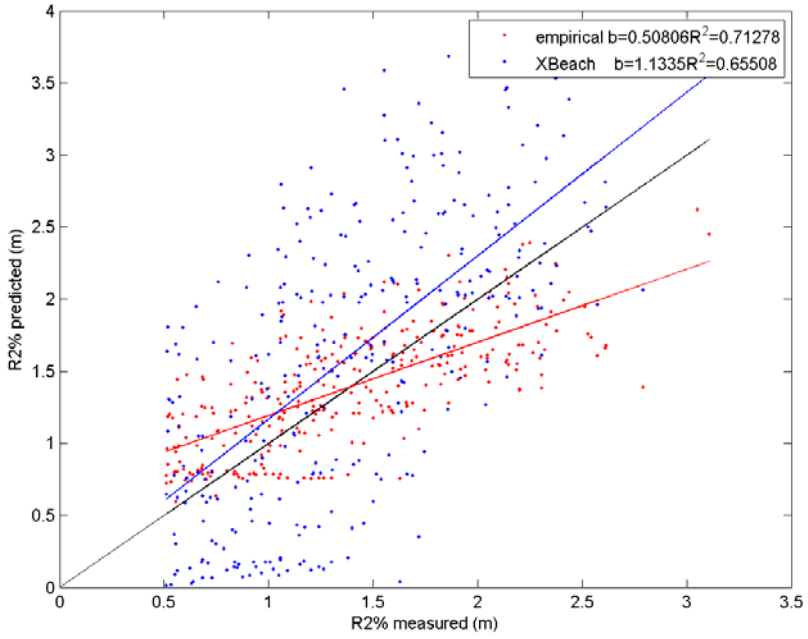

Figure 7-6 Observed vs simulated $R_{2\%}$ run-up height and regression curves; 1D surf-beat.

7.3.3 Summary of required input data

The following data are required:

- Cross-sectional profile.
- Maximum offshore water level or tide level time series (including surge).
- H_{m0} wave height (single value or time series).
- Tp wave period (single value or time series).
- D_{50} of sediment (in case of morphology).
- Thickness of sediment along cross-section (in case of hard structures or unerodible layers).
- Level of bottom of groundwater layer (in case groundwater module is used).
- Permeabilityof groundwater layer (in case groundwater module is used).
- Duration of the run.
- Mode of simulation (surfbeat, nonhydrostatic, XBeach-G).

7.4 Multi-hazard outputs

Since XBeach provides full time-dependent cross-shore distributions of all possible variables such as bed level, water level, wave height, bottom change, cross-shore discharge, current speed etc., dedicated postprocessing is required to retrieve the coastal hazard indicators of interest. Given NetCDF output of the relevant parameters, Matlab functions are available to calculate:

- $R_{2\%}$ runup height (m).
- Mean and peak overtopping discharge ($m^3/m/s$).
- Dune erosion volume (m^3/m).
- Retreat of coastline at specified height.
- Reduction of dune crest height.

7.5 Conclusions

An alternative is presented to the parametric/empirical approaches presented in the previous chapters, in the form of 1D XBeach simulations with appropriate pre- and postprocessing. The proof-of-concept has been shown in the Workpackage 3.2 report where validation exercises have been carried out that included hundreds of runs each.

At present, the methodology consists of a collection of easily adaptable Matlab functions, that can be tailored to specific field sites, simulation modes and available data formats.

8 Flash floods

8.1 Introduction

Flash floods in coastal areas are generally controlled by two main variables: heavy rains and the short response times of the basins. In coastal areas the terrain frequently promotes the convection of warm wet air from the sea, producing (and/or enhancing) convective storms and mesoscale convective systems that sometimes remain stationary over the coastal catchments producing enhanced precipitation with high spatio-temporal variability resulting in local flash floods.

The short response times of coastal basins affected by flash floods (typically of the order of 0.5-6 hours) are the result of the combination of several ingredients:

- *Small catchment areas*. Flash floods typically occur in basins of the order of 0.5-500 km^2, although sometimes flash floods affect larger basins for precipitation events lasting up to 24 hours (Gaume et al., 2009).
- *Steep terrain*. High slopes promote the fast propagation of the flood wave, reducing the hydrograph attenuation during the routing phase.
- *Low permeability*. Factors such as the geology or the soil type and the land use strongly influence the capacity of infiltration of the basin. In highly urbanized catchments, the low permeability promotes the fast propagation of the flood wave and reduces the flood attenuation capacity of the basin. Similarly, factors such as the moisture conditions of the basin or the recent impact of forest fires have important roles on determining the catchment response to certain rainfall events (e.g. Lavabre et al., 1993; Norbiato et al., 2008; Versini et al., 2012).

Finally, the presence of hydrologic/hydraulic structures and measures in the catchment, such as reservoirs, SUstainable Drainage Systems (SUDSs, Butler and Davies, 2011), or narrow stream sections due to structures such as bridges may also play a significant role in the effects of significant runoff events.

In this context, the EU Floods Directive (2007/60/EC) aims to reduce and manage flood risks and prompted the Member States to (i) carry out a preliminary assessment of river basins at risk of flooding by 2011, (ii) draw up flood risk maps by 2013, and (iii) establish flood risk management plans focused on prevention, protection and preparedness by the end of 2015.

This has resulted in a detailed assessment of the areas potentially affected by significant risk of flooding all throughout Europe. In Spain, these areas have been called "Areas with significant potential flooding risk" (ARPSIs; http://www.magrama.gob.es/es/cartografia-y-sig/ide/descargas/agua/ARPSIs.aspx) and have been mapped and characterized by the water authorities in charge of each hydrological area.

As an example, Figure 8-1 shows the areas identified by the Catalan Water Agency (2013) as potentially at risk of flooding in the Tordera basin, which is a case study site of RISC-KIT. These analyses are typically based on crossing the hazard information (obtained as the flooded area calculated with a hydraulic model for a runoff of a given

return period or based on geomorphologic criteria) and the vulnerability maps in the affected areas (as shown in the example of Figure 8-2).

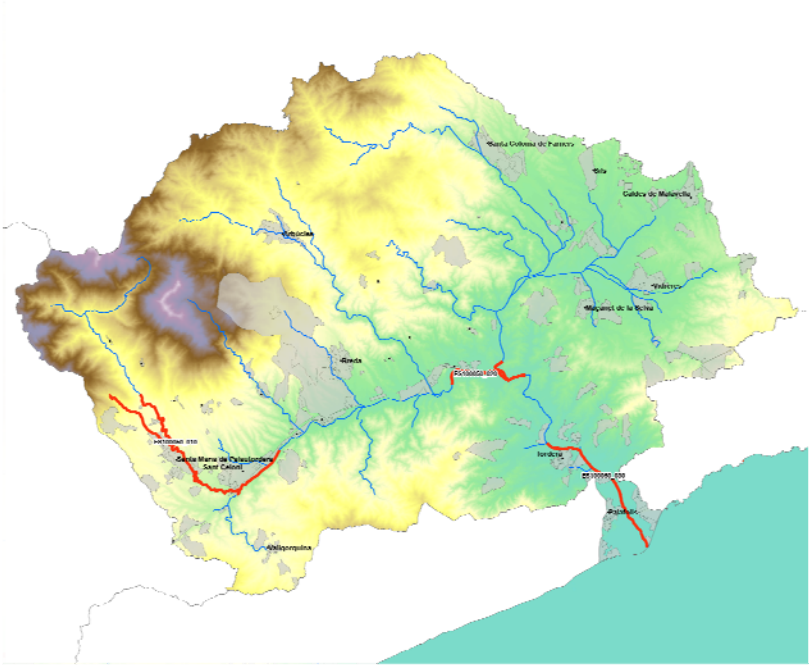

Figure 8-1: Analysis of the Areas of Potential Risk Areas in the Tordera catchment. Catalan Water Agency (http://aca-web.gencat.cat/aca/documents/ca/publicacions/espais_fluvials/prevencio/risc/apri/*9038_01I06_ARPSI_ES100050_v1.pdf).*

Alternatively, the objective of the work proposed here is to implement an automatic method to identify the areas prone to be affected by flash floods (flash flood hotspots) based on the climatic and geomorphological characteristics of the study area. This information is complementary to the real-time flash flood hazard assessment module developed in WP3 (Section 4 of Roelvink et al., 2015), in which, for a given precipitation situation, the flash flood hazard (expressed in terms of the return period) is characterized based on the rainfall accumulation aggregated over the basin upstream of each point of the analysis domain (or basin-aggregated rainfall). In this context, information about the flash flood susceptibility of the areas affected by intense rain provides valuable qualitative information of the expected magnitude of the resulting flash flood.

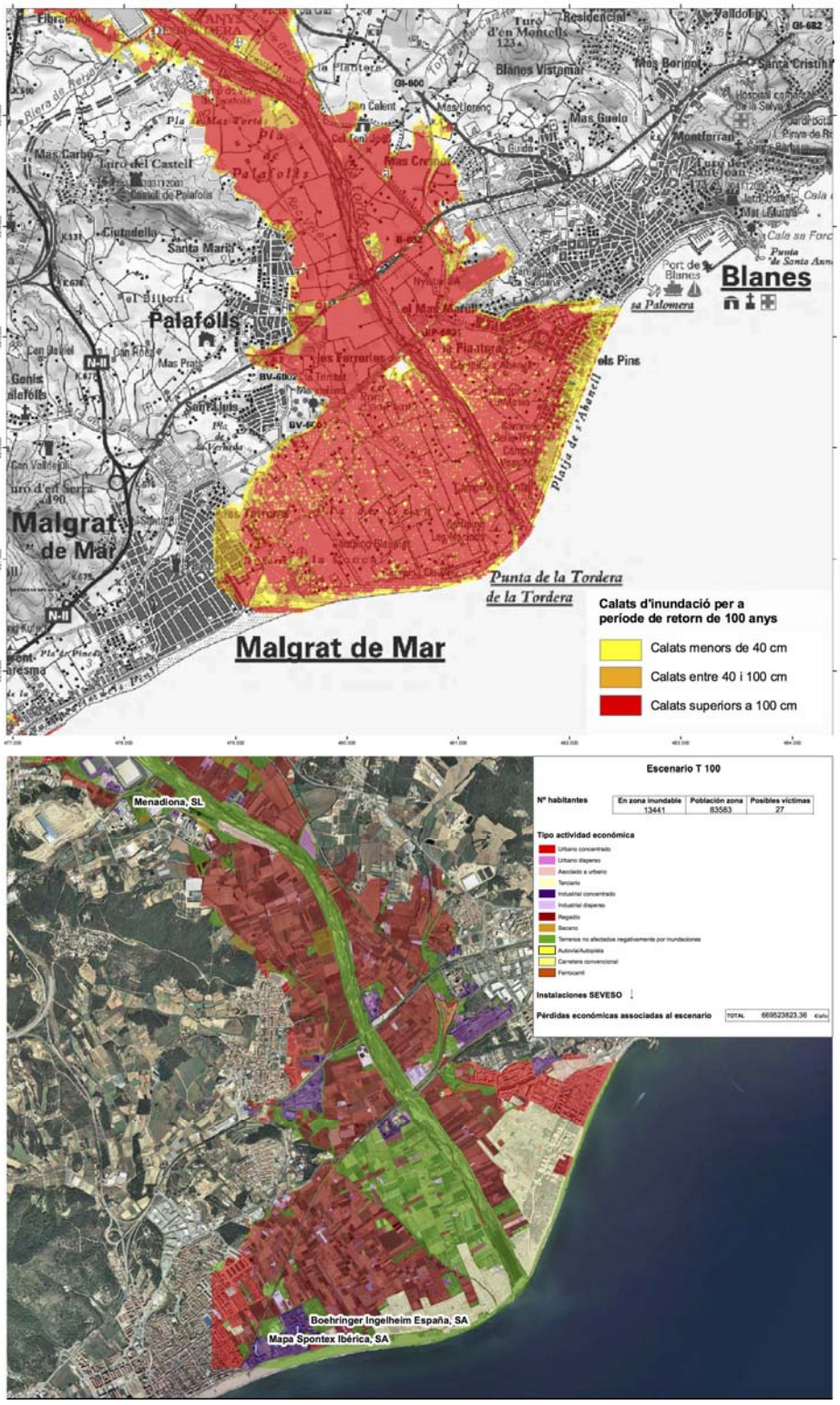

Figure 8-2: Top: Hazard map of flooded areas under a scenario of the 100-year return period flood in the case study site of the Tordera Delta. Bottom: Risk map associated to the 100-year return period flood. Source: Catalan Water Agency (http://aca-web.gencat.cat/aca/documents/ca/publicacions/espais_fluvials/prevencio/risc/apri/09038_01_Planols.htm).

8.2 Description of the ingredients

The analysis of flash flood susceptibility informs us of the likelihood of a dangerous event occurring in an area on the basis of the local conditions. This term is widely used in landslide hazard assessment, but it has been used to identify flash flood hotspots based on geomorphological information (e.g. Collier and Fox, 2003; Smith, 2003 Collier, 2007; Marchi et al., 2010; Versini et al., 2010; Santangelo et al., 2011; Douvinet et al., 2015). The majority of these approaches characterize flash flood susceptibility with arbitrary indexes based on the information extracted from morphologic variables (extracted from Digital Elevation Models), land use and geological maps and climatic information.

Table 8-1: Overview of climatic, hydrological and physical variables that can be useful for characterizing flash flood hotspots (adapted from Ali et al., 2012; Smith, 2013).

Climatic	Daily rainfall statistics.
	Maximum annual daily precipitation.
	Long-term mean annual rainfall.
	Actual or potential evapotranspiration.
Hydrologic	Mean daily flow.
	Mean annual maximum flow date / flood seasonality.
	Slope of the flow duration curve.
	Baseflow indices.
	Long-term ratio of baseflow to runoff.
	Rainfall-runoff lag time.
	Concentration time.
	Runoff coefficient.
	Moisture conditions of the catchment.
Geomorphologic	Drainage area.
	Elevation.
	Catchment slope.
	Topographic index.
	Longest flow path length.
	Channel slope.
	Land use.
	Soil type and geology.

These ingredients are used to identify the catchments with the characteristics (described above) that make them prone to flash floods (see Table 8-1 for a non-exhaustive list of variables that could be used with this aim).

Climatic variables characterize the amounts of precipitation in the area of study. For the analysis of flash flood hotspots, we are typically interested on the upper tail of the distribution (extreme events). Consequently, the information provided by Intensity-Duration-Frequency (IDF) curves is preferred. These tell us the expected rainfall accumulated during a certain duration associated to a certain probability of exceedance (return period).

Probably, runoff observations would be the most useful for monitoring flash flood hot spots (especially in those points where long records exist). However, when the analysis domain is done at regional scale, this information is only limited to a number of points where runoff is monitored. Other variables listed in Table 8-1 such as the concentration time, or the runoff coefficient could be estimated based on hydrological models, and, finally, and, finally, the online monitoring of the moisture conditions of the catchment would require the use of a continuous model (at European scale, the European Flood Awareness system uses the LISFLOOD model; see Thielen et al., 2009) or soil moisture products based on satellite observations.

Finally geomorphologic variables (especially those that can be derived from a Digital Elevation Model or those related to land use) are nowadays available in most of the countries in Europe. Because of this, the variables that have a strong incidence on the hydrological response of the catchments are the ones we have chosen to identify flash flood susceptibility and hotspots: local slope of the terrain, land use, soil type and vegetation coverage (if available).

Based on these criteria, the variables proposed to characterize flash flood hot spots are those summarized in Table 8-2. However, because of their relevancy, it could be particularly interesting considering the following variables:

- Catchment moisture conditions (that strongly influence the effective runoff coefficient of the catchment).
- Annual season to consider that in many cases are limited (e.g. this is the case of the case of the Western Mediterranean coast, where flash floods occur almost exclusively in the period June-November).
- The existence of significant regulation structures that can attenuate the hydrograph affecting the lower part of the catchment.

Table 8-2: Variables proposed for identifying flash flood hot spots.

Climatic	Daily precipitation for a return period of 10 years.
Geomorphologic	Catchment slope.
	Land use.
	Soil type.
	Forest canopy.

8.3 Methodology

The approach chosen to assess flash flood susceptibility is based on the Flash Flood Potential Index (FFPI) proposed by Smith, 2003 (see also UCAR, 2010). The method is based on combining the ingredients that characterize the occurrence of flash floods into an index that assess flash flood susceptibility. The original formulation of the FFPI is based on the following equation:

$$FFPI = \frac{M + L + S + V}{N} \tag{8.1}$$

where *M*, *L*, *S* and *V* are indexes in the range 1-10 that assess the susceptibility to flash floods given, respectively, the local slope, land use, soil type and vegetation. *N* is the number of features used to assess flash flood susceptibility (in the original formulation, *N*=4). In the various applications of the FFPI (e.g. Ceru, 2012; Zogg and Deitsch, 2013), the calculation of *M*, *L*, *S* and *V* used the look-up tables provided by Smith (2003), which transform each variable into the indexes (*M*, *L*, *S*, *V*) that characterize flash flood susceptibility.

The result of equation 8.1 is a FFPI map in the range 1-10 (see top panel of Figure 8-3) assessing the flood susceptibility at the resolution of the input layers: areas with high values of FFPI (which typically result from high slopes, impervious areas and little vegetation), are those identified as more susceptible to flash floods (in yellow in the top panel of Figure 8-3). Smith (2003) also proposed to remap and rescale the FFPI at subbasin scale to identify those more prone to the occurrence of flash floods (bottom panel of Figure 8-3).

Here, we propose to apply the method and include information about the climatology of extreme precipitation, as depicted by annual maximum daily rainfall statistics. With this aim, a new index *R* (in the range 1-10) will be added in equation 8.1 to account for the spatial variability of daily rainfall statistics in the study domain. For the computation of the index, the 10-year return period daily precipitation values will be linearly transformed into an index in the range 1-10.

It has to be noted that by using the climatic and geomorphological ingredients detailed above, the FFPI remains as static information (this means that the identified hot spots remain stationary and independent of the hydrological conditions of a given day).

However, the simplicity of the method allows the inclusion of new variables to characterize flash flood susceptibility, and, in particular, including dynamic variables (as suggested by Smith, 2003). In this sense, including the moisture conditions of the catchment as depicted with a continuous rainfall-runoff model or the day of the year (to account for the seasonality of flash floods) should be relatively simple, and it would probably enhance the interest of the method.

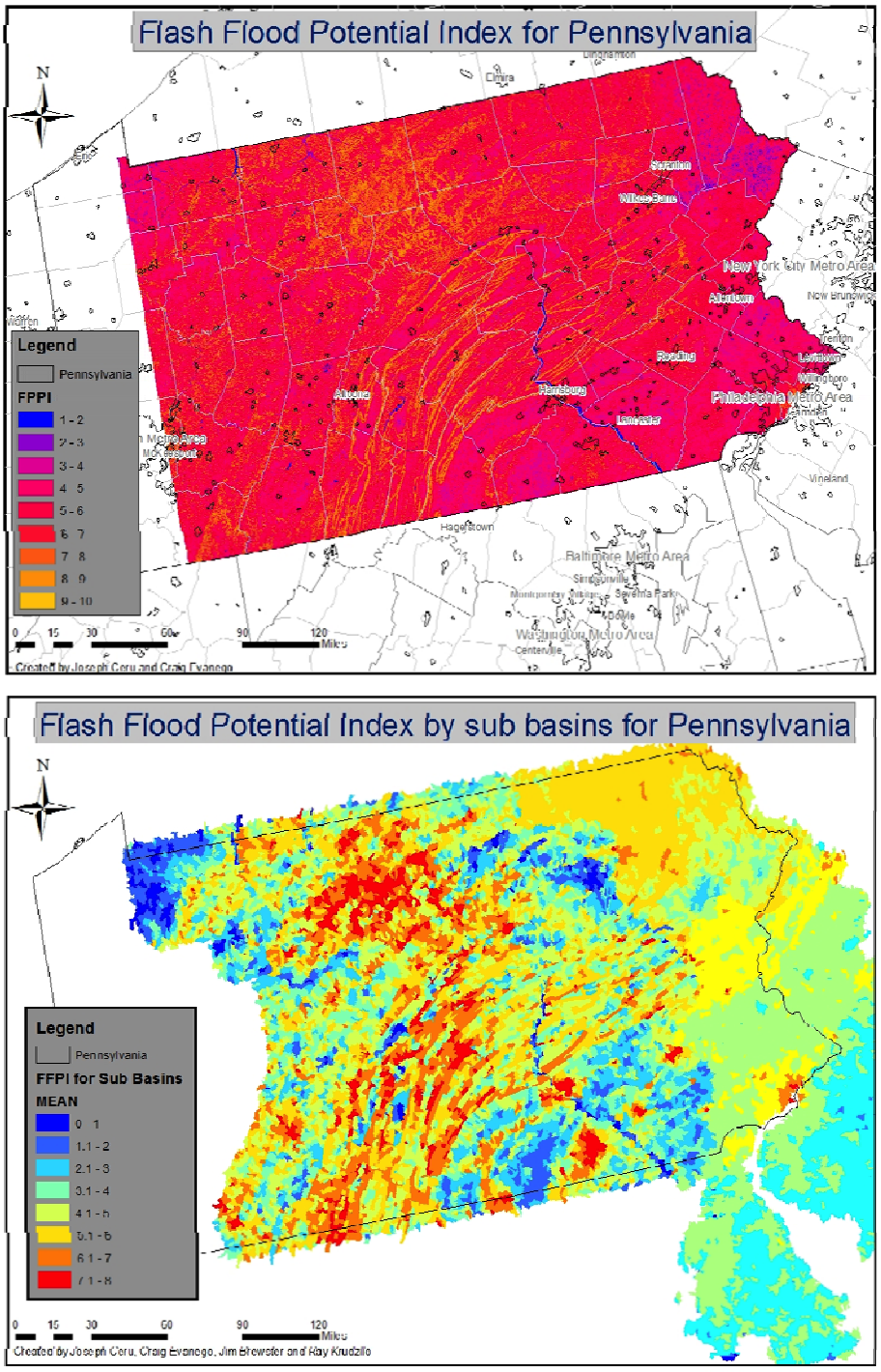

Figure 8-3: FFPI estimated for Pennsylvania. Top panel: at pixel scale (resolution, 30 m); bottom: averaged at subbasin scale. (Ceru, 2012).

8.4 Example of application

In what follows, an example of application of this method to assess flash flood susceptibility in the Catalan coast (Figure 8-4) is presented. Here we describe the datasets that will be used (the ingredients), and the steps needed for the successful implementation of the method to identify flash flood hotspots.

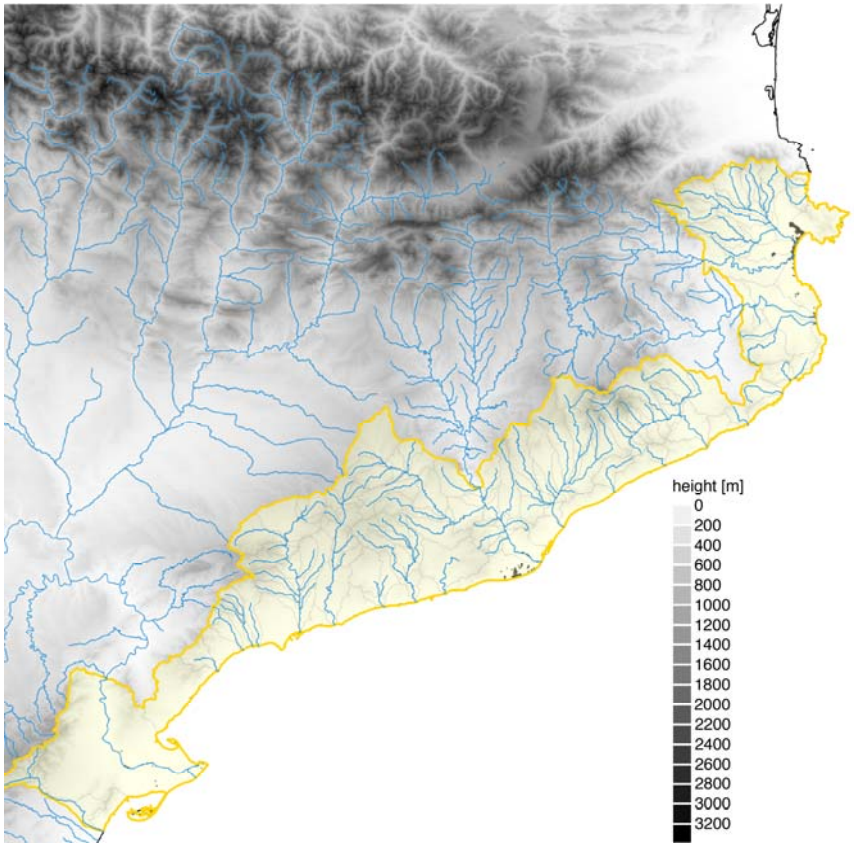

Figure 8-4: Shaded in yellow, domain where the coastal flash flood hotspots will be identified using the FFPI approach.

Table 8-3: Ingredients for Flash flood hotspot identification.

Description	Source	Original resolution
Digital Elevation Model	Institute of Cartography and Geography of Catalonia	30 m
Corine Land Cover	European Environment Agency	100 m
Soil texture	Joint Research Centre, Soil Database	1000 m
Maximum green vegetation fraction (Broxton et al., 2014)	USGS Land Cover Institute	1000 m
Daily rainfall accumulation for a return period of 10 years (INM, 2007)	Spanish Agency of Meteorology	1000 m

Table 8-4: Steps for Flash flood hotspot identification.

Step 1	Resample the 5 datasets to a common resolution of 250 m over the same grid as the one used for the flash flood hazard assessment module developed in WP 3 (Roelvink et al., 2015).
Step 2	Process the DEM to retrieve the slope map of the analysis domain (Figure 8-5).
Step 3	Transform the slope, land cover, soil and vegetation fields (Figure 8-5 - Figure 8-8) into the indexes *M*, *L*, *S* and *V* used in equation 8.1
Step 4	Propose a transformation of the field of daily precipitation for a return period of 10 years (Figure 8-9) into an index *R* (in the range 1-10) to be include as a new term in equation 8.1 to account for the spatial variability of extreme precipitation in the analysis domain.
Step 5	Combine the 5 ingredients according to equation 8.1 to retrieve the *FFPI*.
Step 6	Average the FFPI field at catchment scale to identify the highly susceptible subbasins.

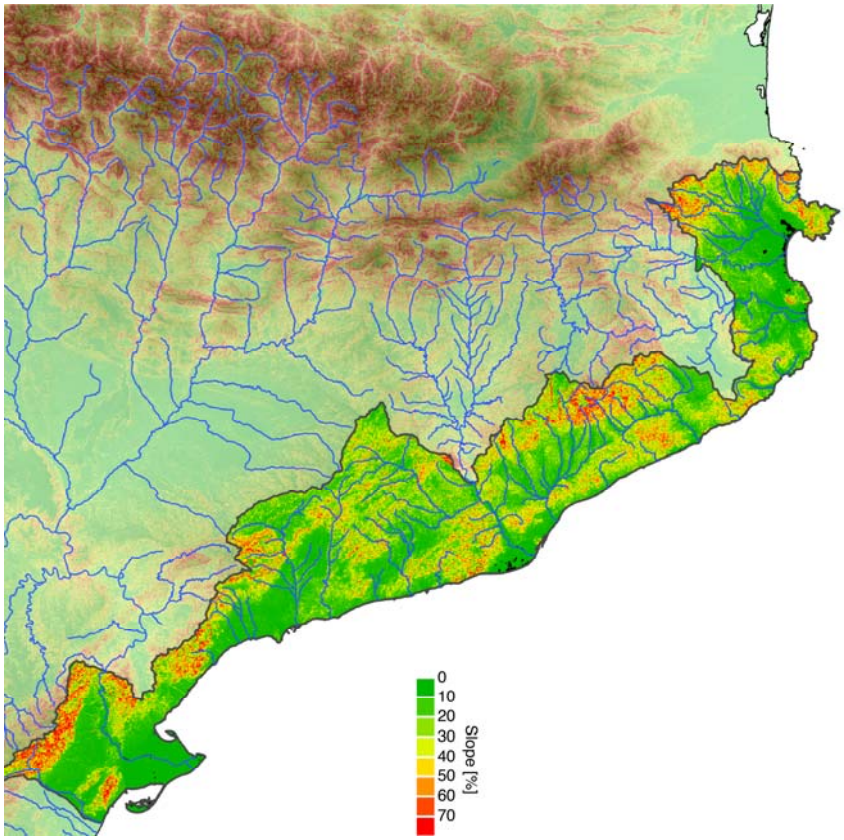

Figure 8-5: Map of local terrain slope (%) in the analysis domain.

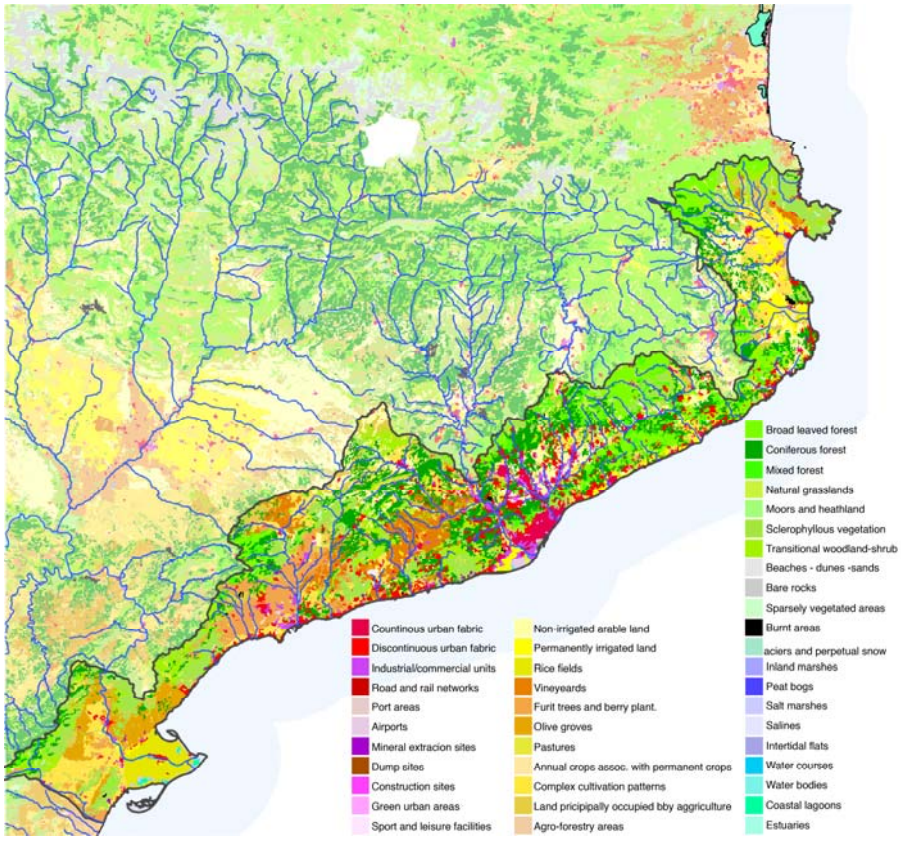

Figure 8-6: Map of land use in the analysis domain.

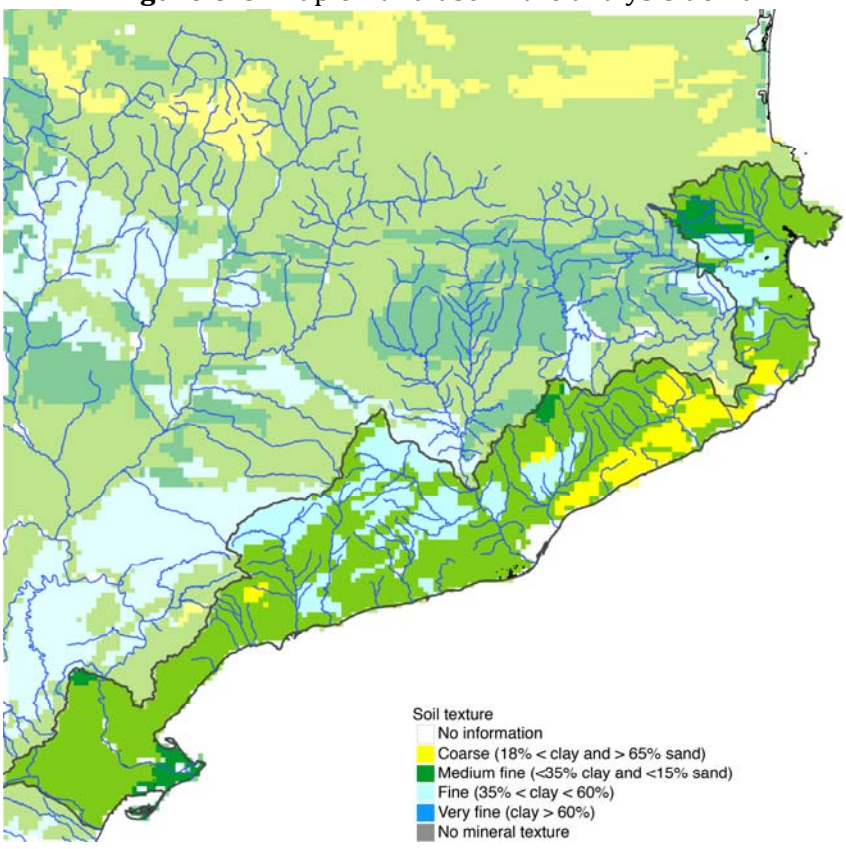

Figure 8-7: Map of soil texture in the analysis domain.

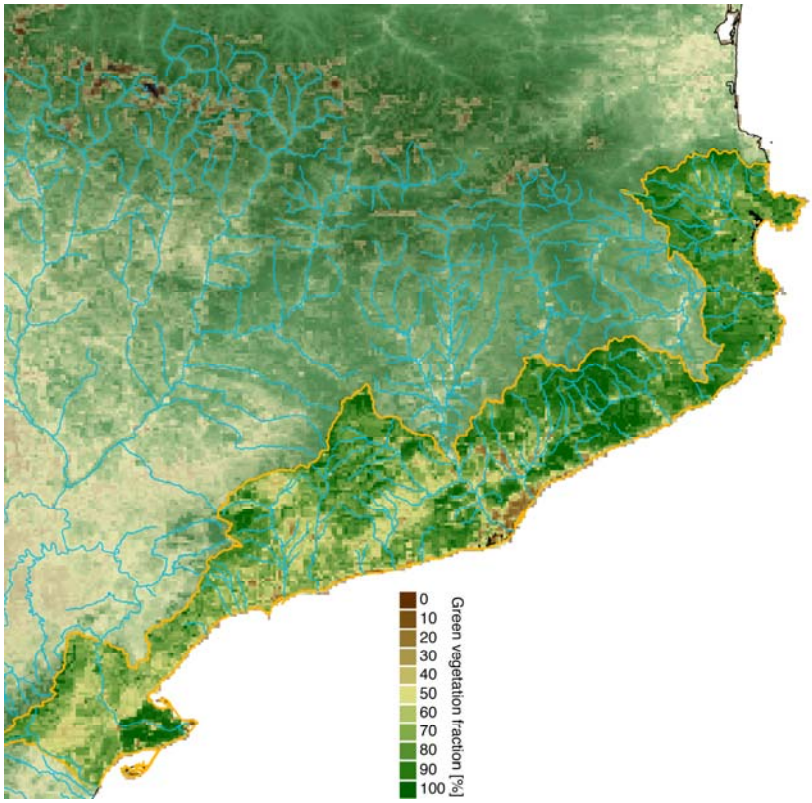

Figure 8-8: Map of green vegetation fraction (%) in the analysis domain.

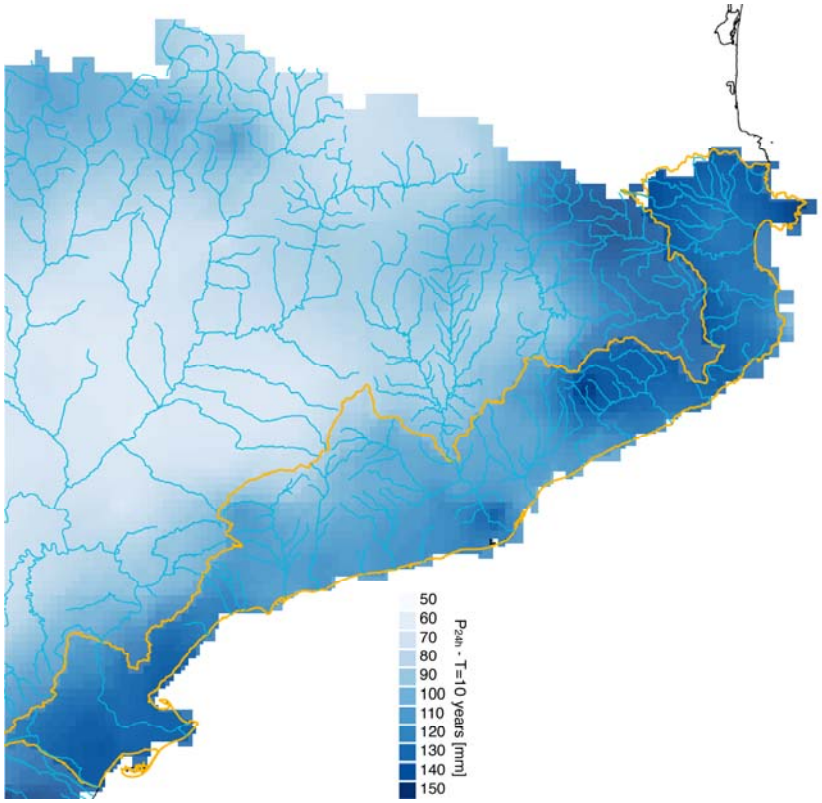

Figure 8-9: Map of the daily rainfall (in mm) for a return period of 10 years in the analysis domain.

9 Long-term assessment

9.1 Introduction

When doing Coastal Risk Assessment within the general framework of Coastal Management, it is important to consider its validity at long time scales which are the usual ones in coastal planning, i.e. several decades. At long-term scales, the Hazard Assessment can be influenced in different ways: (i) change in time of coastal geomorphology; (ii) change in time of forcing conditions and, (iii) new forcing conditions.

The first one can be easily taken into account by applying the framework for a modified coastal morphology. In essence, this implies to periodically update the characterisation of the coastal system to be analysed by gathering new data on coastal morphology and/or by modelling its expected evolution. This means that any performed assessment will be associated to a given coastal morphology and it will be valid whereas this morphology does not significantly change, i.e. without significantly affecting hazards' intensity and/or capacity of response. The inclusion of an existing background erosion in a coastal stretch will imply the reduction of the beach width when projecting the morphology at the long term. Although this does not necessarily imply any change in the hazards (which are mainly controlled by the maritime climate), it will affect the capacity of the beach to cope with such hazards.

The second one can be easily taken into account by applying the framework for modified forcing conditions. When referring to storms, this means a modification in storminess (intensity and frequency). Existing studies at global scale (e.g. Caires et al., 2006; Mori et al., 2010) and/or at regional scale (Lionello et al., 2008) have found different trends in storminess depending on the site and with a high variability in modelled extreme wave climates for the different used models. In spite of this variability, the inclusion of this potential long-term effect on the Hazard Assessment is a relatively easy task. The procedure consists in simulating the new wave and water level climates under a selected climate scenario which will be used as the forcing data to apply the framework.

Finally, the third one refers to the appearance of new hazards or forcings when increasing the time scale. The most typical example is sea level rise (SLR), with a nearly-negligible contribution at the short-term scale (very small magnitude) but measurable one when integrating at long-term ones (cumulative effect).

Whereas the first two mentioned long-term effects do not involve any modification in the proposed framework but to change the coastal characterisation or to change the forcing data, the inclusion of SLR requires to modify the framework by including a new elements. In this chapter we propose a methodology to apply the proposed framework at the long-term scale by considering the potential effects of SLR on the storm-induced coastal hazards.

9.2 SLR-induced changes in storm-induced hazards

9.2.1 Static approach

The trivial way to assess SLR contribution on storm-induced coastal hazards would be to simply consider the existence of a new (raised) sea level. In terms of inundation, this will not affect runup intensity (because it only depends on wave climate and beach slope) although it will modify overwashing/overtopping due to a decrease of the beach freeboard. This approach is only valid for passive coasts and rigidized ones (artificial coast such as those characterized by the presence of revetments or dikes).

Thus, if the area of interest is a passive or protected coast, the application of the hazard assessment framework at the long-term scale do not imply any change in forcing conditions. In consequence water level (runup and surge) extreme climates calculated under present conditions will be valid. However, since runup and/or surge will occur under a raised mean sea level, there will be a change in the induced coastal flooding in terms of frequency and intensity.

The change in the frequency of flooding of a given coastal stretch due to SLR can easily be assessed by adding to the total water level climate calculated under present conditions the corresponding increase in mean sea level for the desired time projection. Figure 9-1 shows an example of application of this static approach in the Tordera delta for a SLR projection of 0.50 m. A coastal stretch protected by a coastal structure with a freeboard of +5.0 m under present conditions will be flooded for events associated to return periods of 25 years or longer. However, without any change in storminess, under a SLR scenario of 0.5 m, the same site will be affected more frequently, since the minimum event to exceed the new (lower) freeboard will be 13 years.

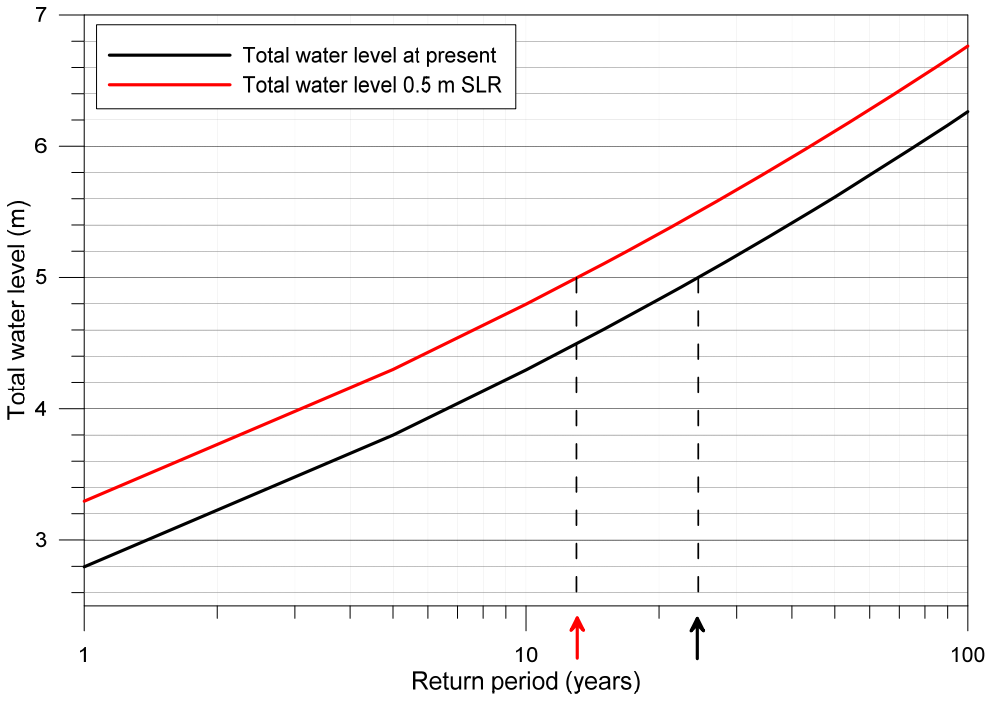

Figure 9-1: Total water level extreme climate under present conditions and for a 0.50 m increase in mean sea level.

The change in the magnitude of storm-induced flooding of a given coastal stretch under SLR can also be assessed by re-calculating overtopping rates. In this case, the overtopping model is fed with the same wave-induced runup climate with a modified freeboard (decreasing the coastal freeboard a magnitude equivalent to the projected sea level). Figure 9-2 shows the change in overtopping climate for a coastal stretch with a freeboard of +2.5 m under present conditions due to a SLR of 0.5 m. This is equivalent to calculate the overtopping rates associated to the same probability (there is no change in storm properties) for a 0.5 m lower coast. Thus, in the presented example, the overtopping discharge associated to a return period of 50 years increases from a rate of 0.014 $m^3/m/s$ under present conditions to a rate of 0.04 $m^3/m/s$ for a 0.50 SLR.

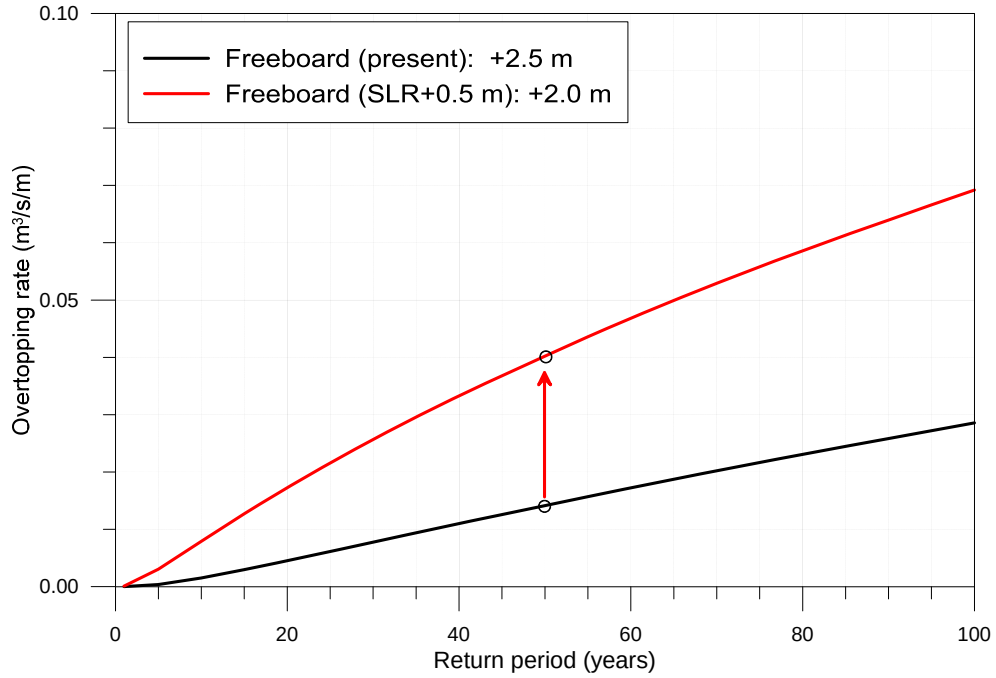

Figure 9-2: Effect on overtopping discharge rates at a coastal stretch with a freeboard of 2.5 m with respect to present mean sea level and a SLR of 0.50 m.

The SLR-induced effect on storm-induced erosion assuming this simple approach is also straightforward. If the storm-induced erosion hazard magnitude is calculated by using a process-oriented model such as XBeach 1D or Sbeach, the procedure will be to apply the model as in current conditions (there is no change in wave climate) but increasing the water level by the projected SLR. This should be equivalent to calculate the induced erosion under the presence of constant surge during the impact of the storm equivalent to the SLR. Figure 9-3 shows the application of this approach to calculate the magnitude of the storm-induced erosion in a profile typical of the Tordera delta under present conditions and two SLR scenarios. As it can be seen, the inclusion of SLR by modifying the water level where waves will be acting increases thee induced erosion with respect to that calculated under current conditions. Thus, the adoption of this static approach can be considered as a conservative approach to assess the impact of SLR on storm-induced erosion hazard.

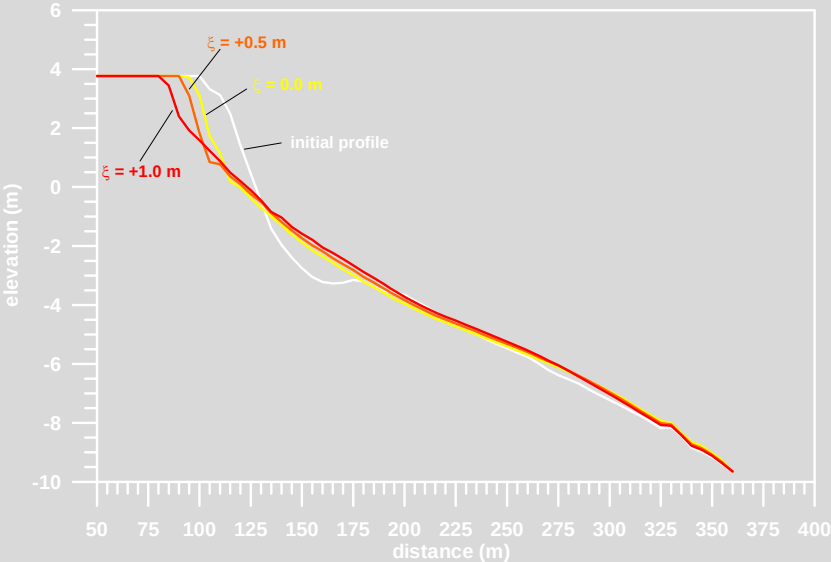

Figure 9-3: Effect of SLR on storm-induced erosion calculated using Sbeach and the static approach for SLR projections of 0.5 and 1.0 m.

9.2.2 Dynamic approach

Although the previous presented approach can be useful for certain coastal sites, it would not reproduce realistic conditions in sedimentary coasts which cannot be considered as static systems. Due to this, we have developed a simple method to account for the dynamic response of sedimentary coasts to RSLR (relative sea level rise which add the contribution of local processes such as subsidence to SLR) to be included in the hazard assessment.

The key question to include RSLR-induced changes on storm-induced hazards from a dynamic perspective is how to simulate the RSLR-induced changes in morphology. Here we assume sedimentary coasts dynamically respond to RSLR following an equilibrium type of response (e.g. Fitzgerald et al. 2008) which can be estimated by using the Bruun model (Bruun, 1962). The model assumes the existence of an equilibrium profile which reacts to RSLR by experiencing an upward and landward translation and maintaining its shape since there is no change in forcing conditions. In any case, the model also implicitly assumes the conservation of mass applies across- and along-shore.

In spite of its wide use in the literature, it has limitations that have to be considered (e.g. Cooper & Pilkey, 2004) and, unless in the case of absence of littoral transport gradients and presence of sediment sources/sinks, it is not recommended for local scale assessments in which precise quantitative estimations are needed (Stive et al., 2009). Bearing in mind these limitations, Ranasinghe et al., (2011) have recently proposed a probabilistic model to estimate coastal recession due to sea-level rise (PCR model). However, this model also has several simplifying assumptions that need to be taken into account. Moreover, an extensive validation analysis should also be required before to widely use it.

Under this scenario of lacking a generally validated morphological model to predict RSLR-induced coastal response, we propose to characterize its magnitude following

the axiom of the simpler the better. Thus, we accept that the coastal response can be characterised by using the Bruun rule, with an induced shoreline retreat given by:

$$\Delta x_{RSLR} = s\frac{L}{B_{\max} + d} = s\frac{1}{sl} \tag{9.1}$$

where Δx_{RSLR} is the expected beach retreat, s is the RSLR, L is the extension of the active profile (from berm to closure depth), B_{max} is the maximum berm height (beach elevation), d is the closure depth and sl is the active profile average slope.

One of the consequences of accepting a Bruun-type of coastal response to RSLR is that the beach profile will be reconstructed in such a way that under the new raised water level, the relative beach configuration will be the same. However, this should only be valid provided there is enough accommodation space, i.e. there is no barrier/obstacle to landward profile migration.

However, in developed coasts where vulnerability assessments are mostly applied, beaches are frequently backed by rigid boundaries that may limit their landward migration. Under this situation, the availability of accommodation space is one of the limiting factors to control the magnitude of the coastal response and, in consequence, the final beach configuration.

To account the effect of the existing accommodation space, we propose a method which assumes that a critical width is required to permit the beach to fully response to RSLR and thus, to maintain its relative elevation with respect to MWL (Bosom, 2014; Bosom et al. under review). This critical beach width (W_c) is taken as the actual distance between the maximum elevation of the beach/dune (B_{max}) and the shoreline, which can be calculated as:

$$W_c = \frac{B_{\max}}{\tan\beta} \tag{9.2}$$

where $tan\beta$ is the beach-face slope.

According to this assumption, under a given RSLR scenario, the beach profile will adjust to new conditions as predicted by the Bruun rule as long as the projected beach width is wider than the critical value (W_c). Otherwise, the lack of accommodation space will prevent the full development of the beach profile and its relative elevation will decrease.

Figure 9-4 illustrates the different possibilities of coastal response to RSLR taking into account the critical beach width criterion. Configuration 1 corresponds to a natural beach without any obstacle in the hinterland (similar to pristine/natural conditions) where the actual width is wider than the critical value, resulting in a condition without any restriction in accommodation space. Under this condition, the beach profile responds as predicted by the Bruun rule with an upward and landward translation without any change in the relative beach height.

The second situation is the most common in developed coasts where the beach is backed by a rigid boundary. In this case, the profile response will depend on the actual

beach width (considered as the distance between the shoreline and the obstacle): if it is wider than the critical value, the beach will respond as described for configuration 1. On the other hand, if it is narrower than the critical value, the beach will tend to follow the response predicted by the Bruun model, although will not have enough space to fully develop it. In this case, the shoreline retreat will be accompanied by a beach lowering due to a decrease in the relative height. If these conditions maintain, the final situation will be given by configuration 3 (Figure 9-4) where the beach has fully disappeared due to RSLR-induced retreat and only a rigid shoreline remains to face RSLR-induced effects with a decreasing relative height for rising water levels.

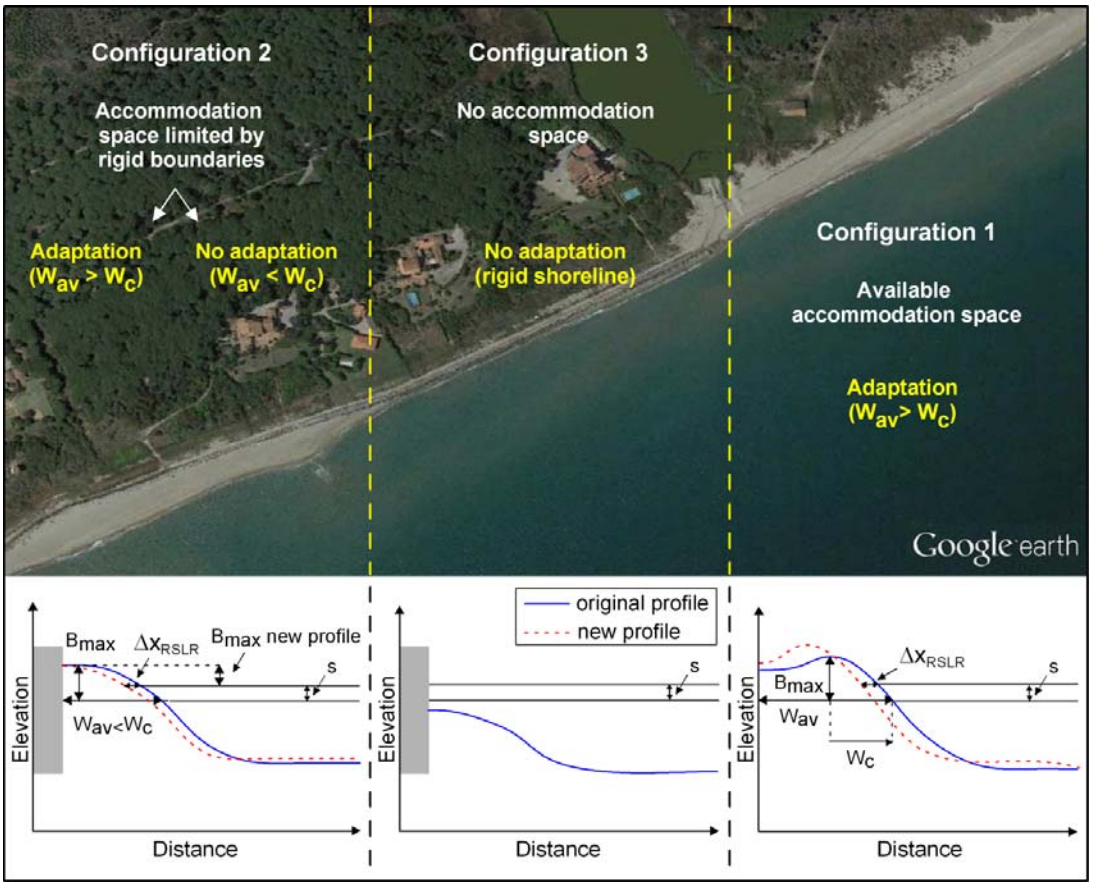

Figure 9-4: Expected beach response to RSLR for three different baseline configurations of varying accommodation space (Bosom et al. in review).

In order to quantify the RSLR-induced changes on storm-induced hazards, beach width and maximum berm height are projected at the selected time horizons and used to determine the adaptation ability of the coast.

In the case of erosion, the magnitude of the hazard which is the storm reach associated to a given probability of occurrence is the same than under present conditions (Δx). However, the capacity of the beach to cope with this induced erosion which is parameterized by its width, is lower because the storm will be acting on a narrower beach. This can be modeled as:

$$EV = \Delta x / (W + \Delta x_{RSLR}) \qquad (9.3)$$

where Δx is the storm-induced beach retreat associated to a given return period, W is the average beach width at the baseline (2010) and Δx_{RSLR} is the SLR-induced shoreline retreat at a given time projection (Equation 9.1). As it can be clearly deduced, although no changes in storm-induced erosion are produced by the presence of SLR, the capacity of protection provided by the coast will be lower, i.e. the hazard magnitude is the same but the vulnerability increases.

In the case of inundation, because the magnitude of the inundation depends on the coastal freeboard, no SLR-induced variations are expected in dynamic sedimentary coasts when enough accommodation space exists. Under these conditions, the beach profile fully responds and the active profile is fully rebuilt maintaining its relative elevation to mean sea level.

However, when the projected beach width is lower than the before described critical value, the beach would not be able to maintain its elevation and, under this situation the procedure applied in the previous section (static approach) should be applied. This approach means that the effects of SLR on the storm-induced inundation can vary along the coast from a zero impact for wide beaches to a significant influence for narrow beaches. They vary also in time, for SLR-induced eroding beaches reaching a width narrower than the critical value.

Figure 9-5 shows the potential consequences of applying this approach in the Catalan coast for different SLR scenarios. This is done in terms of coastline length with a projected beach width narrower than the critical value and, thus, varying its freeboard with respect to mean sea level and, in consequence, suffering a lager inundation for same probability events. As it can be seen, this affected length increases with time and, also, when the time horizon is increased, a significant part of the coast should disappear (should be fully eroded).

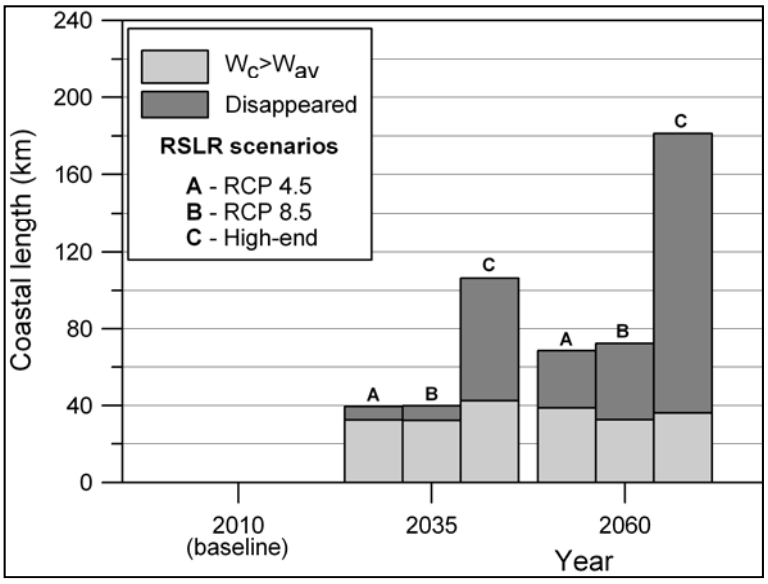

Figure 9-5: Coastline length narrower than the critical value at different time horizons under different RSLR scenarios (adapted from Bosom et al. in review).

10 Framework implementation

10.1 Introduction

The proposed framework for the assessment of storm-induced hazards within the RISC-KIT project can be seen in Figure 2-3 where two phases are shown: (i) A *first phase* to identify sensitive (hotspots) areas along the coast to the impact of extreme events and, (ii) a *second phase*, where the XBeach (1D) advanced model is applied in selected sensitive stretches to define the hotspots.

In this section we shall describe the main steps to implement the framework from the practical standpoint. This will be illustrated with the initial phase of the framework (Figure 10-1) since it is at this stage where most of the presented modules are applied, with the only left part being the application of the XBeach transect mode which will essentially applied in those areas identified as hotspots.

10.2 Data input requirements

The first task with to implement the framework consists of the selection and preparation of data to be used through the process. This include two main activities: (i) characterization of the coast and (ii) forcing.

Data input requirements to characterize the Flash Flood hazard can be seen in Chapter 8 together an example for the Catalan coast.

10.2.1 Coast characterization

To characterize the coast (from the hazard assessment standpoint), we have to select coastal (beach/barrier) transects to represent the area of analysis at a proper spacing (in the order of 1 km). This spacing must reflect the alongshore variability of the coast of interest in terms of relevant parameters (slope, berm/barrier/dune height, barrier, sediment grain size, beach profile shape, etc.).

The following information is required for the considered different hazards:

Flooding/overwash: beachface slope (for run-up), beach/dune height (to calculate freeboard and compute overtopping and inundation), beach width (to calculate overwash extension).

Erosion: sediment grain size, beach profile slope (for volume changes), beach width (to account for beach resilience).

Barrier breaching: in addition to the previous one barrier width.

Protected coasts: dimensions of detached breakwaters.

Flash Floods: terrain slope and identification of river basins (MDT).

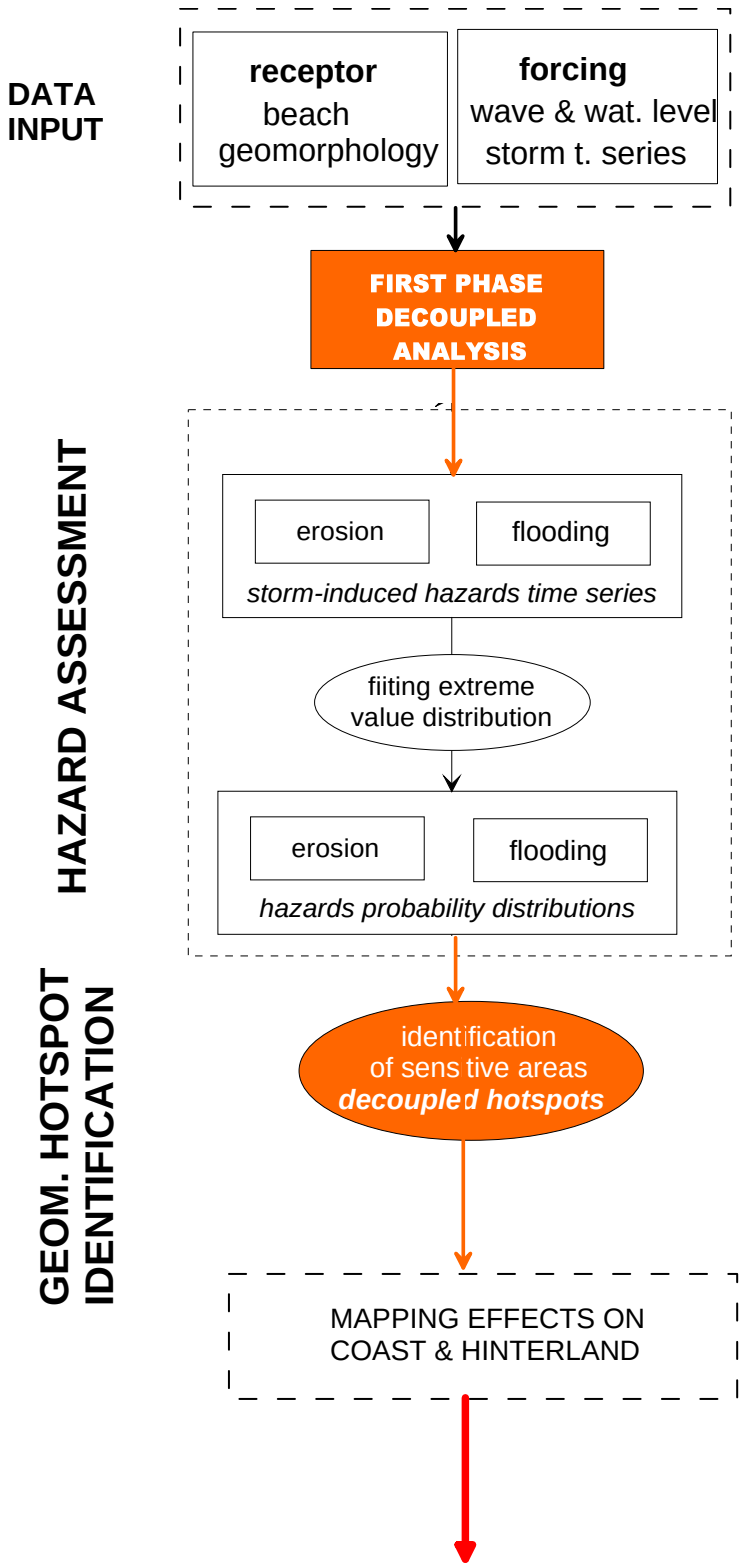

Figure 10-1: Initial phase (identification of hotspots) of the Hazard Assessment Module.

In what follows, an example of different data sources to be used is briefly described.

DTM: Digital Terrain Model with resolution enough to properly reproduce the topography of the study site. This will be used for inundation modeling (e.g. small scale applications or estuary application) and to extract beach profiles along the coast which will be used to compute storm-induced hazards. These profiles will have a spacing of about 1 km. A fine grid and high-resolution data (e.g. from Lidar) are required since parameters such as *beach slope* and *berm/dune height* are going to be extracted from this source. (e.g. in the Catalan coast we are working with a DTM with a grid of 5 m x 5 m, obtained with a topographic Lidar).

Beach profiles: cross-shore profiles including the submerged part as an extension of the ones obtained from the emerged beach DTM. They are needed to calculate storm-induced erosion with XBeach or with another erosion model. Although the ideal spacing is about 1 km, it could be possible to use a smaller number of data. Thus, it will be enough to select typical profiles representing large coastal. Depending on the spatial variability of the coastal morphology of the area to be analyzed, it should be relevant not only to characterize it by taking a profile at a regular spacing but to select an "average" and a "worst case" state. The first one will be given by a representative profile of the 1 km long sector, whereas the second one will be characteristic of the weakest morphology (from the hazard standpoint) within that sector (e.g. representative of the area with the lowest dune).

Sediment size: Information of sediment size along the coast in the same sites where beach profile are given. They are needed to calculate storm-induced erosion with any erosion model (parametric or process-oriented).

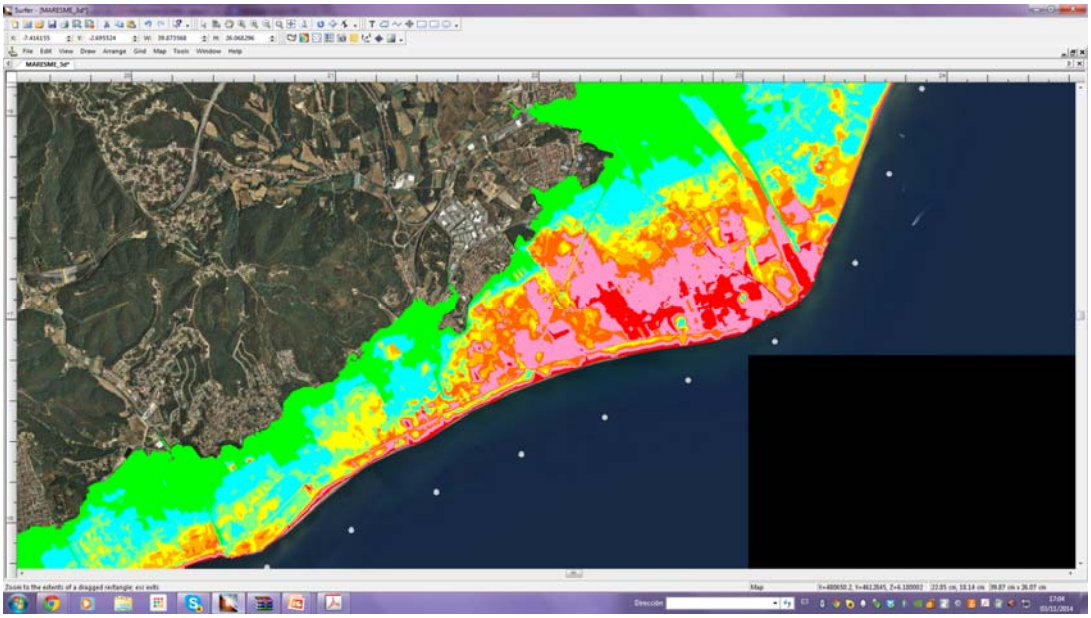

Figure 10-2: Profile selection at 1 km spacing along the N part of the Maresme (Catalan coast, NW Mediterranean).

One of the elements to be considered when selecting the profiles representative of the study area is the sensitivity of the analysis to the used beach morphology. As it has

been previously mentioned, although the usual spacing at this regional scale should be in the order of 1 km, small scale spatial variability could determine the existence of an expected relatively large variability in calculated hazard magnitude. Figure 10-2 shows the selection of beach profile location every 1 km along the Maresme coast as a first approach.

There is not a general rule to select which should be the representative profile and this will be site-dependent. Thus, a first screening of spatial variability of main geomorphic parameters controlling hazards magnitude should be done. According to obtained results, a proper selection will be done (averaged profile, minimum profile, profile associated to a given frequency of occurrence). Just to illustrate this variability, Figure 10-3 shows the frequency distribution of beachface slopes (which control the runup magnitude) in the area included in Figure 10-2 obtained from a beach profile sampling every 100 m. As it can be seen, the beach slope significantly varies and due to this, the use of an averaged slope will not necessarily be the best option to identify the existence of flooding-related hotspots.

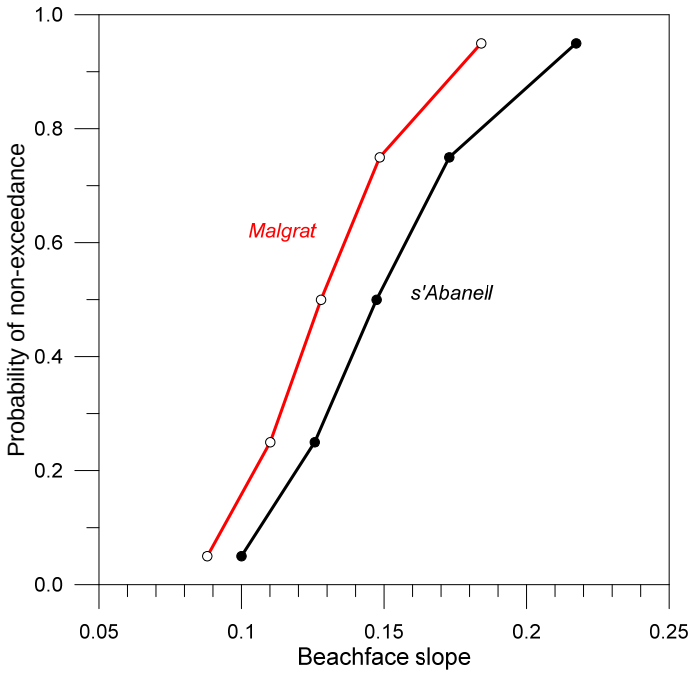

Figure 10-3: Frequency distribution of beachface slopes around the Tordera delta.

Once we have selected the beach profiles, an optimization procedure can be implemented to reduce the number of computations. To do this, we classify the measured profile variables (e.g. beach face slope) in classes representing all possible values in the study area. Hazard magnitude (e.g. runup) will be calculated only for these *representative* profile classes, whereas the final response (e.g. inundation) will be *individually* calculated. Figure 10-4 shows this for the case presented above. Here we have different profiles which showed similar beach slopes values that are grouped into a representative profile (class 7) in such a way that runup is calculated just for one representative slope. However, when the flooding potential is going to be calculated they are individually considered by comparing the representative runup with the individual beach/dune heights. In this last case, we propose to do the analysis

with a representative "average" profile and a worst-case profile to properly identify the potential hotspots.

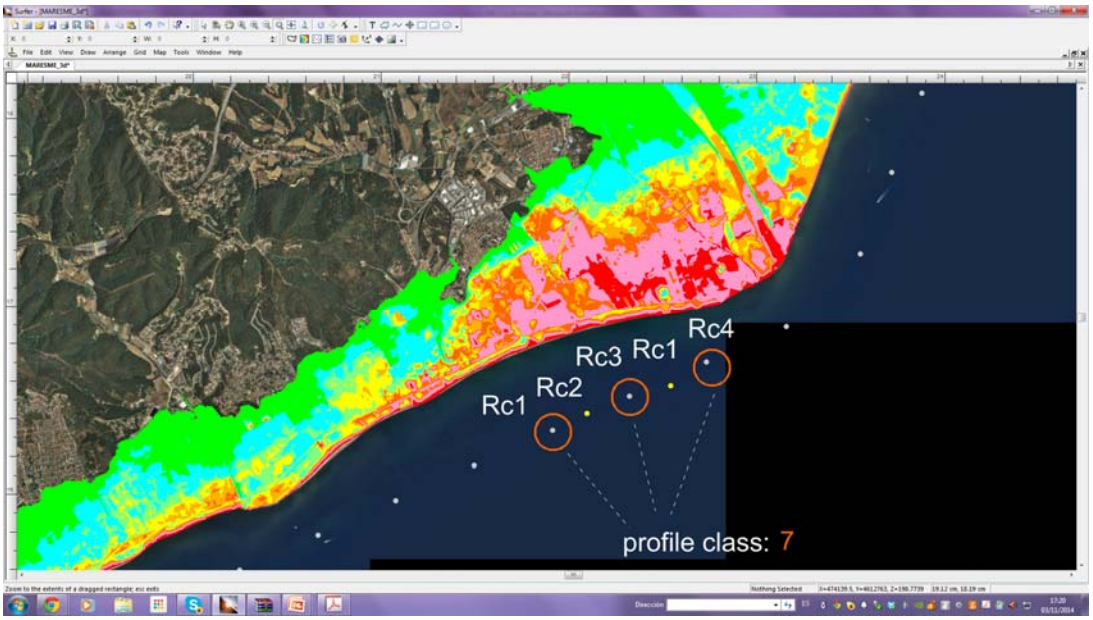

Figure 10-4: Identification of representative profiles along the N part of the Maresme (Catalan coast, NW Mediterranean).

10.2.2 Forcing characterization

To characterize the forcing -storms-, we have to select long-term time series of waves and water level representative of the spatial variability of maritime climate along the study area.

In order to properly reproduce the spatial variability of the maritime climate of the study area (coastal length of about 100 km or larger), we have to consider the spatial variation of storm conditions along the coast. To do so, we need to compile data able to capture such variability.

Each site must analyze existing forcing (wave and water level) data to assess which is the minimum set of conditions to be used. This has to be done in a site-specific manner to account the local maritime climate characteristics. Figure 10-5 shows the selection of the minimum set of forcing conditions to be used in the Maresme coast. Existing data sources are a series of nodes where hindcast wave and water level are provided. After a pre-analysis of maritime climate conditions, it was decided that the use of just 2 sectors (one at the N and one at the S) was enough to represent the spatial variability in forcing conditions. Thus, all coastal sectors belonging to a given quadrant will be analyzed using the same forcing conditions.

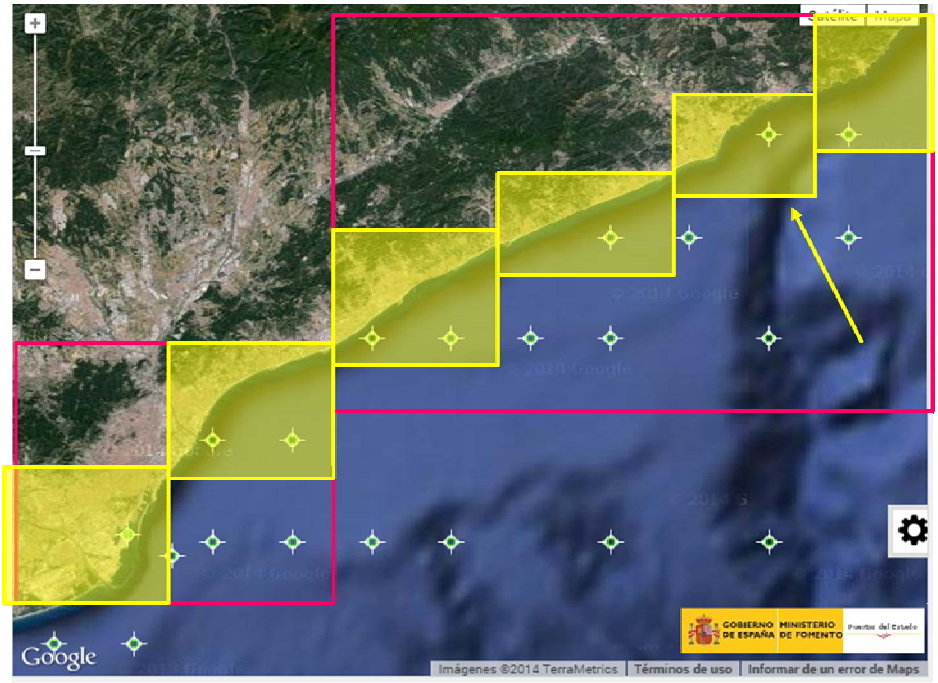

Figure 10-5: sectors to characterize wave and water level forcing conditions in the Maresme coast. Yellow blocks represent the existing local data and red ones are the 2 selected maritime climate sectors to define the forcing for coastal hazards.

Since we are adopting a probabilistic approach in which the hazards are characterized through their extreme climate, time series must be long enough to have a reliable estimation of such climate. This means to have time series in the order of several decades of length. There are two possibilities: (i) instrumental recorded data (from wave buoys and tide gauges) and/or (ii) hindcasting. As an example, in the Catalan coast we have different datasets (instrumental and model-derived ones) such as the 44-years long time series of hindcasted data obtained within the Hipocas FP5 project.

In what follows, an example of different data sources to be used is briefly described.

Wave time series: Long time series (recorded or hindcasted) of wave data. Usually H, T, θ data every 1 or 3 hours.

Water level time series: Long time series (recorded or hindcast) of water level. In the case of recorded, they are usually given as total water level every ***n*** minutes. This data has to be processed to extract surge component. In the case of hindcast data, they are usually given as surge height every ***n*** hours.

Wind time series: Long time series of wind data. Usually V, θ data every ***n*** minutes.

Rainfall data: Rainfall probabilistic distribution in a given basin (see chapter 8).

10.3 Procedure

In what follows, main steps to be followed to apply the framework in the exploratory phase are presented.

10.3.1 Initial Phase

A. Identify the number of maritime sectors to be used in your application to select forcing conditions (Figure 10-5).

B. Retrieve wave and water level data (long time series).

C. Identify storm events in wave time series. Retain main variables defining the storm (*Hs*, *Tp*, direction, duration, water level).

D. Select segments along the coast (about 1 km long).

E. Select beach profiles to represent each segment taking into account the small scale spatial variability of the sector: average and worst case scenarios (Figure 10-4).

F. Represent each profile in terms of beachface slope, berm/dune height, beach width, sediment grain size, barrier width (if applicable).

G. Classify beach profiles in beach types as a function of beach slope and grain size (recommended bins of 0.01 in slope and 0.1 mm in grain size)

Protected coasts by detached breakwaters (if applicable)

C'. Calculate for protected sections of the coast equivalent storm deepwater wave characteristics by using the proposed methodology (chapter 6).

Flooding-related hazards

H. Calculate for each profile type (each selected beachface slope), the wave-induced runup for each storm identified in (C or C') using the selected model (section 3.2).

I. Add the corresponding water level (storm surge) recorded during each storm to runup calculated in (H) to obtain a set of extreme total water levels (if applicable - significant storm surges).

J. Fit total water level calculated in (I) to an extreme probability distribution (e.g. G.P.D. when using POT to identify storms or G.E.V. when using annual maxima).

K. Obtain from (J) water levels associated to selected return periods (e.g. 10, 50, 100, 500).

L. Calculate for each profile (sector) along the coast the susceptibility to be inundated at a given probability (return period) by comparing the local beach/dune height with the water level associated to such return period for the corresponding beach type (slope) calculated in (K). (susceptibility = total level / beach height).

M. Calculate for each probability (return period) and for each profile (sector) along the coast with high susceptibility to be inundated (total water level/beach height > 1) the corresponding overtopping rates (section 3.3).

N. Calculate for each probability (return period) and for each profile (sector) along the coast with high susceptibility to be inundated (total water level/beach height > 1) the corresponding overwash extension (section 3.3) when appropriated.

O. Calculate for each probability (return period) and for each profile (sector) along the coast with high susceptibility to be inundated (total water level/beach height > 1) the maximum potential inundation area (section 3.4).

P. Delineate for each probability (return period) the extension of the area to be (temporarily) inundated (section 3.4).

Erosion hazard

Q. Calculate for each profile type (each selected beachface slope and each selected sediment size), the induced erosion (eroded volume and shoreline retreat) for each storm identified in (C or C') using the selected erosion parametric model (chapter 4).

R. Fit calculated erosion variables in (P) to an extreme probability distribution (e.g. G.P.D. when using POT to identify storms or G.E.V. when using annual maxima).

S. Obtain from (Q) shoreline retreats associated to selected return periods (e.g. 10, 50, 100, 500).

T. Calculate for each profile (sector) along the coast the susceptibility to erosion at a given probability (return period) by comparing the local beach width with shoreline retreat associated to such return period for the corresponding beach type (slope and grain size) calculated in (R). (susceptibility = shoreline retreat / beach width).

Breaching hazard (if applicable)

U. Apply for each profile along the coast (barrier) the table for susceptibility to breaching (chapter 5) using values of inundation and erosion hazards previously calculated (N and R).

Flash flood (if applicable)

V. Calculate for the study area values of required indicators to build up the Flash Flood Potential Index FFPI to map susceptibility to Flash Flood at a small spatial scales (resolution of initial grid data). See steps in Table 8-4.

W. Integrate values obtained at small spatial scale up to sub-basin scale (after previous identification of sub-basins) to identify areas of high susceptibility to flash floods.

Long-term assessment (if applicable)

X. Obtain for selected SLR scenarios the target sea level rise value at the selected time horizon.

Y. Estimate for the target sea level rise the induced shoreline retreat.

Z. For static coastal sectors -fixed boundaries- estimate new relative water level and overtopping rates using the static approach (section 9.2.1).

AA. For active coastal sectors -with sandy coastlines- estimate new coastal configuration and corresponding relative water level and overtopping rates using the dynamic approach (section 9.2.2).

10.3.2 Second Phase

II-A. Identify from results obtained in the Exploratory Phase (10.3.1) the most sensitive stretches to storm-induced coastal hazards.

II-B. Apply to each selected beach profile (E) for identified hotspots (II-A) the 1D XBeach model (chapter 7) to compute storm-induced coastal hazards for each identified/selected storm (C).

II-C. Fit calculated magnitudes of storm-induced hazards in (II-B) to an extreme probability distribution (e.g. G.P.D. when using POT to identify storms or G.E.V. when using annual maxima).

II-D. Calculate for each selected probability (return period) and for each profile (sector) along the coast the final vulnerability to storm-induced hazards (inundation/erosion/breaching).

10.4 Final remarks

The module here presented is composed by a series of models calibrated and validated in numerous sites. However its application to a specific site requires to verify the validity of standard coefficients for the local conditions.

Thus, for instance, simple models as the runup ones presented here predict different values for the same wave conditions. If all models were good enough to predict runup at a given site, all of them had to predict the same result when fed by the same forcing conditions. However, this is not the case, since they predict different runup values. Thus, before applying the module, it is the responsibility of each site to select the most proper one for the study site.

This is also applicable for the process-oriented model XBeach that although able to model the effects of local conditions such as sediment grain size, beach profile, wave conditions, still has some coefficients that need to be locally calibrated.

Finally, the Hazard Assessment Module and the CRAF have been designed to be applied following the response approach in which hazards are characterized by means of a probabilistic distribution. This is the most generic case and, as discussed in chapter 2, it can be considered as the most realistic approach for hazard characterization in most of the coasts. However, when the coast of interest is highly protected, hazards associated to low and medium return periods are not relevant for stakeholders since the coast is already protected to their impact. In this case, the module can also be applied but instead of obtaining the probability distribution of the hazards, by directly estimating the hazard associated to a long return period event.

Thus, if the event approach is going to be followed the route of application of the Hazard Assessment Module will be the same than outlined in section 10.3 but the quantification of the storm-induced hazards. In this case, the starting point should be a extreme wave height climate (*Hs* associated with given return periods) and relationships between involved variables (*Hs-Tp, Hs-storm duration, Hs-surge*). Then, for selected return periods, the magnitude of analyzed hazard will be calculated by applying the corresponding model.

11 References

ACA (Water Agency of Catalonia). 2014. *Mapes de perillositat i risc d'inundació del districte de conca fluvial de Catalunya. Memòria*. Generalitat de Catalunya, Barcelona.

ACA (Water Agency of Catalonia). 2013. *Avaluació preliminar del risc d'inundació en el districte de conca fluvial de Catalunya.* Generalitat de Catalunya, Barcelona, 55pp.

Ali, G., Tetzlaff, D.,Soulsby, C., McDonnell, J.J., Capell, R. 2012. A comparison of similarity indices for catchment classification using a cross-regional dataset. *Advances in Water Resources*, 40**,** 11-22.

Almeida, L.P., Vousdoukas, M.V., Ferreira, O., Rodrigues, B.A., Matias, A. 2012. Thresholds for storm impacts on an exposed sandy coastal area in southern Portugal. *Geomorphology,* 143–144, 3-12.

Armaroli, C., Perini, L. 2012. A simplified methodology for the estimation of wave runup on armoured rubble slopes for vulnerability assessment. *Proc. 7th Euregeo Conference*, I, 355-356, Bologna.

Armaroli, C., Ciavola, P., Masina, M. 2009a. Morphological thresholds for the definition of the vulnerability of coastal dunes in northern Italy. *Proc. AGU Conference*, 90(52), EOS Transaction.AGU, San Francisco, California.

Armaroli, C., Ciavola, P., Masina, M., Perini, L. 2009b. Run-up computation behind emerged breakwaters for marine storm risk assessment. *Journal of Coastal Research*, SI 56, 1612 – 1616.

Armaroli, C., Grottoli, E., Harley, M.D., Ciavola, P. 2013. Beach morphodynamics and types of foredune erosion generated by storms along the Emilia-Romagna coastline, Italy. *Geomorphology*, 199, 22-35.

Armaroli, C., Ciavola, P., Perini, L., Calabrese, L., Lorito, S., Valentini, A., Masina, M. 2012a. Critical storm thresholds for significant morphological changes and damage along the Emilia-Romagna coastline, Italy. *Geomorphology*, 143-144, 34-51.

Armaroli, C., Perini, L., Calabrese, L., Luciani, P., Salerno, G., Ciavola, P. 2012b. Cartografia di rischio da mareggiata della fascia costiera della Regione Emilia-Romagna. *Proc. Meeting Marino*, D'Angelo S. and Fiorentino A. (Eds.), ISPRA, 25-33, Roma.

Bates, P.D., De Roo, A.P.J. 2000. A simple raster-based model for floodplain inundation. *Journal of Hydrology,* 236, 54-77.

Bates, P.D., Dawson, R.J., Hall, J.W., Horritt, M.S., Nicholls, R.J., Wicks, J., Hassan, M.A.A.M. 2005. Simplified two-dimensional numerical modeling of coastal flooding and example applications. *Coastal Engineering,* 52, 793-810.

Beniston, M., Stephenson, D.B. 2004. Extreme climatic events and their evolution under changing climatic conditions. *Global and Planetary Change*, 44, 1-9.

Bosom, E. 2014. *Coastal vulnerability to storms at different time scales. Application to the Catalan coast*. Universitat Politècnica de Catalunya, Barcelona.

Bosom, E., Jiménez, J.A., Nicholls, R. 2015. Increase of vulnerability to storms due to relative sea-level rise: the example of the Catalan coast. (in review).

Broxton, P. D., Zeng, X., Scheftic, W., Troch, P.A. 2014. A MODIS-Based Global 1-km Maximum Green Vegetation Fraction Dataset. *Journal of Applied Meteorology and Climatology*, 53**,** 1996-2004.

Bruun, P. 1962. Sea level rise as a cause of shore erosion. *J Waterway Harbour Division,* 88, 117-130.

Burcharth, H.F. and Hughes, S.A. 2011. Fundamentals of Design. In: Vincent, L., and Demirbilek, Z. (editors), *Coastal Engineering Manual, Part VI, Design of Coastal Project Elements, Chapter VI-5, Engineer Manual 1110-2-1100*, U.S. Army Corps of Engineers, Washington, DC.

Butler, D., Davies, J. 2011. *Urban Drainage*, 3rd Edition. Spon Press, New York, 632pp.

Caires, S., Swail, R., Wang, X. L. 2006. Projection and Analysis of Extreme Wave Climate, *Journal of Climate*, 19, 5581–5605.

Callaghan, D.P., Ranasinghe, R., Roelvink, D. 2013. Probabilistic estimation of storm erosion using analytical, semi-empirical, and process based storm erosion models. *Coastal Engineering* 82, 64-75.

Callaghan, D.P., Nielsen, P., Short, A., Ranasinghe, R. 2008. Statistical simulation of wave climate and extreme beach erosion. *Coastal Engineering* 55, 375-390.

Cañizares, R., Irish, J.L. 2008. Simulation of storm-induced barrier island morphodynamics and flooding. *Coastal Engineering*, 55, 1089-1101.

CEM. 2011. *Coastal Engineering Manual*, US Army Corps of Engineers.

Ceru, J. 2012. The Flash Flood Potential Index for Pennsylvania. *2012 ESRI Federal GIS Conference.* (http://proceedings.esri.com/library/userconf/feduc12/papers/user/JoeCeru.pdf.)

Ciavola, P., Armaroli, C., Perini, L., Luciani, P. 2008. Evaluation of maximum storm wave run-up and surges along the Emilia-Romagna coastline (NE Italy): A step towards a risk zonation in support of local CZM strategies. In: *Integrated Coastal Zone Management - The Global Challen*ge, 505-516, Research Publishing Services, Singapore.

Collier, C. G. 2007. Flash flood forecasting: What are the limits of predictability? *Quarterly Journal of the Royal Meteorological Society*, 133, 3-23.

Collier, C. G., Fox, N.I. 2003. Assessing the flooding susceptibility of river catchments to extreme rainfall in the United Kingdom. *International Journal of River Basin Management*, 1, 225-235.

Cooper, J. A. G., Pilkey, O. H. 2004. Sea-level rise and shoreline retreat: time to abandon the Bruun Rule. *Global Planetary Change*, 43(3-4), 157–171.

Daly, C., Roelvink, J. A., van Dongeren, A. R., van Thiel de Vries, J. S. M., McCall, R. T. 2012. Validation of an advective-deterministic approach to short wave breaking in a surf-beat model. *Coastal Engineering*, 60, 69–83.

d'Angremond, K., van der Meer, J.W., de Jong, R.J. 1996. Wave transmission at low crested structures. *Proc. 25th ICCE*, ASCE, 3305– 3318.

Dean, R.G. 1977. Equilibrium beach profiles: U.S. Atlantic and Gulf Coasts. Oc. Engrg. Report No. 12, Univ. of Delaware, Newark, De.

Divoky, D., McDougal, W.G. 2006. Response-based coastal flood analysis. *Proc.30th Int. Conf. on Coastal Engineering*, ASCE, 5291-5301.

Donnelly, C. 2008. *Coastal Overwash: Processes and Modelling*. Ph.D. Thesis, University of Lund, 53 pp.

Donnelly, C., Ranasinghe, R., Larson M. 2006. Numerical Modeling of Beach Profile Change Caused by Overwash. *Coastal Dynamics 2005*, ASCE, 1-14.

Douvinet, J., van De Wiel, M.J., Delahaye, D., Cossart, E. 2014. A flash flood hazard assessment in dry valleys (northern France) by cellular automata modelling. *Natural Hazards*, 75, 2905-2929.

EC. 2007. Directive 2007/60/EC of the European Parliament and of the Council of 23 October 2007 on the assessment and management of flood risks**.** *Official Journal L 288, 06/11/2007, 27-34.*

FEMA. 2005. *Wave runup and overtopping. FEMA Coastal Flood Hazard Analysis and Mapping guidelines. Focused Study Report.* Federal Emergency Management Agency.

FEMA. 2007. *Guidelines and Specifications for Flood Hazard Mapping*: *Atlantic Ocean and Gulf of Mexico coastal guidelines update.* Federal Emergency Management Agency.

Figlus, J., Kobayashi, N., Gralher, C., Iranzo, V. 2010. Wave overtopping and overwash of dunes. *Journal of Waterway, Port, Coastal and Ocean Engineering*, *137*(1), 26-33.

FitzGerald, D. M., Fenster, M. S., Argow, B. A., Buynevich, I. V. 2008. Coastal impacts due to sea-level rise. *Annu. Rev. Earth Planet. Sci.*, *36*, 601-647.

García Sorinas, L. 2014. *Estimación probabilística de la erosión por tormentas en la costa catalana*. M.Sc. Thesis, Faculty of Civil Engineering, UPC, Barcelona.

Garrity, N.J., Battalio, R., Hawkes, P.J., Roupe, D. 2006. Evaluation of the event and response approaches to estimate the 100-year coastal flood for Pacific coast sheltered waters. *Proc. 30th ICCE*, ASCE, 1651-1663.

Gaume, E. et al. 2009. A compilation of data on European flash floods. *Journal of Hydrology*, 367**,** 70-78.

Geeraerts, J., Troch, P., Rouck, J.D., Verhaeghe, H.,Bouma, J.J. 2007. Wave overtopping at coastal structures: prediction tools and related hazard analysis. *Journal of Clear Production*, 15, 1514-1521.

Goda, Y. 1985. *Random Seas and Design of Maritime Structures*. University of Tokyo Press. Tokyo, Japan.

Harley, M.D., Ciavola, P. 2013. Managing local coastal inundation risk using real-time forecasts and artificial dune placements. *Coastal Engineering,* 77, 77–90.

Hedges, T., Reis, M. 1998. Random wave overtopping of simple seawalls: a new regression model. *Water, Maritime and Energy Journal,* 1(130), 1-10.

Holthuijsen, L.H., Booij, N., Herbers, T.H.C. 1989. A prediction model for stationary, short-crested waves in shallow water with ambient currents. Coastal Engineering, 13(1), 23–54. doi:10.1016/0378-3839(89)90031-8.

Holman, R.A. 1986. Extreme value statistics for wave run-up on a natural beach. *Coastal Engineering* 9, 527–544.

Idroser, 1982. *Piano progettuale per la difesa della costa Emiliano-Romagnola - Aspetti meteomarini e determinazione del trasporto litoraneo, vol. III*, Regione Emilia-Romagna, 57p.

Instituto Nacional de Meteorología (INM). 2007. *Estudio sobre precipitaciones máximas diarias y periodos de retorno para un conjunto de estaciones pluviométricas seleccionadas de España*. CD.

Jiménez, J.A., Sánchez Arcilla, A., Stive, M.J.F. 1993. Discussion on prediction of storm/normal beach profiles. *Journal of Waterway Port, Coastal and Ocean Engineering,* 19(4), 466-468.

Kerper, D.R., Sakumoto, L., Zyserman, J.A., Baek, S. 2006. Application of FEMA Guidelines for Coastal Flood Hazard Mapping to a site in Northern California. *Proc. 30th ICCE*, ASCE, 1812-1825.

Kobayashi, N., Tega, Y., Hancock, M.W. 1996. Wave reflection and overwash of dunes. *Journal of Waterway, Port, Coastal, and Ocean Engineering*, *122*(3), 150-153.

Kriebel, D., Dean, R.G., 1993. Convolution model for time-dependent beach-profile response. Journal of Waterway, Port, Coastal and Ocean Engineering, 119, 204-226.

Larson, M., Kraus, N.C. 1989. *SBEACH: Numerical Model for Simulating Storm-Induced Beach Change.* CERC-89-9. US Army Corps of Engineers, Vicksburg.

Laudier, N., Thornton, E., MacMahan, J., 2011. Measured and modelled wave overtopping on a natural beach. *Coastal Engineering* 58, 815-825.

Lavabre J., Sempere D., Cernesson, F. 1993. Changes in the hydrological response of a small Mediterranean basin a year after a wildfire. *Journal of Hydrology*, 142, 273–99.

Lionello, P., Cogo, S., Galati, M. B., Sanna, A. 2008. The Mediterranean surface wave climate inferred from future scenario simulations. *Glob. Planet. Change*, 63(2-3), 152–162.

Marchi, L., Borga, M., Preciso, E., Gaume, E. 2010. Characterisation of selected extreme flash floods in Europe and implications for flood risk management. *Journal of Hydrology*, 394, 118-133.

Martinez, G. et al. 2014. *Synthesis of data collection consultation organised at local level.* RISC-KIT Deliverable D1.2.

Mather, A., Stretch, D., Garland, G. 2011. Predicting extreme wave run-up on natural beaches for coastal planning and management. *Coastal Engineering Journal* 53, 87-109.

Matias, A., Blenkinsopp, C.E., Masselink, G., 2014. Detailed investigation of overwash on a gravel barrier. *Marine Geology* 350, 27-38.

McCall, R. T., Masselink, G., Poate, T. G., Roelvink, J. A., Almeida, L. P., Davidson, M., Russell, P. E. 2014. Modelling storm hydrodynamics on gravel beaches with XBeach-G. *Coastal Engineering*, *91*, 231-250.

Mendoza, E.T., Jiménez, J.A., 2006. Storm-Induced Beach Erosion Potential on the Catalonian Coast. *Journal of Coastal Research.* SI 48, 81-88.

Mendoza, E.T., Jiménez, J.A., Mateo, J. 2011. A coastal storms intensity scale for the Catalan sea (NW Mediterranean). *Natural Hazards and Earth System Sciences* 11, 2453-2462.

Minea, G. 2013. Assessment of the flash flood potential of Bâsca River Catchment (Romania) based on physiographic factors. *Central European Journal of Geosciences*, 5, 344-353.

Mori, N., Yasuda, T., Mase, H., Tom, T., Oku, Y. 2010. Projection of Extreme Wave Climate Change under Global Warming, *Hydrol. Res. Lett.,* 4, 15–19.

Morton, R.A. 2002. Factors controlling storm impacts on coastal barriers and beaches - A preliminary basis for near real-time forecasting. *Journal of Coastal Research*, 18, 486-501.

Morton, R.A., Sallenger, A.H.Jr. 2003. Morphological impacts of extreme storms on sandy beaches and barriers. *Journal of Coastal Research*, 19, 560-573.

Nairn, R.B., Roelvink, J.D., Southgate, H.N. 1990. Transition zone width and implications for modeling surfzone hydrodynamics. *Proc. 22nd ICCE,* ASCE, 68-81.

Nederhoff, C. M., Lodder, Q. J., Boers, M., Den Bieman, J. P., Miller, J. K. 2015. Modeling the effects of hard structures on dune erosion and over-wash - a case study of the impact of Hurricane Sandy on the New Jersey coast. *Proceedings Coastal Sediments*, San Diego, CA.

Nielsen, P., Hanslow, D.J. 1991. Wave runup distributions on natural beaches. *Journal of Coastal Research* 7, 4, 1139-1152.

Norbiato, D., Borga, M., Esposti, S.D., Gaume, E., Anquetin, S. 2008. Flash flood warning based on rainfall thresholds and soil moisture conditions: An assessment for gauged and ungauged basins. *Journal of Hydrology*, 362**,** 274-290.

Owen, M., 1980. *Design of seawalls allowing for wave overtopping,* Wallingford, UK.

Puertos del Estado. 2001. *ROM 0.0. General procedure and requirements in the design of harbor and maritime structures*. Spanish Ministry of Public Works, Madrid.

Pullen, T., Allsop, N.W.H., Bruce, T., Kortenhaus, A., Schüttrumpf, H., van der Meer, J.W. 2007. *EurOtop. Wave overtopping of sea defences and related structures: Assessment manual*. www.overtopping-manual.com.

Ranasinghe R, Callaghan D, Stive, M.J.F. 2012. Estimating coastal recession due to sea level rise: beyond the Bruun rule. *Climatic Change,* 110, 561-574.

Raynaud, D., Thielen, J., Salamon, P., Burek, P., Anquetin, S., Alfieri, L. 2014. A dynamic runoff co-efficient to improve flash flood early warning in Europe: evaluation on the 2013 central European floods in Germany. *Meteorological Applications***,** doi: 10.1002/met.1469.

Reeve, D. 2010. *Risk and Reliability: Coastal and Hydraulic Engineering*. Spon Press, London, 304 pp.

Reis, M., Hu, K., Hedges, T. Mase, H. 2008. A comparison of empirical, semiempirical and numerical wave overtopping models. *Journal of Coastal Research,* 24, 250-262.

Roberts, T.M., Wang, P., Kraus, N.C. 2010. Limits of wave runup and corresponding beach profile change from large scale laboratory data. *Journal of Coastal Research* 26, 184-198.

Roelvink, J. A. 1993. Dissipation in random wave group incident on a beach. *Coastal Engineering*, 19, 127–150.

Roelvink, D., Reniers, A., van Dongeren, A.P., de Vries, J.V.T., McCall, R., Lescinski, J. 2009. Modelling storm impacts on beaches, dunes and barrier islands. *Coastal Engineering*, 56(11), 1133-1152.

Roelvink, D., Dastgheib, A., Spencer, T., Möller, I., Christie, E., Berenguer, M., Sempere-Torres, D. 2015. *Improvement of physical processes.XBeach improvement & validation; wave dissipation over vegetated marshes and flash flood module*. *Updated Physical models.* RISC-KIT Deliverable D3.2. (http://www.risckit.eu/np4/file/23/RISCKIT_D.3.2_Improvement_of_Physical_Pr.pdf),

Sánchez-Arcilla, A., Jiménez, J.A., Peña, C. 2009. Wave-induced morphodynamic risks. Characterization of extremes. *Coastal Dynamics 2009*, World Scientific (CD), paper 127.

Sanuy, M., Jiménez, J.A., Ortego, M. 2015. Differences resulting from coastal flooding analysis in Mediterranean conditions based on the adopted approach: event *vs* response. (in review).

Santangelo, N., Santo, A., Di Crescenzo, G., Foscari, G., Liuzza, V., Sciarrotta, S., Scorpio, V. 2011. Flood susceptibility assessment in a highly urbanized alluvial fan: the case study of Sala Consilina (southern Italy). *Natural Hazards and Earth System Sciences*, 11, 2765-2780.

Schuettrumpf, H., Oumeraci, H. 2005. Layer thicknesses and velocities of wave overtopping flow at seadikes. *Coastal Engineering* 52, 473-495.

Shand, R.D., Shand, T.D., McComb, P.J., Johnson, D.L. 2011. Evaluation of empirical predictors of extreme run-up using field data. *20th Australasian Coastal and Ocean Engineering Conference,* Perth.

Smith, G., 2003. *Flash Flood Potential: Determining the Hydrologic Response of FFMP Basins to Heavy Rain by Analyzing Their Physiographic Characteristics*. A white paper available from the NWS Colorado Basin River Forecast Center website at http://www.cbrfc.noaa.gov/papers/ffp_wpap.pdf, 11 pp.

Stephenson, D.B. 2008. Definition, diagnosis, and origin of extreme weather and climate events. In: Diaz, H.F., Murnane, R.J. (Eds), *Climate Extremes and Society*. Cambridge University Press, Cambridge, 11-23.

Stive, M. J., Ranasinghe, R., Cowell, P. 2009. Sea level rise and coastal erosion. In: Kim Y (ed) *Handbook of Coastal and Ocean Engineering*. World Scientific, pp 1023-1038.

Stive, M.J., De Vriend, H.J. 1994. Shear stresses and mean flow in shoaling and breaking waves. *Proc. 24th Int. Conference on Coastal Engineering,* ASCE, 594-608.

Stockdon, H.F., Holman, R.A., Howd, P.A., Sallenger, A.H.Jr. 2006. Empirical parameterization of setup, swash and run-up. *Coastal Engineering,* 56, 573-588.

Svendsen, I.A. 1984. Wave heights and set-up in a surf zone. *Coastal Engineering*, 8, 303–329. doi:10.1016/0378-3839(84)90028-0.

Teatini, P., Ferronato, M., Gambolati, G., Bertoni, W., Gonella, M. 2005. A century of land subsidence in Ravenna, Italy. *Environmental Geology*, 47, 831-846.

Thielen, J., Bartholmes, J., Ramos, M.H., de Roo, A. 2009. The European Flood Alert System - Part 1: Concept and development. *Hydrology and Earth System Sciences*, 13**,** 125-140.

Tuan, T.Q., Verhagen, H.J., Visser, P., Stive, M.J. 2006. Wave overwash at low-crested beach barriers. *Coastal Engineering Journal*, *48*(04), 371-393.

UCAR. 2010. *Flash Flood Early Warning System Reference Guide*. NOAA National Weather Service. (http://www.meted.ucar.edu/hazwarnsys/haz_fflood.php).

Van der Meer, J.W., Briganti, R., Zanuttigh, B., Wang, B. 2005. Wave transmission and reflection at low-crested structures: Design formulae, oblique wave attack and spectral change. *Coastal Engineering*, 52, 915–929.

Van der Meer, J.W., Daemen, I.F.R. 1994. Stability and wave transmission at low-crested rubble-mound structures. *Journal of Waterway, Port, Coastal, and Ocean Engineering*, 120(1), 1–19.

Van Dongeren, A., Lowe, R., Pomeroy, A., Trang, D.M., Roelvink, D., Symonds, G., Ranasinghe, R. 2013. Numerical modeling of low-frequency wave dynamics over a fringing coral reef. *Coastal Engineering*, 73, 178–190.

Versini, P. A., Gaume, E., Andrieu, H. 2010. Assessment of the susceptibility of roads to flooding based on geographical information – test in a flash flood prone area (the Gard region, France). *Natural Hazards and Earth System Sciences*, 10, 793-803.

Versini, P. A., Velasco, M., Cabello, A., Sempere-Torres, D. 2012. Hydrological impact of forest fires and climate change in a Mediterranean basin. *Natural Hazards*, 66**,** 609-628.

Vila-Concejo, A., Matias, A., Pacheco, A., Ferreira, O. and Dias, J.A. 2006. Quantification of inlet-related hazards in barrier island systems. An example from the Ria Formosa (Portugal). *Continental Shelf Research* 26, 1045-1060.

Vousdoukas, M.I., Wziatek, D., Almeida, L.P. 2012. Coastal vulnerability assessment based on video wave run-up observations at a mesotidal, steep-sloped beach. *Ocean Dynamics* 62, 123-137.

Wise, R.S., Smith, S.J., Larson, M. 1996. *SBEACH. Numerical Model for Simulating Storm-Induced Beach Change.* CERC. US Army Corps of Engineers, Vicksburg.

Zijlema, M., Stelling, G. S., Smith, P.B. 2011. SWASH: An operational public domain code for simulating wave fields and rapidly varied flows in coastal waters. *Coastal Engineering*, 58(10), 992–1012. doi:10.1016/j.coastaleng.2011.05.015.

Zogg, J., Deitsch. K. 2013. The Flash Flood Potential Index at WFO Des Moines, Iowa. *National Weather Service working paper*. Available from http://www.crh.noaa.gov/ images/dmx/hydro/FFPI/FFPI_WriteUp.pdf.